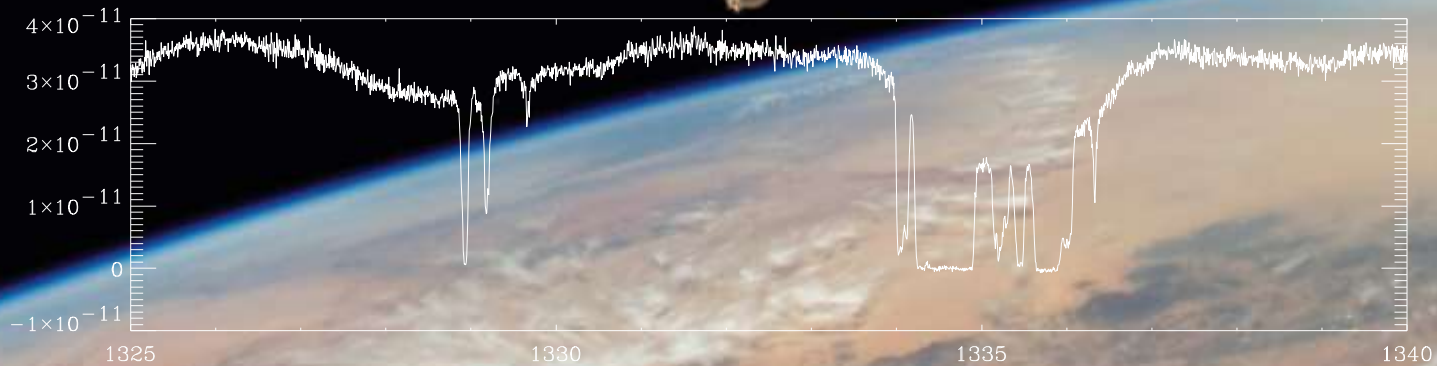


THE LEGACY OF HST SPECTROSCOPY



Edward B. Jenkins
Princeton University Observatory

HST Spectroscopic Capabilities in the Ultraviolet

Current instruments:

- **ACS prism:** $R \approx 100$ @ 1500 Å, λ coverage = 1250 — 1800 Å, $A_{\text{eff}} = 800 \text{ cm}^{-2}$
- **COS:** 7 different **1st order grating modes:** $3000 \leq R \leq 20,000$, λ coverage = 900 — 3000 Å, $200 \leq A_{\text{eff}} \leq 2000 \text{ cm}^{-2}$
- **STIS:** 11 spectral modes:
 - **1st order gratings:** $500 \leq R \leq 10,000$, λ coverage = 1150 — 3200 Å, $300 \leq A_{\text{eff}} \leq 1200 \text{ cm}^{-2}$
 - **Echelle gratings:** $30,000 \leq R \leq 114,000$, λ coverage = 1150 — 3100 Å, $130 \leq A_{\text{eff}} \leq 300 \text{ cm}^{-2}$
 - **Prism:** R highly variable, λ coverage = 1150 — 3620 Å, $A_{\text{eff}} \approx 500 \text{ cm}^{-2}$
 - Wide selection of entrance slits, including ones 52" long \perp to disp.

HST Spectroscopic Capabilities in the Ultraviolet

- Previous instruments:

- **FOS:** $250 \leq R \leq 1300$, λ coverages = 1150 — 5400 Å & 1620 — 8500 Å, capable of doing spectropolarimetry (but only for $\lambda > 1650$ Å post costar)
- **GHR:** 1st order and echelle gratings: $2000 \leq R \leq 80,000$, λ coverages = 1150 — 1800 Å & 1680 — 3400 Å

- *While these early-generation instruments were generally inferior to the current ones, an important capability that we no longer have is a tolerance for high detector count rates (e.g. **50,000** counts s⁻¹resel⁻¹ allowed for the Digicons on FOS and GHR, compared with **100** counts s⁻¹resel⁻¹ for the STIS MAMA detectors) ; **this precludes obtaining high S/N in short observing times.***

The Dark Ages

2004-2009

Date: Fri, 13 Aug 2004 16:22:40 -0400 (EDT)

From: STScI-Generic@stsci.edu

To: ebj@astro.princeton.edu

Subject: STIS Update

Dear HST User,

On Tuesday, August 3, STIS entered a "suspend" state in response to the loss of 5-volt power in the Side 2 electronics. The Side 1 electronics suffered a short circuit in May 2001 and are currently not working. Failures in the two redundant Sides make STIS unusable. While it is possible that further investigation will point out a way to restore STIS to a useful state, we believe it unlikely that STIS can be revived without physical servicing. Fortunately, all other science instruments and the observatory itself continue to function normally.

The observing programs that use the unique capabilities of STIS will be suspended. We expect to notify all STIS observers about the status of their programs within the next several weeks

The Dark Ages 2004-2009



The People who do Imaging



Figures of Merit

- Primary:
 - The effective area A_{eff} that is the product of the area of the unobscured primary mirror and the efficiencies of the optics and the detector
 - The multiplexing factor M that represents the number of independent resolution elements that can be recorded in a single exposure
 - The wavelength resolving power $R = \lambda/\delta\lambda$

Figures of Merit

- Secondary:
 - F_{\min} : a minimum flux where noise sources other than the statistical uncertainty of photon counts start to dominate.
 - F_{\max} : a maximum flux that can be tolerated by a detector without suffering long term damage.

Figures of Merit

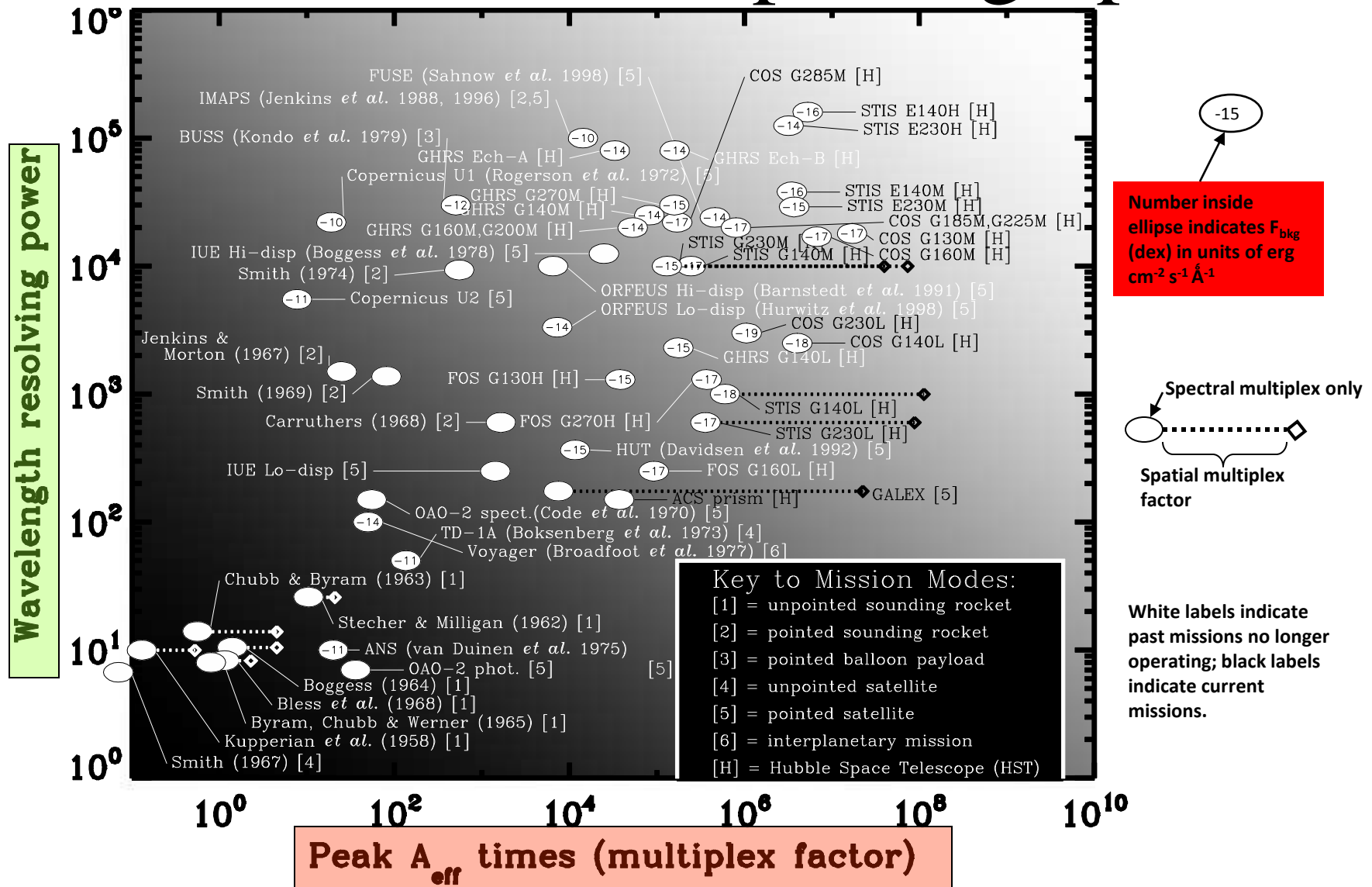
- Which figures of merit matter for a given observing program depends on the nature of a source and the science goals of the research.
- Let us consider two fundamental quantities:

R

and

$$A_{\text{eff}} \times M$$

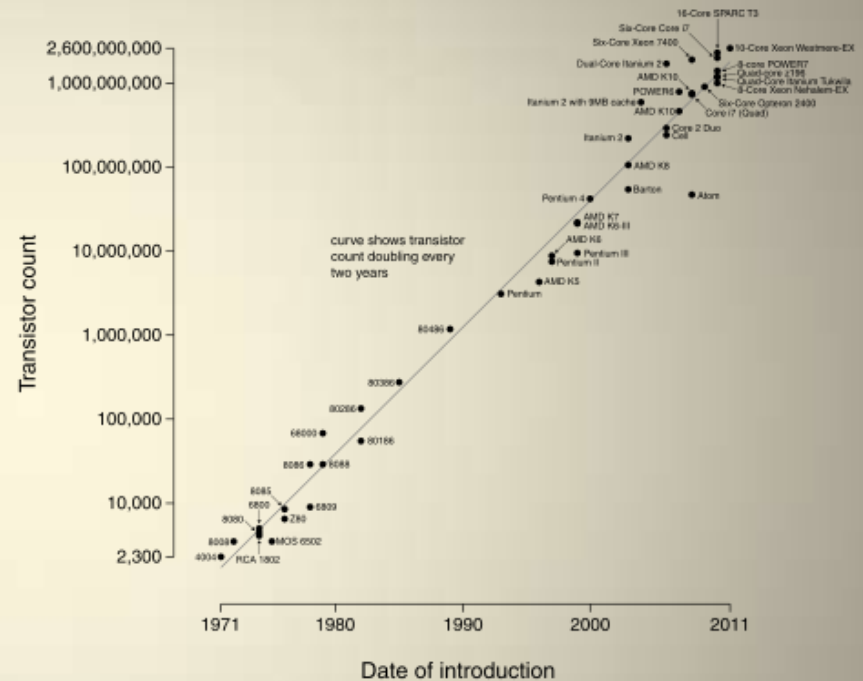
Evolution of UV spectrographs



Moore's Law

The number of transistors that can be placed inexpensively on an integrated circuit doubles approximately every two years

Microprocessor Transistor Counts 1971-2011 & Moore's Law

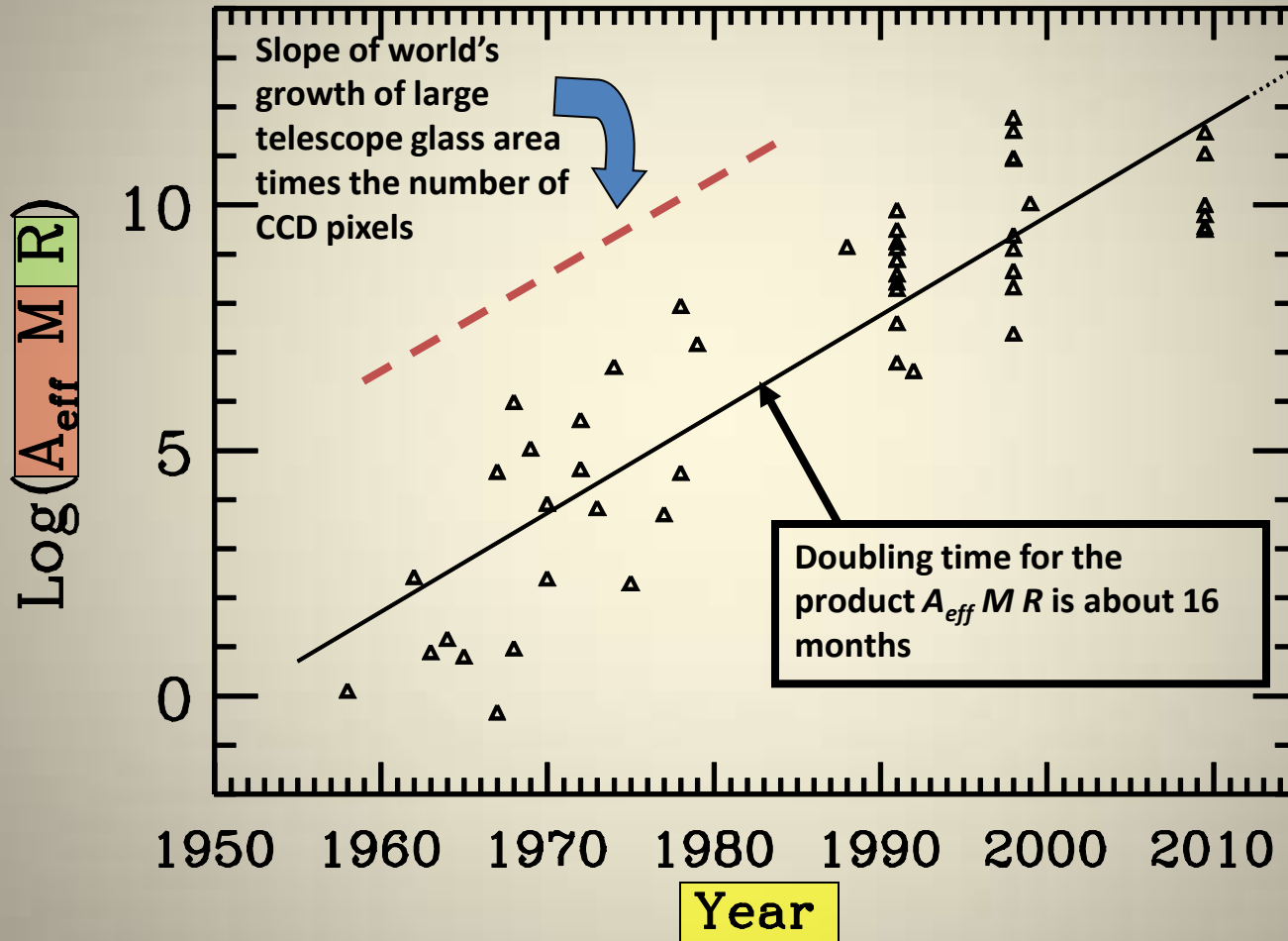


Wirth's Law:

Software is getting slower more rapidly than hardware becomes faster.

Niclaus Wirth
(1995)

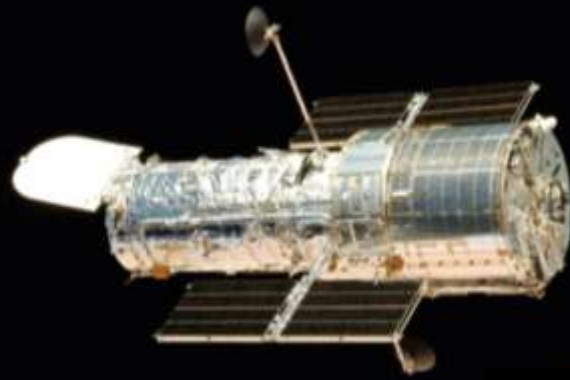
Jenkins's Law



The time needed to analyze and interpret the results increases faster than the increase in observing capability.

My Review of Achievements from HST Spectroscopy

- ⦿ Downloaded articles listed in <http://archive.stsci.edu/hst/bibliography/> and filtered according to usages of FOS, GHRS, STIS or COS
- ⦿ How many of them are there?
 - 2763 (but a few of which used only imaging, not spectroscopy)
 - That means I can spend an average of (30 min)(60 sec/min)/2763 articles = 0.65 sec/article



THE LEGACY OF HST UV SPECTROSCOPY

Edward B. Jenkins

Princeton University Observatory



A REPRESENTATIVE SAMPLE* OF RESULTS FROM HST UV SPECTROSCOPY

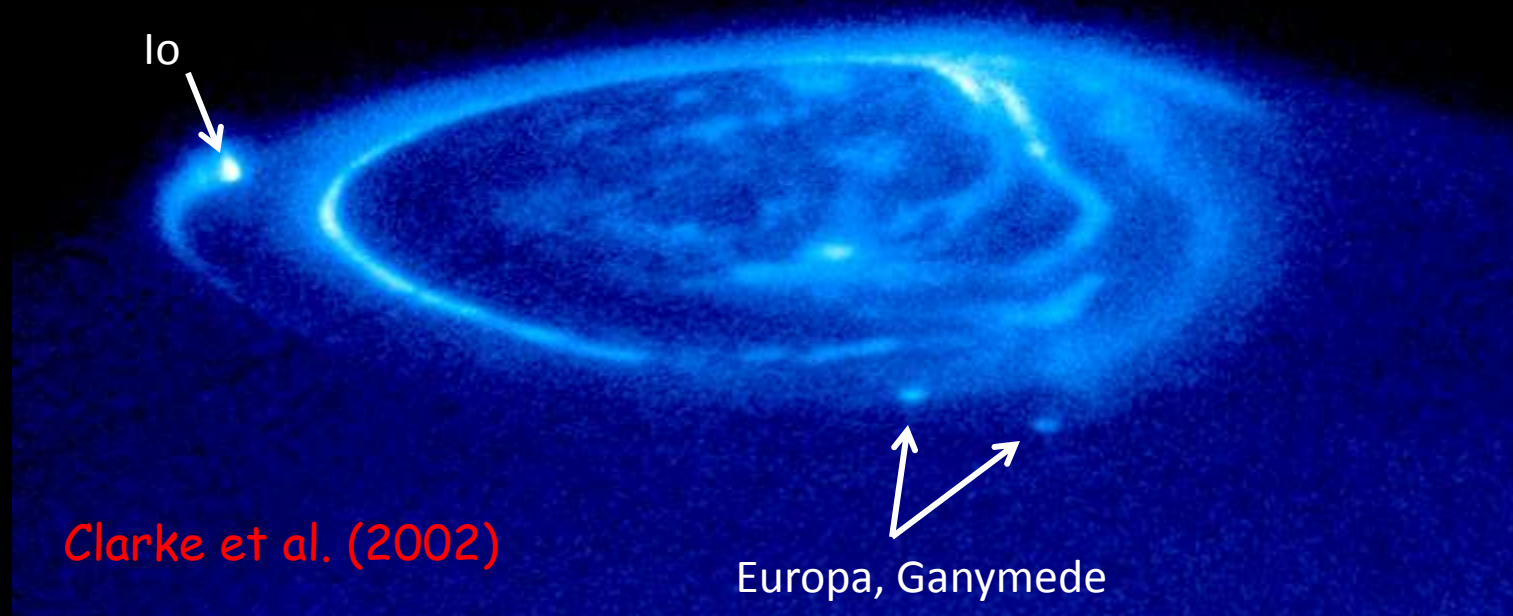
Edward B. Jenkins

Princeton University Observatory

* I tried my best to overcome a bias against subject areas that were unfamiliar to me. Obviously, there is insufficient time to cover many good, interesting papers .

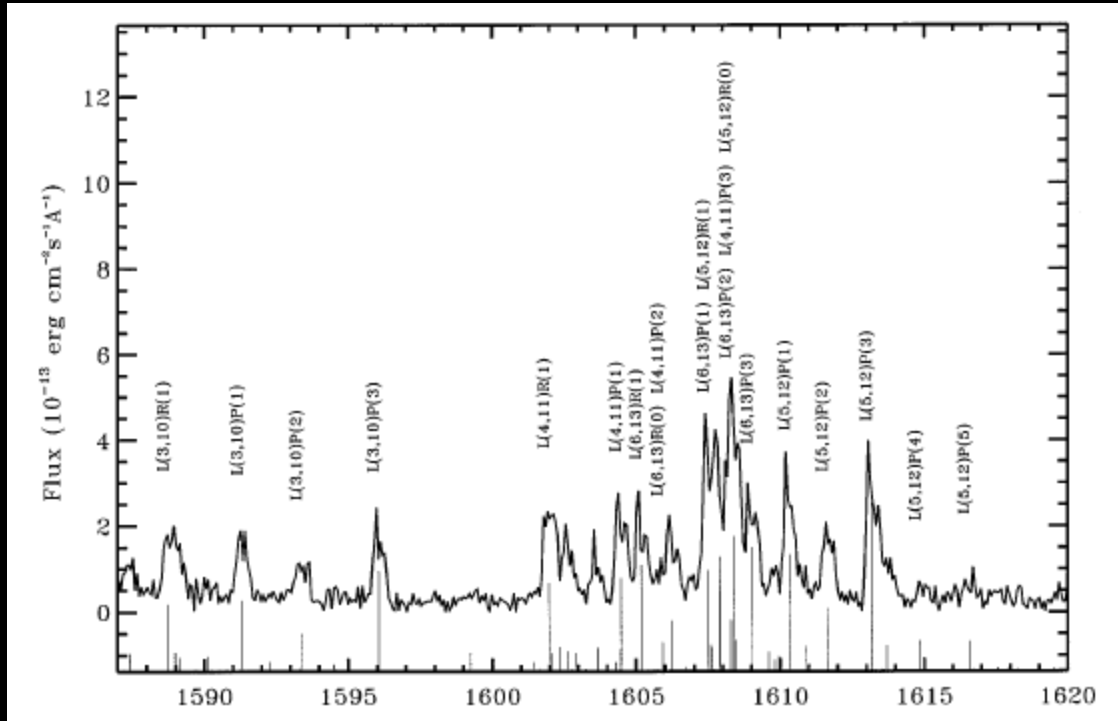
Objects in our Solar System

Footprints of the magnetic flux tubes from the Galilean satellites in the auroral regions of Jupiter

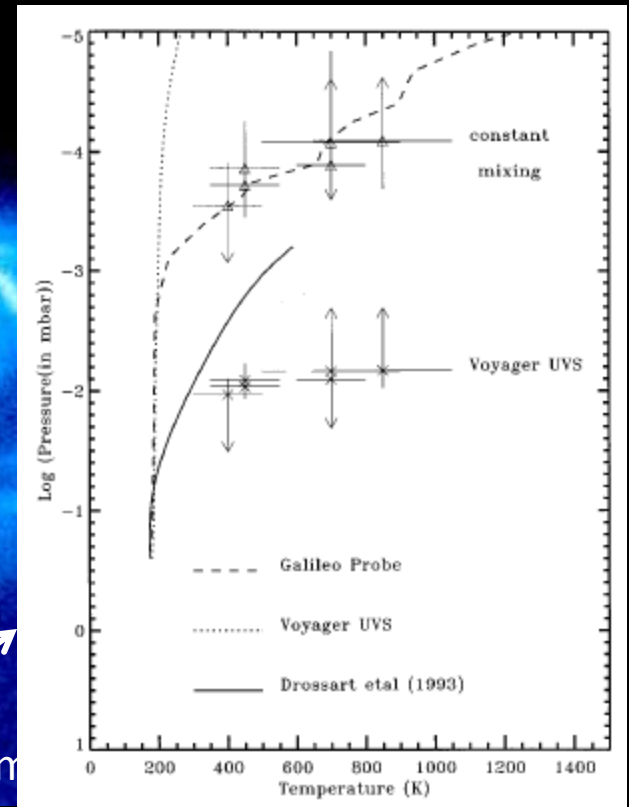


Brightness $\approx 10^3 \times$ terrestrial aurora

Objects in our Solar System



Europa, Ganym



Kim, Fox & Caldwell (1997)

Brightness $\approx 10^3 \times$ terrestrial aurora

Objects in our Solar System



Impact of Comet Shoemaker-Levy on Jupiter
July 1994

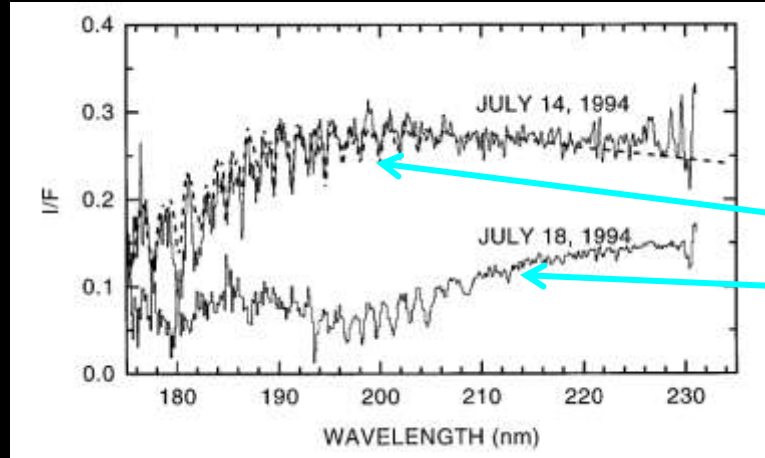
Objects in our Solar System



Impact of Comet Shoemaker-Levy on Jupiter
July 1994

Objects in our Solar System

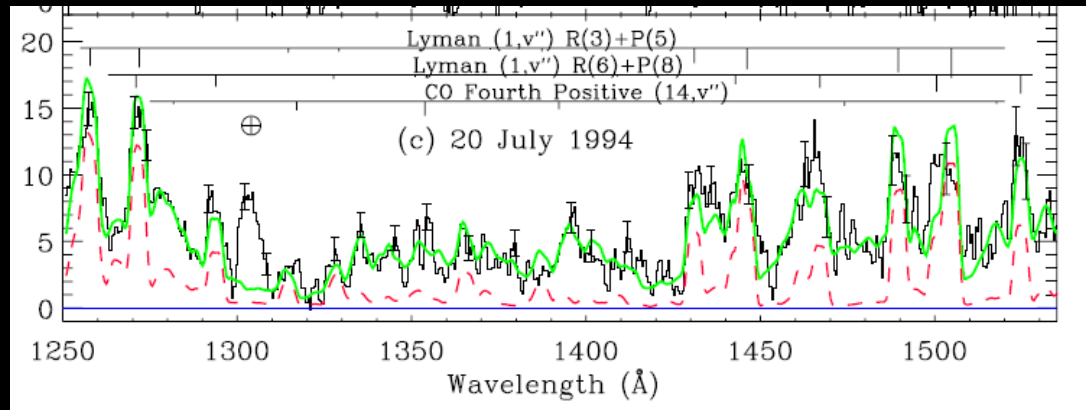
Detected CS_2 , H_2S & NH_3 , but no SO_2



Reflectivities:
Pre-impact
Post-impact

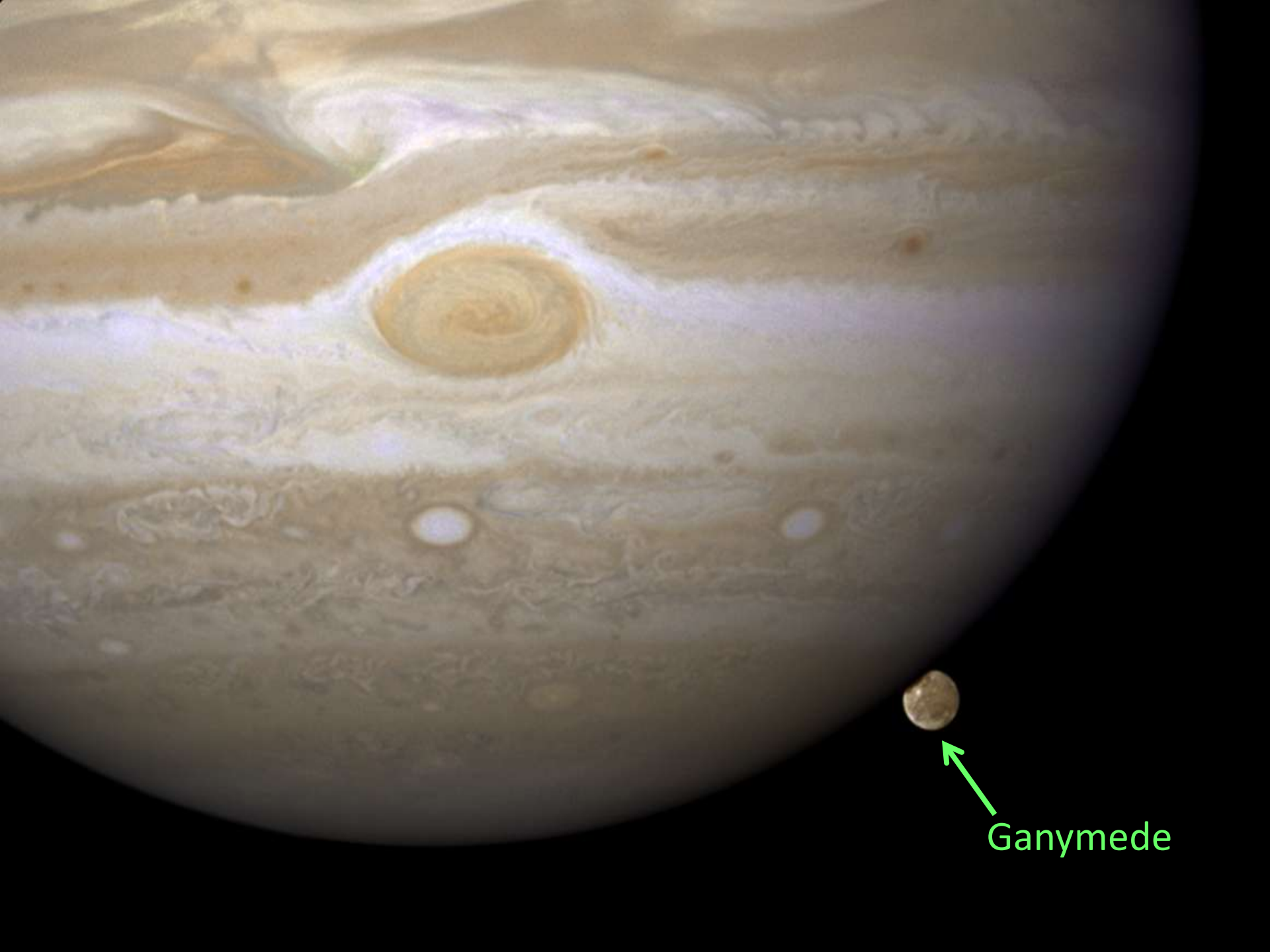
Yelle & McGrath
(1996)

Fluorescence
of H_2 caused
by pumping
from solar $\text{Ly}\alpha$
emission



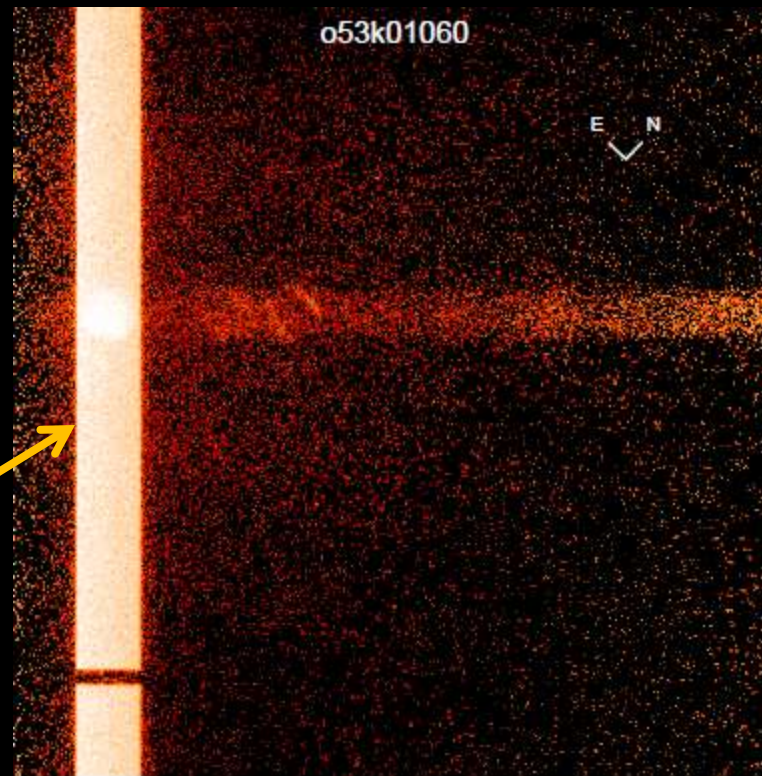
Wolven et
al. (1997)

Impact of Comet Shoemaker-Levy on Jupiter
July 1994



Ganymede

Objects in our Solar System



Raw Image

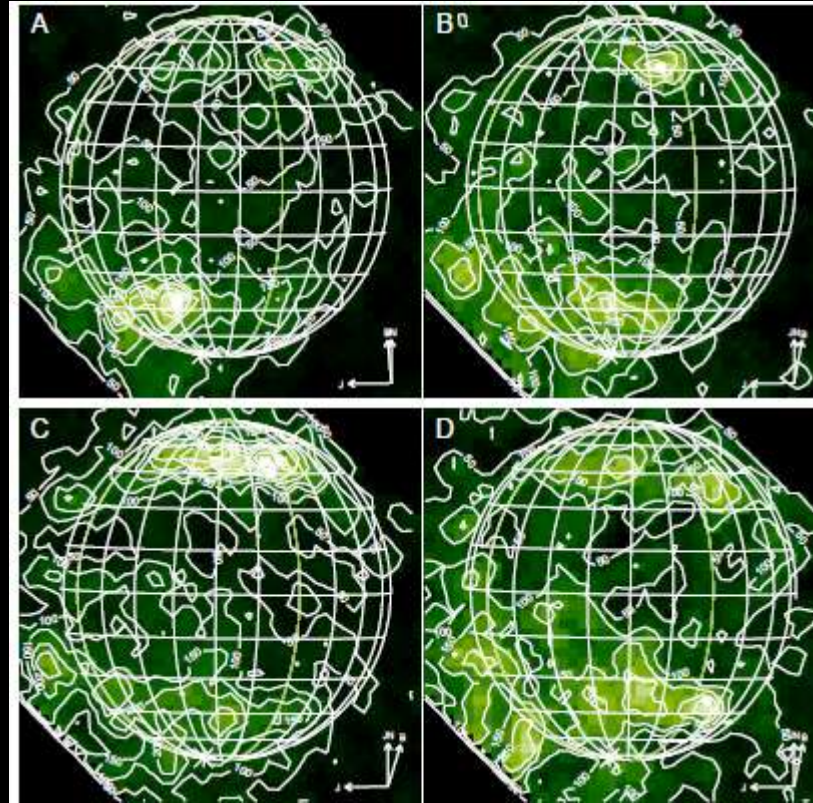
Geocoronal $L\alpha$
filling the 52"×2"
entrance slit of
STIS

STIS Imaging spectrum of
Ganymede in the far UV

Feldman et
al. (2000)

Objects in our Solar System

Derivations
of the
1356Å O I]
emission at
different
times



STIS Imaging spectrum of
Ganymede in the far UV

The ratio of
1356Å to
1302Å line
strengths is
consistent
with electron
impact
excitation of
O₂ with some
contribution
from O I

Feldman et
al. (2000)

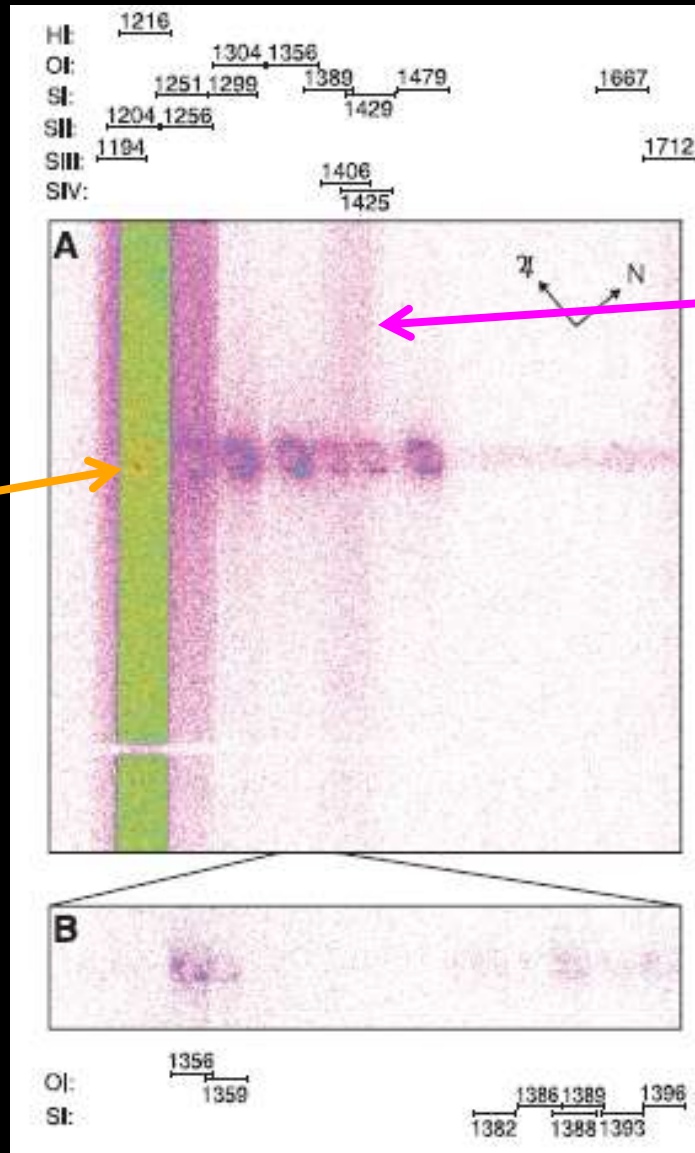
Objects in our Solar System



Io

Objects in our Solar System

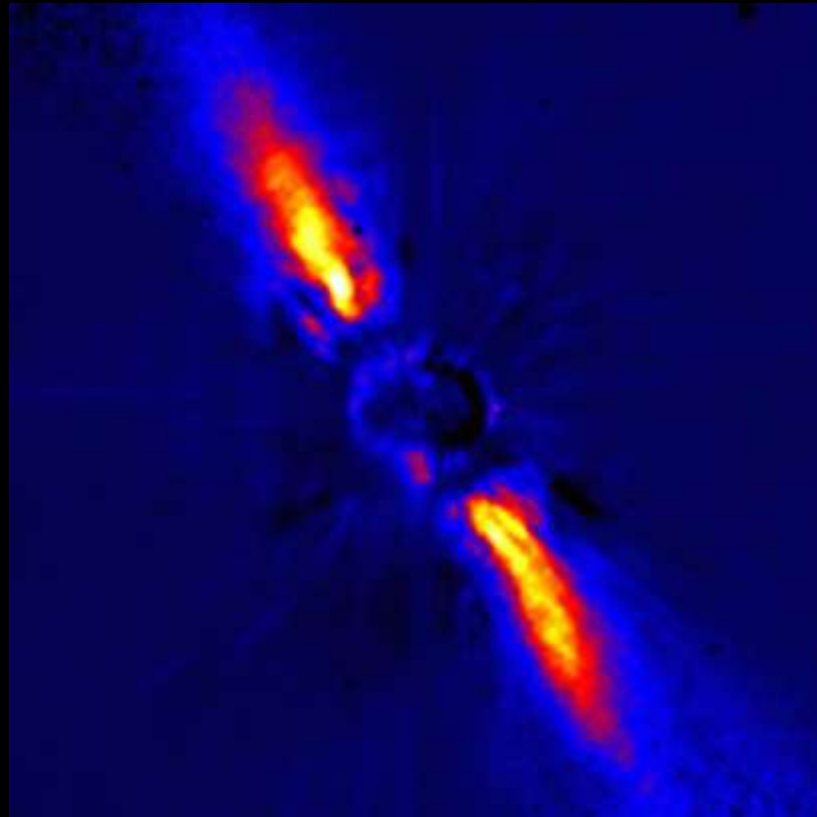
$L\alpha$
emission



Extended
emission from
escaping
neutral sulfur

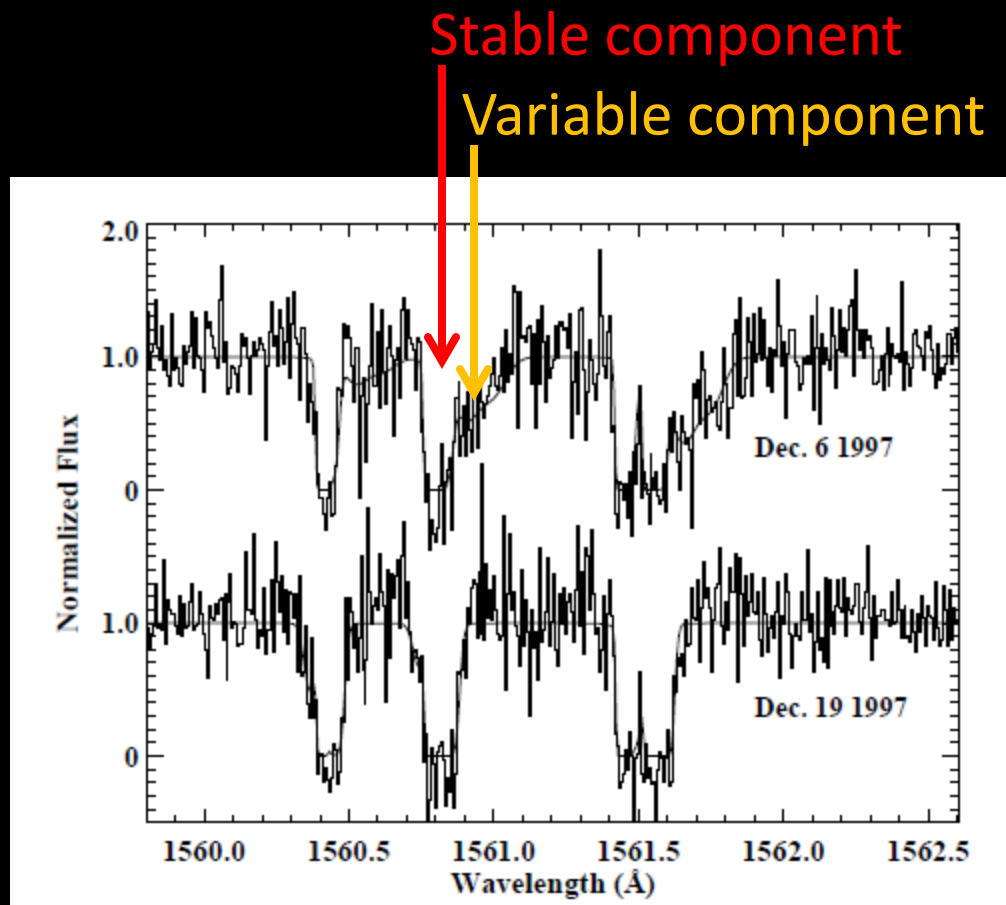
Roessler et al. (1999)

Things around other Stars: The Debris Disk Surrounding β Pic



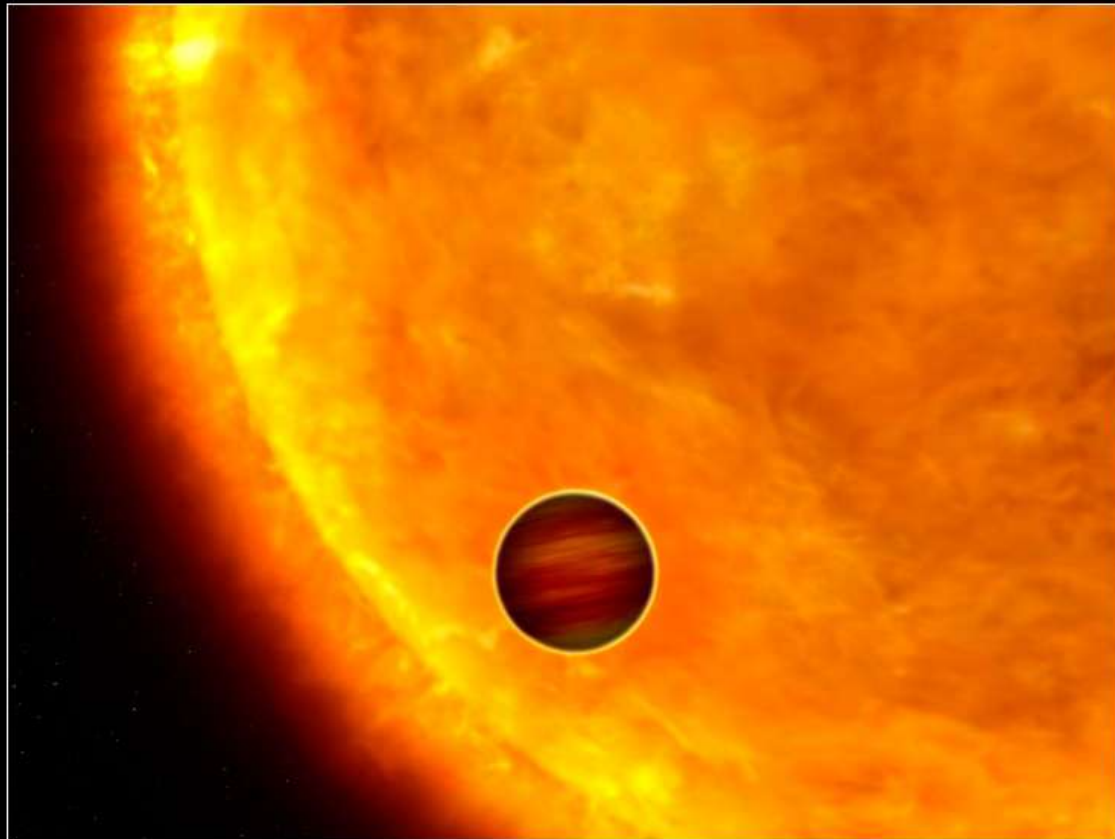
Things around other Stars: The Debris Disk Surrounding β Pic

Absorption
by neutral
carbon
atoms



Roberge et al.
(2000)

Things around other Stars: Transit of HD 209458b



Artist's View of a Transiting Extrasolar Planet

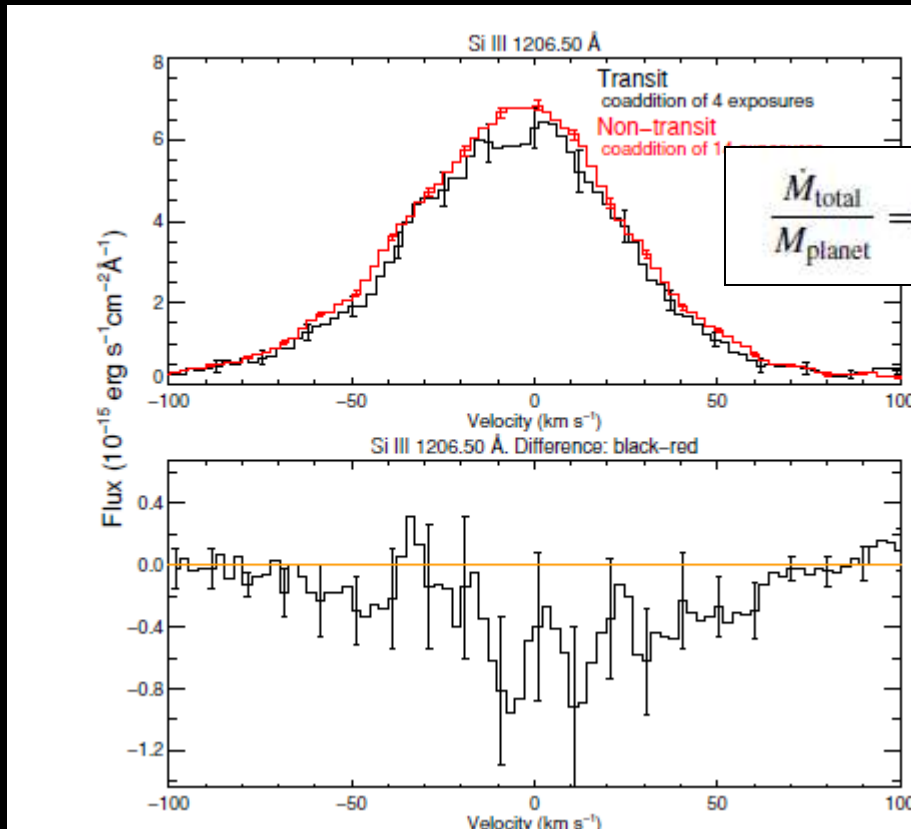
NASA, ESA, and G. Bacon (STScI) ■ STScI-PRC06-34b

Things around other Stars: Transit of HD 209458b

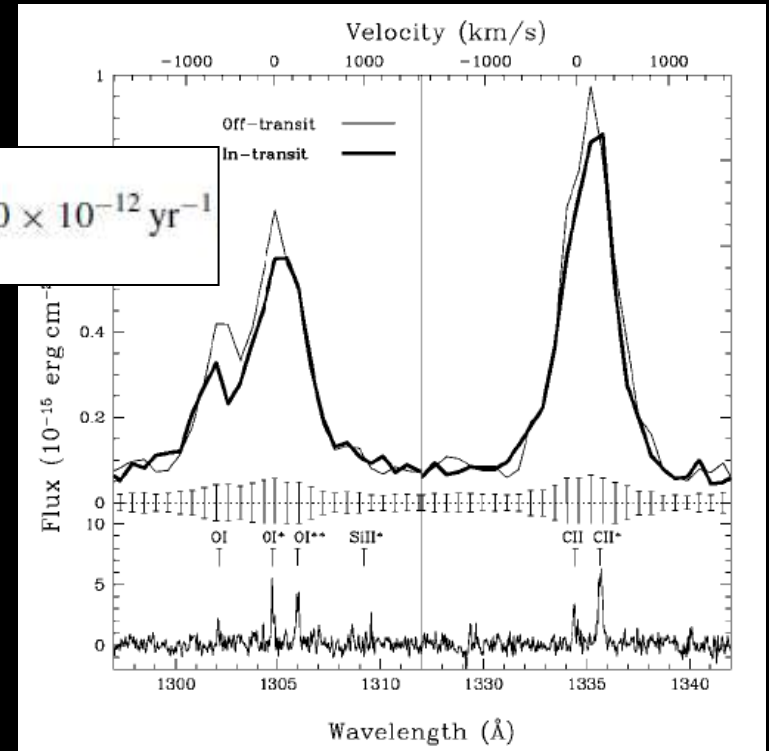
Si III

O I

C II



$$\frac{\dot{M}_{total}}{M_{planet}} = 2.0 \times 10^{-12} \text{ yr}^{-1}$$



Linsky et al. (2010)

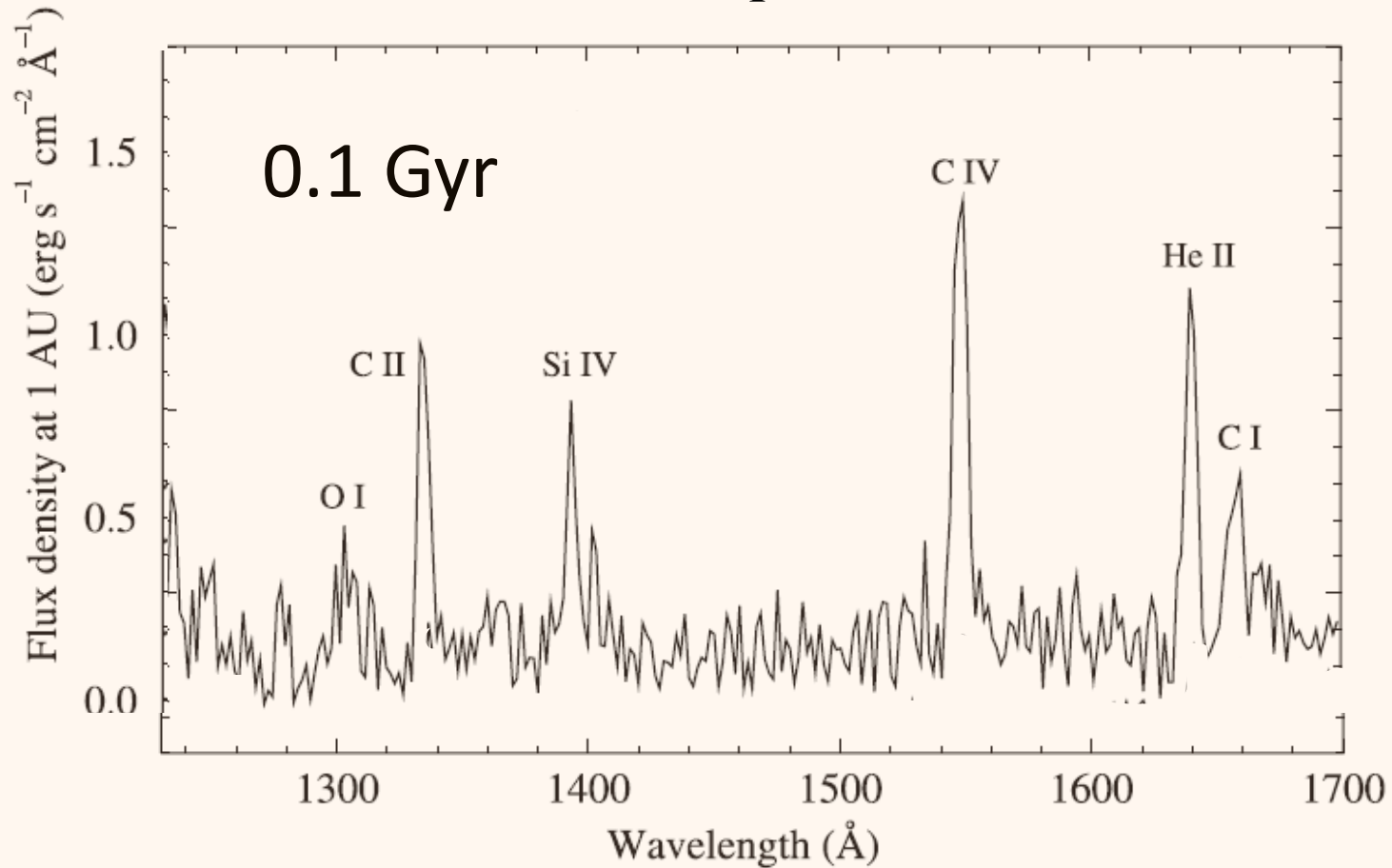
Vidal-Madjar et al. (2004)

Behavior of Solar Analogs with Age

- From the work of Wilson (1963) and Wilson & Skumanich (1964), there has been evidence that the Ca II H & K reversals (and hence chromospheric activity) decrease with stellar age, probably as a result of the decrease in stellar rotation (Wilson 1966).

Behavior of Solar Analogs with Age

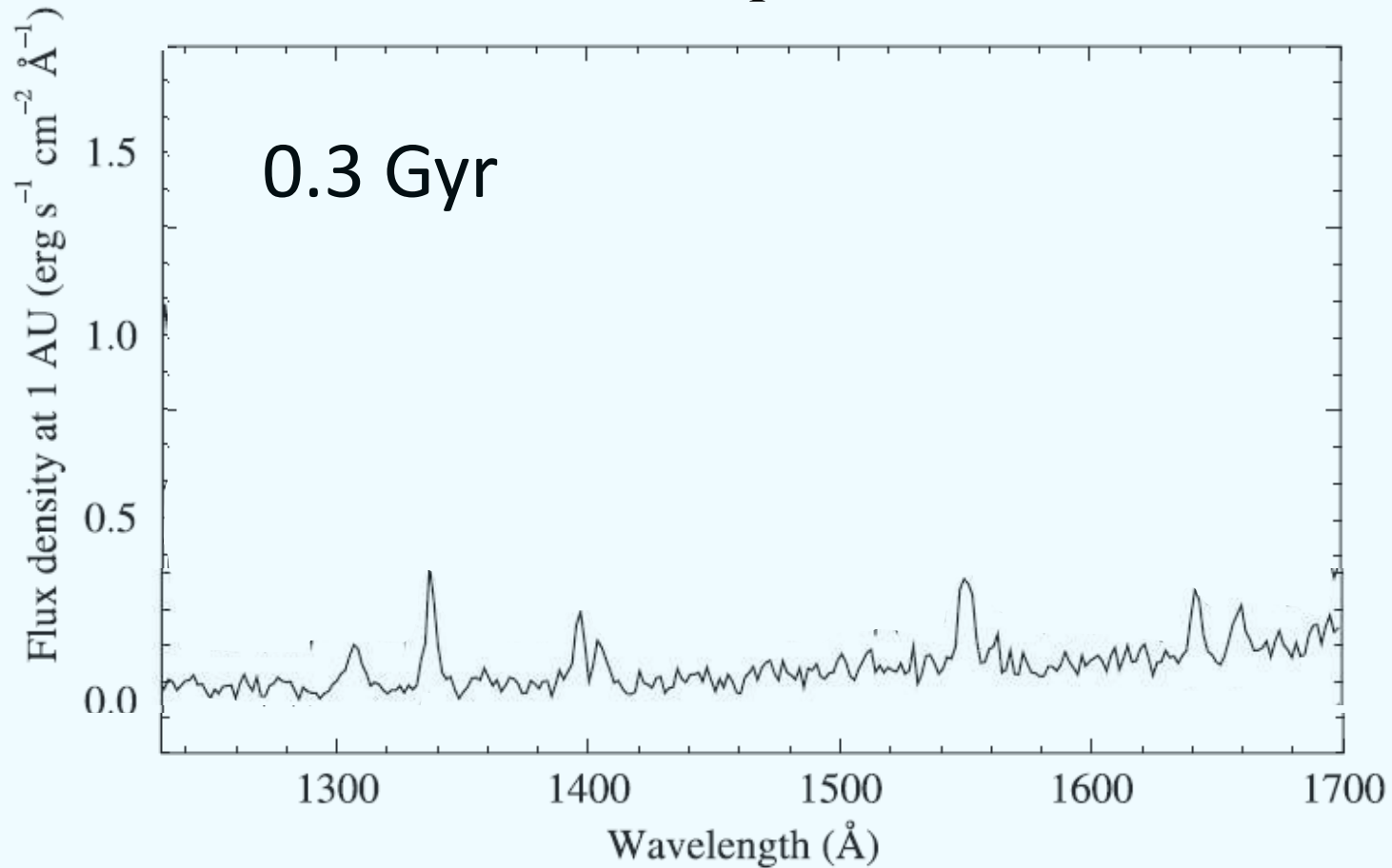
Ultraviolet Chromospheric Emission



Ribas et al (2005)

Behavior of Solar Analogs with Age

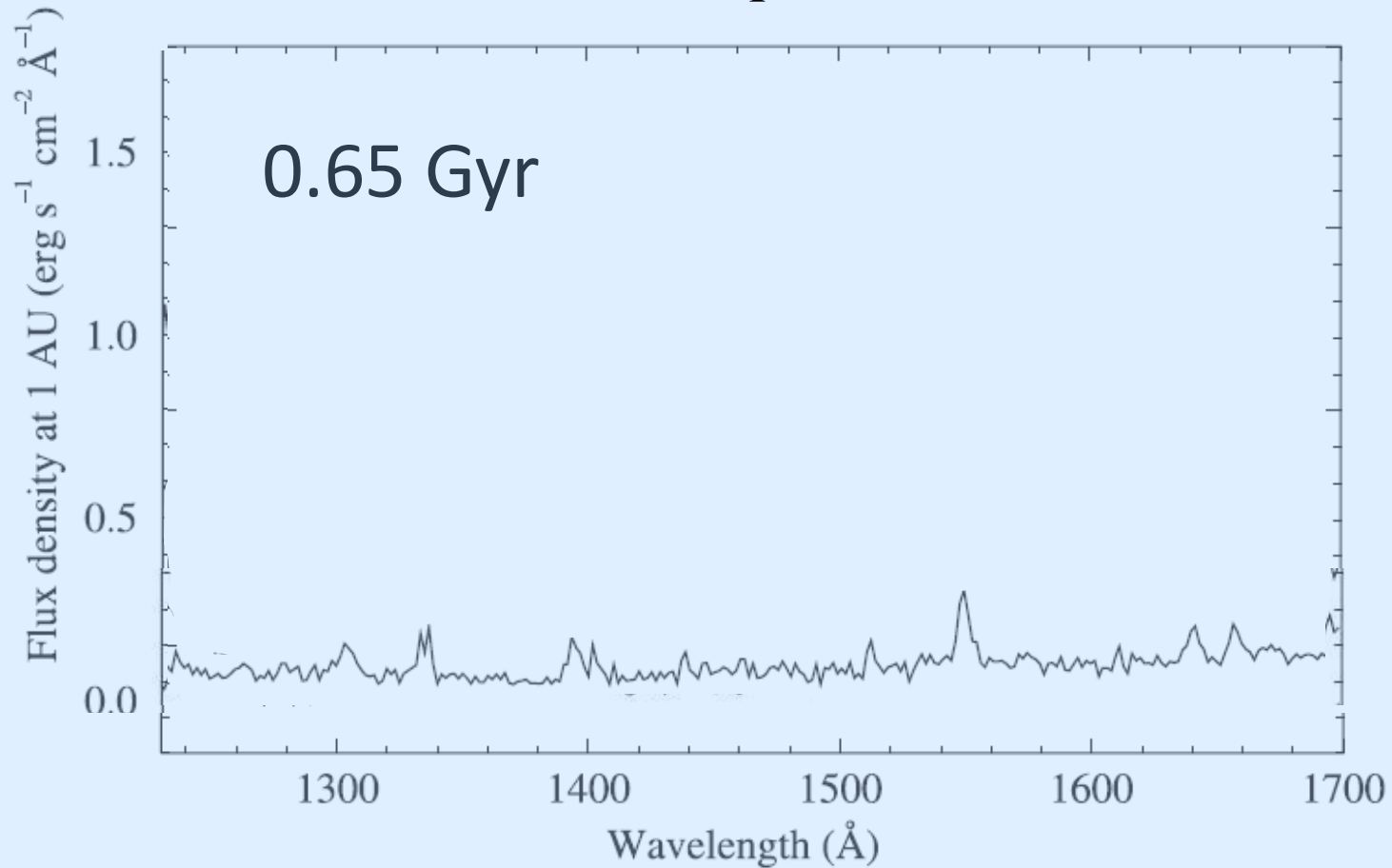
Ultraviolet Chromospheric Emission



Ribas et al (2005)

Behavior of Solar Analogs with Age

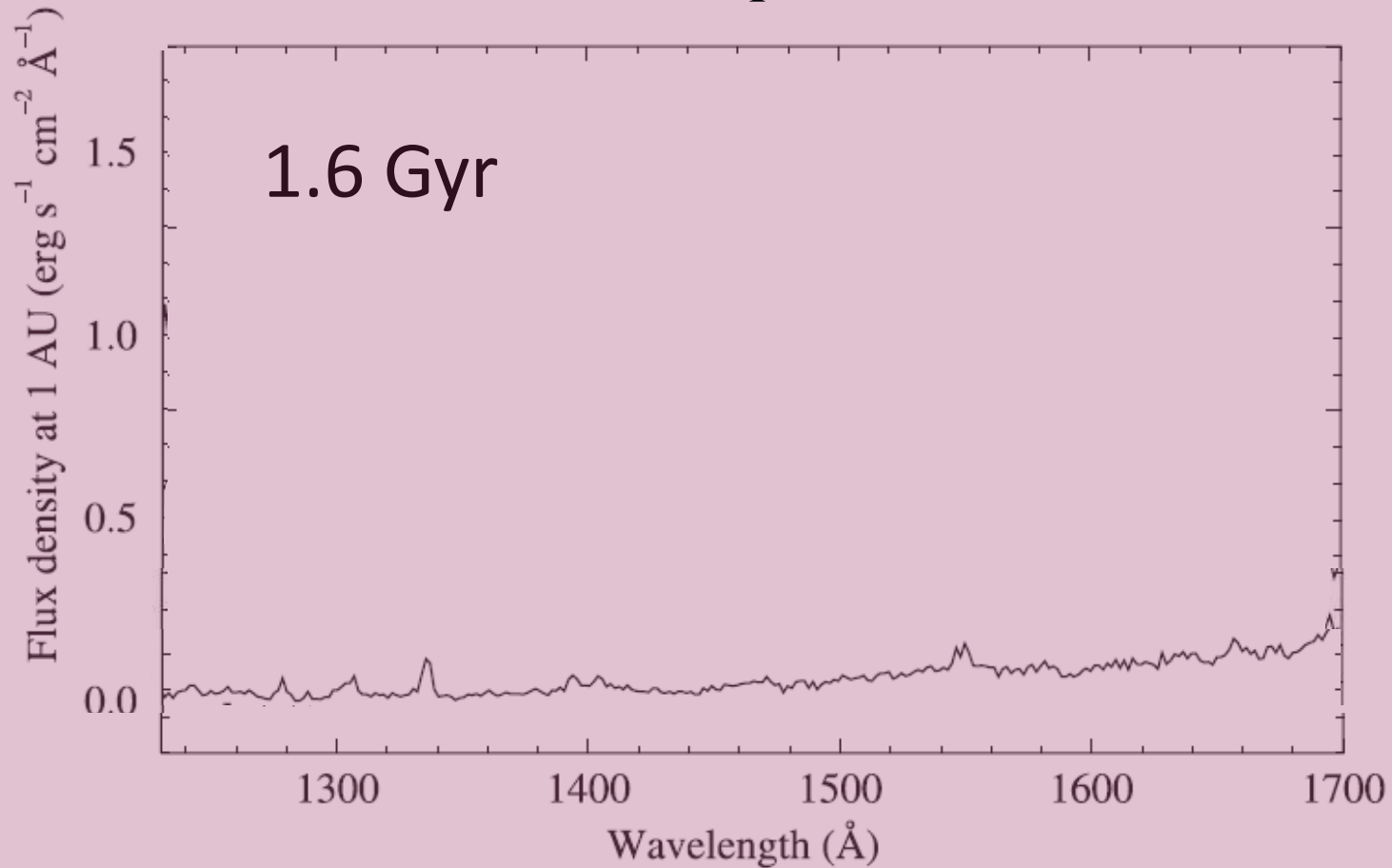
Ultraviolet Chromospheric Emission



Ribas et al (2005)

Behavior of Solar Analogs with Age

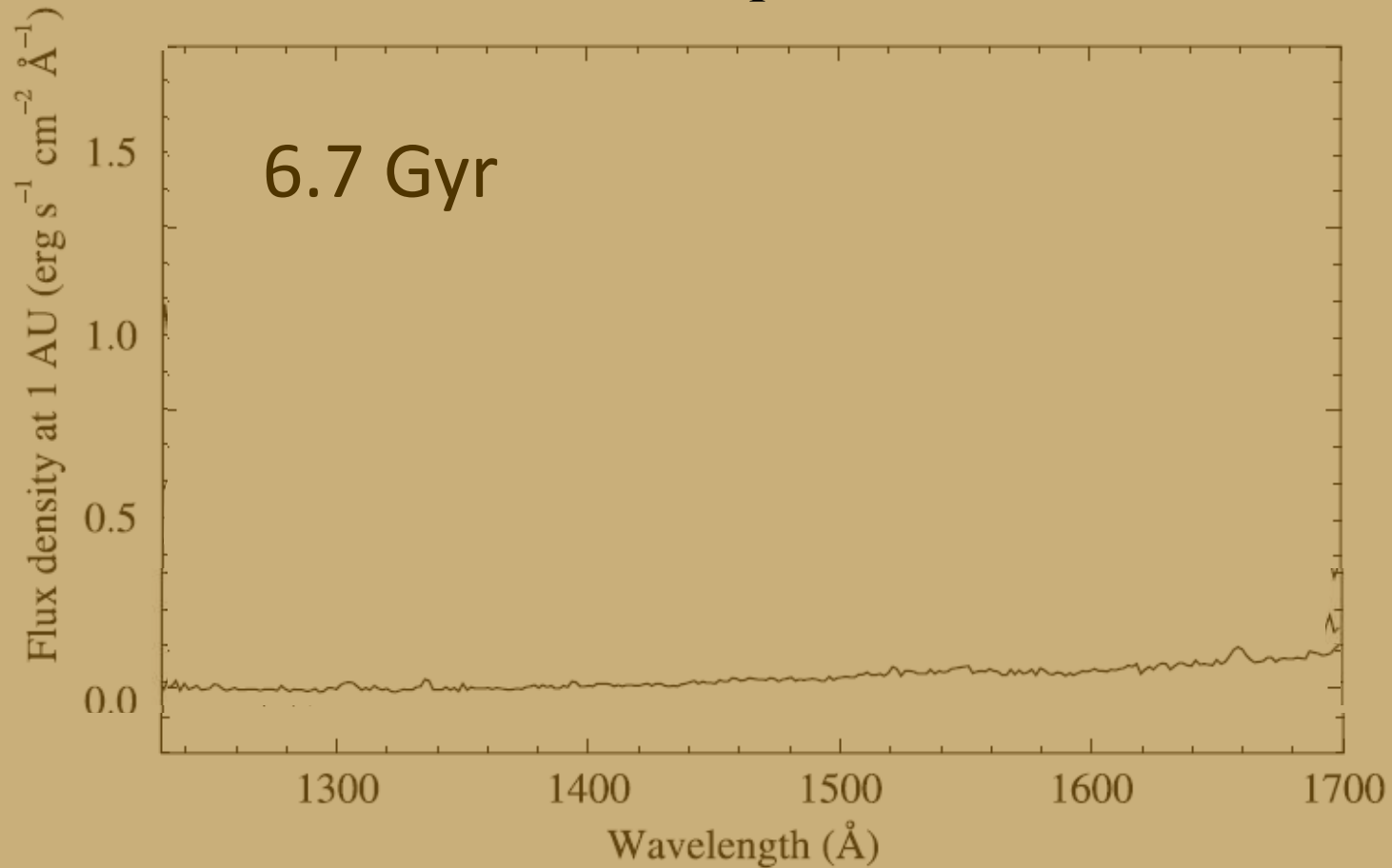
Ultraviolet Chromospheric Emission



Ribas et al (2005)

Behavior of Solar Analogs with Age

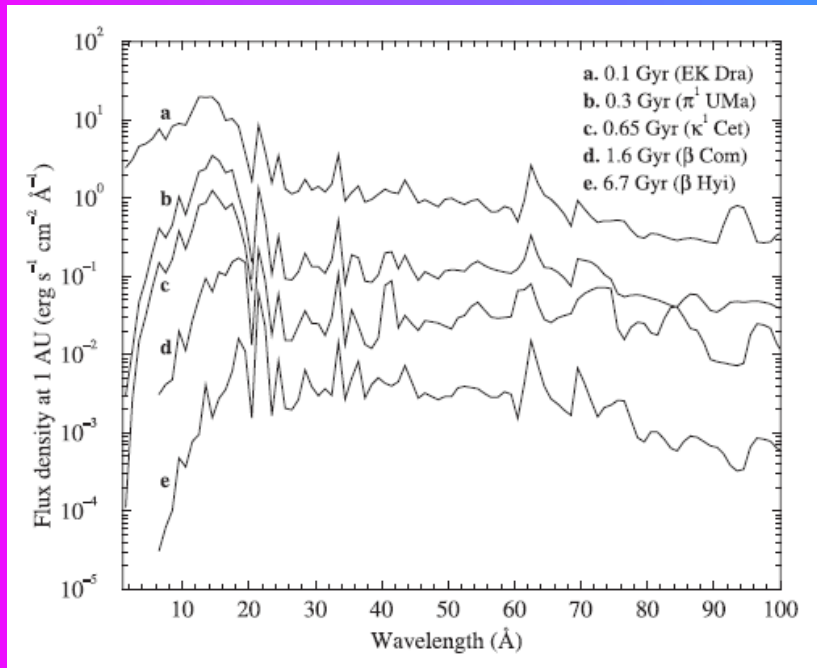
Ultraviolet Chromospheric Emission



Ribas et al (2005)

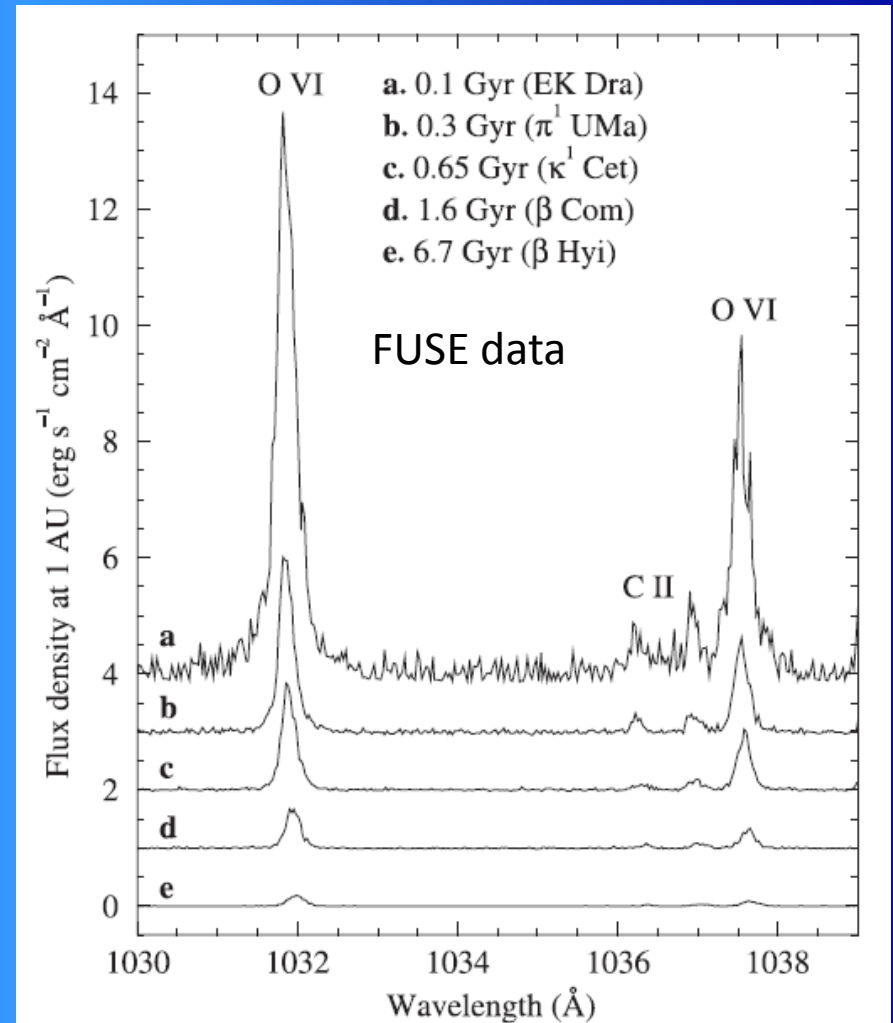
Behavior of Solar Analogs with Age

Shorter
wavelengths



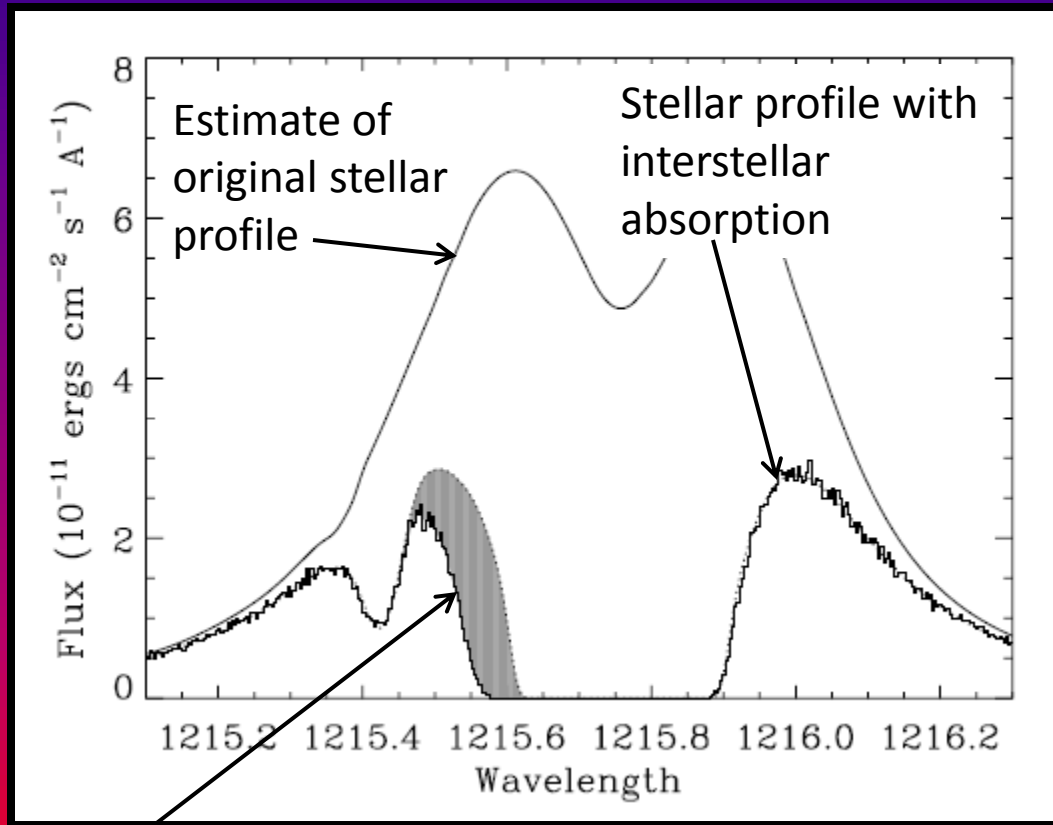
(Based on multi-T
plasma fits to ASCA and
ROSAT observations)

Ribas et al (2005)



Guinan, Ribas & Harper (2003)

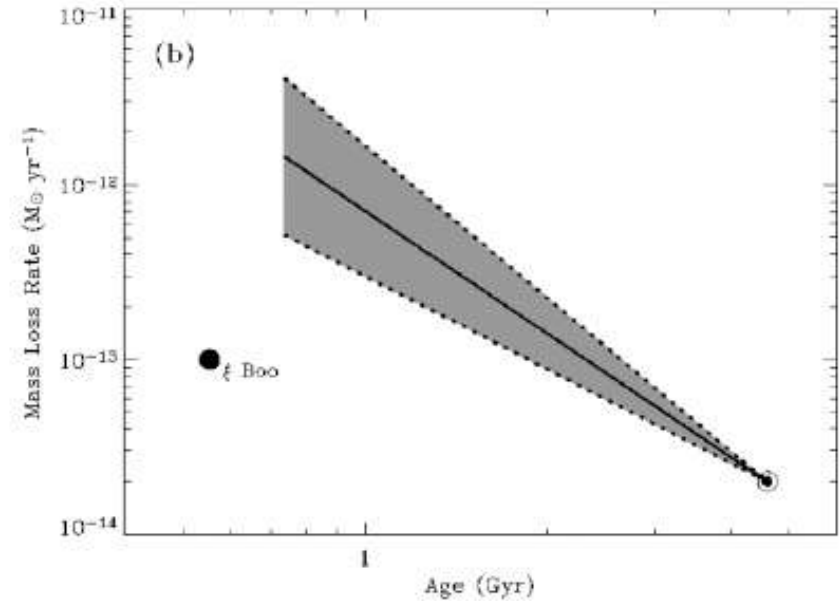
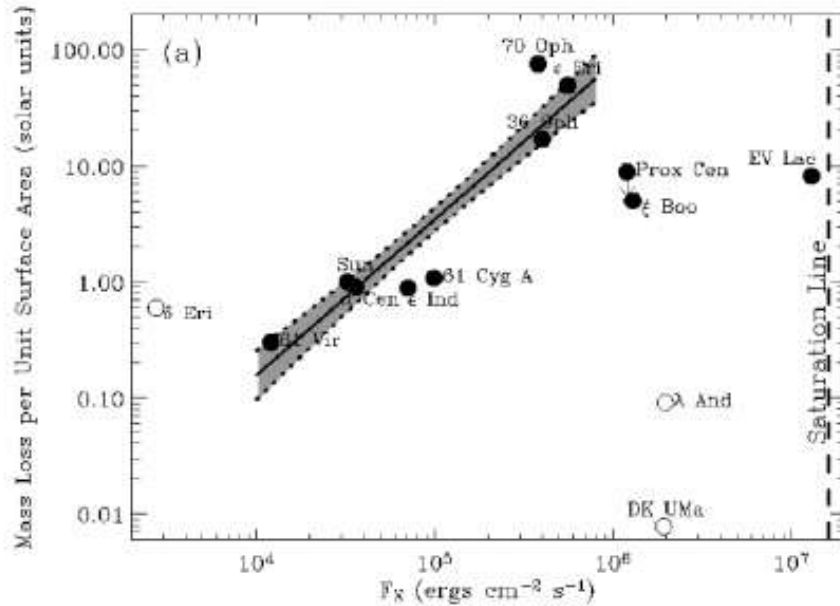
Mass Loss Rates from Astrospheres



Wood et al. (2002)

Astrospheric
absorption

Mass Loss Rates from Astrospheres



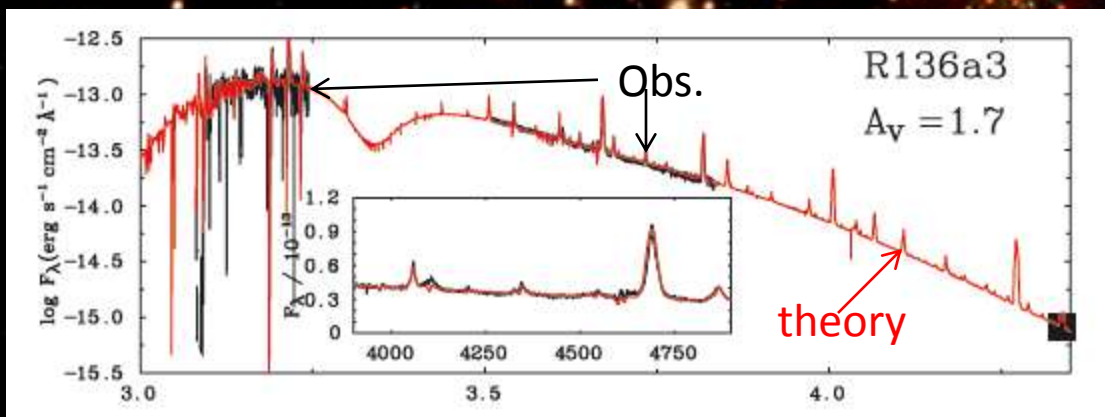
Wood et al. (2005)

Hot Stars

- Much has already been done in the past using IUE
- Much improvement came from better NLTE atmosphere models
- HST particularly good for crowded fields, like this one

Hot Stars

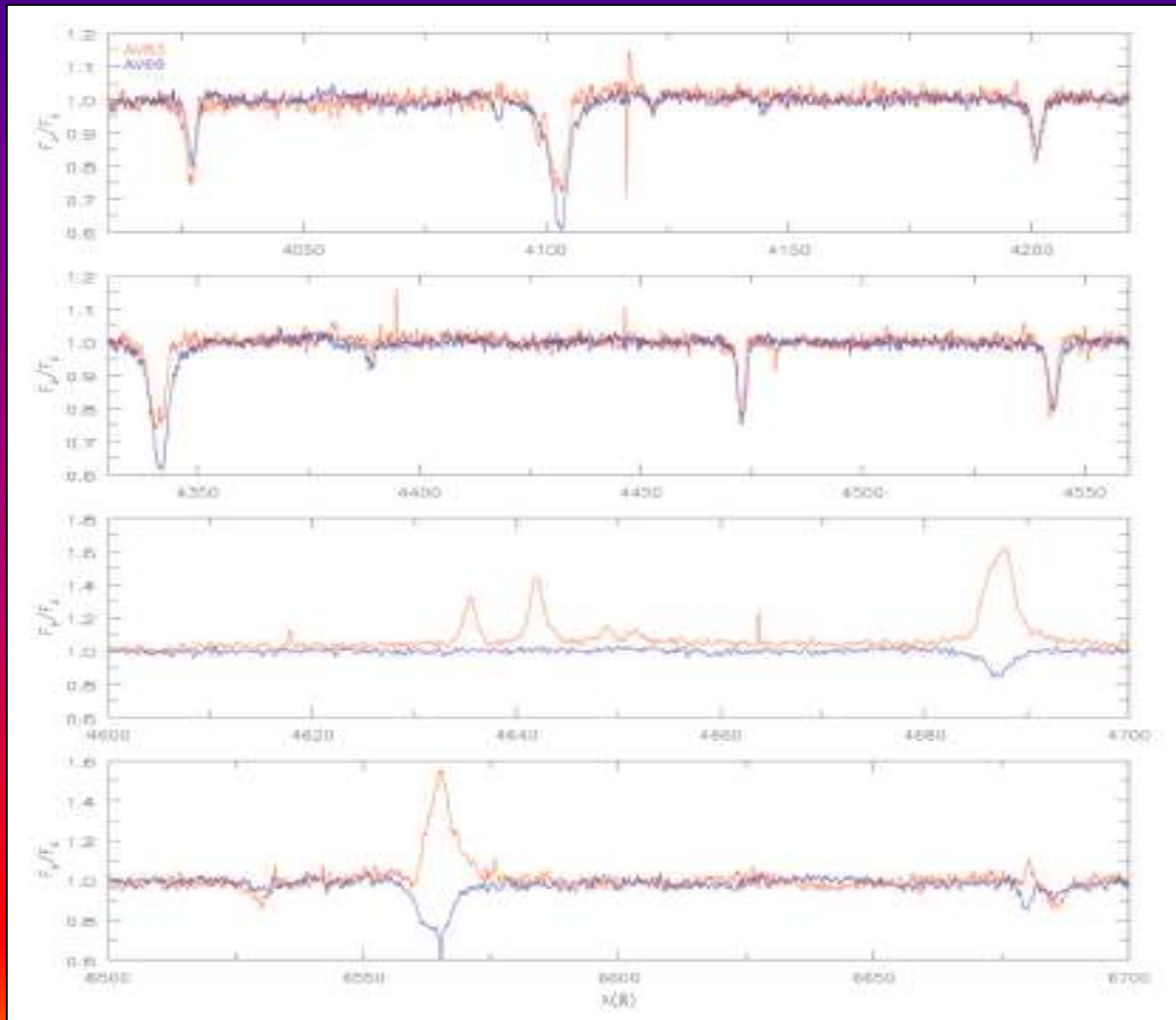
R136 →



Crowther et al.
(2010)

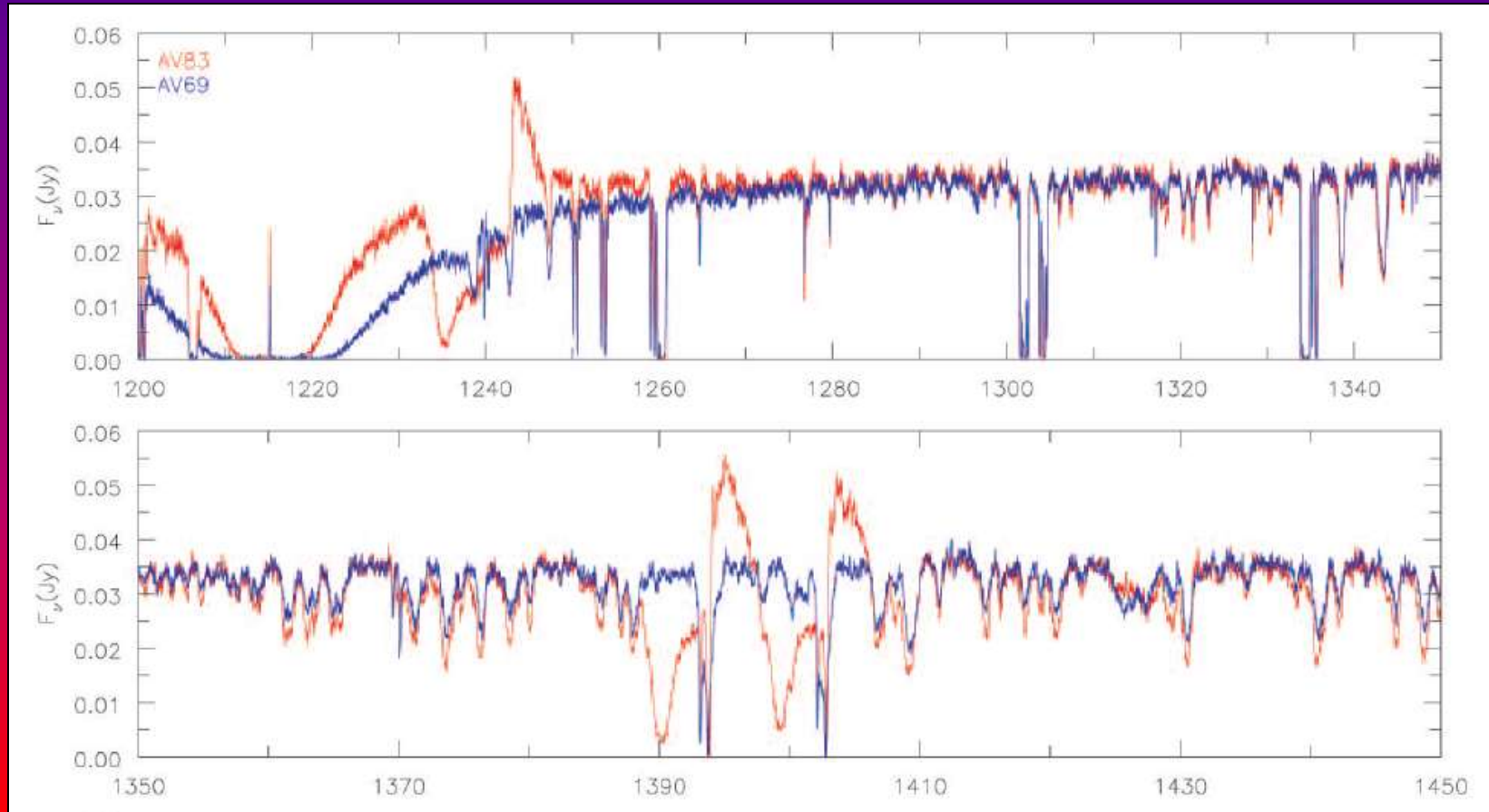
$M_{\text{init}} (M_{\odot})^b$	320^{+100}_{-40}	240^{+45}_{-45}	165^{+30}_{-30}	220^{+55}_{-45}
$M_{\text{current}} (M_{\odot})^b$	265^{+80}_{-35}	195^{+35}_{-35}	135^{+25}_{-20}	175^{+40}_{-35}

Stars: P-Cygni Profiles, Terminal Wind Velocities, Mass Loss Rates



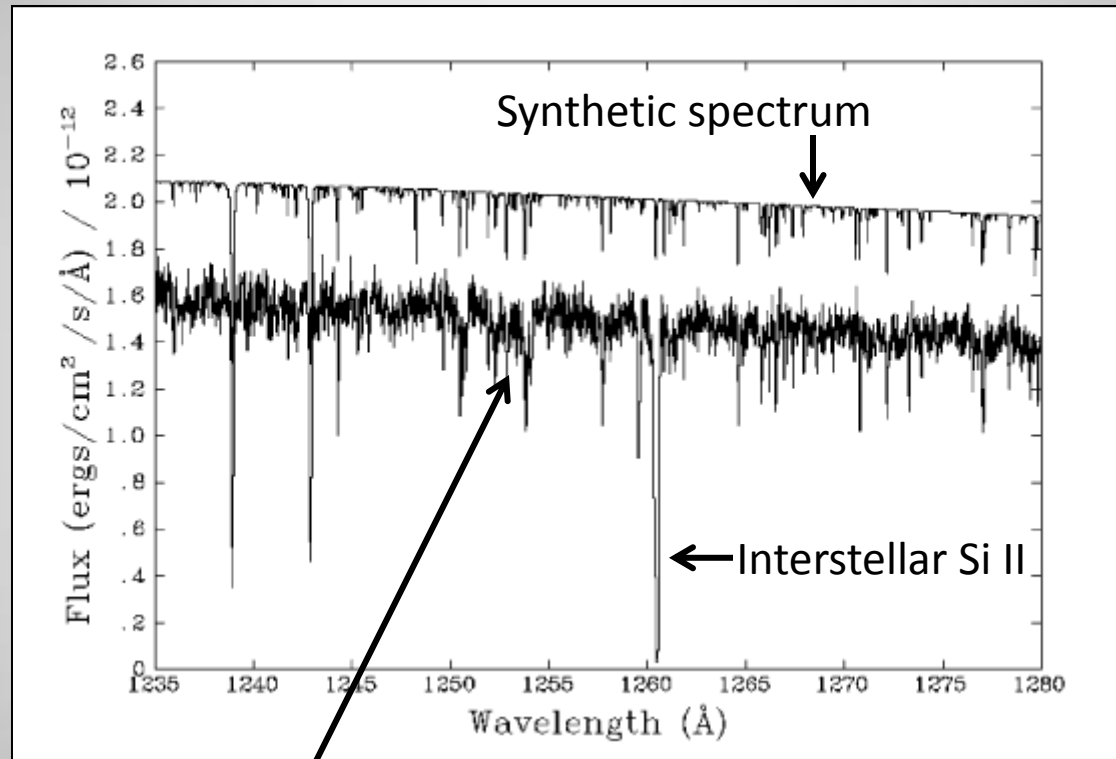
Hillier et al.
(2003)

Stars: P-Cygni Profiles, Terminal Wind Velocities, Mass Loss Rates



Hillier et al. (2003)

Metal Abundances in the Atmospheres of DAZ White Dwarfs



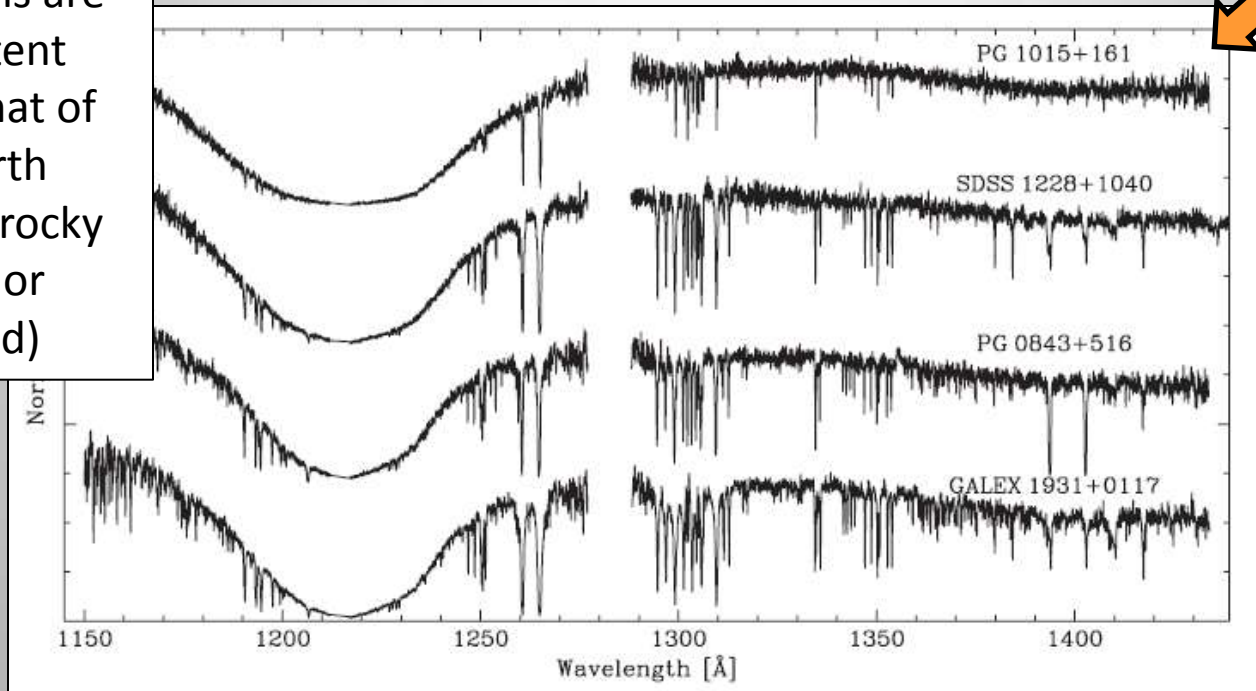
Barstow et al. (2003)

Obs. Spectrum of REJ0558-373
($T_{\text{eff}} = 59,508\text{K}$, $\text{Log } g = 7.70$)

Radiative levitation overcomes
diffusive settling for $T_{\text{eff}} \geq 50,000\text{K}$

Metal Abundances in the Atmospheres of DAZ White Dwarfs

Abundance patterns are consistent with that of the Earth (i.e., a rocky planet or asteroid)

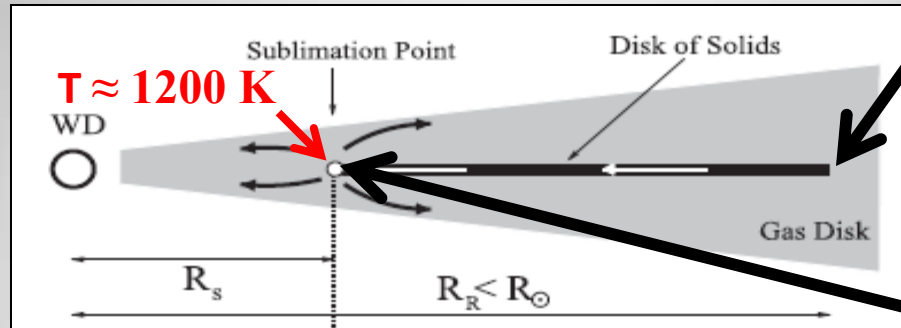


These WD stars have $T_{\text{eff}} \approx 20,000\text{K}$

Diffusive settling times for metals in these atmospheres are of order several days!

Gänsicke et al. (2012)

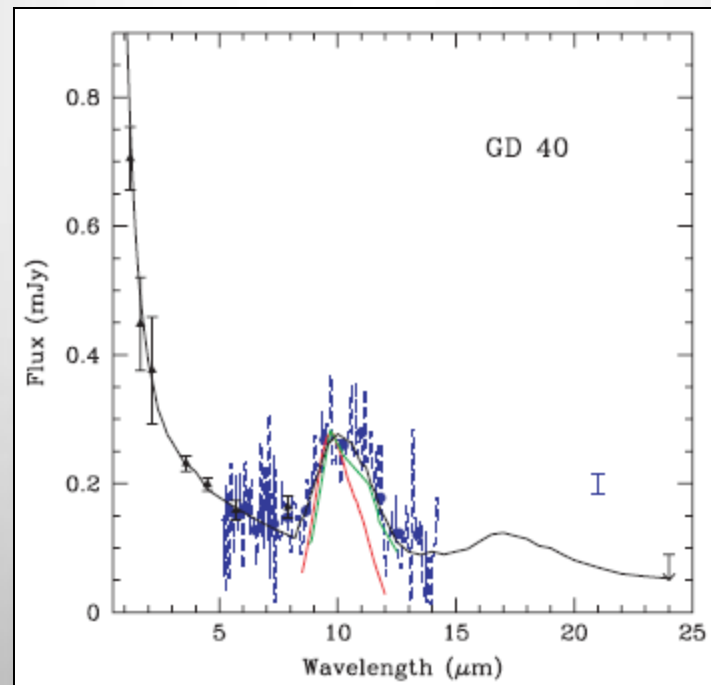
Metal Abundances in the Atmospheres of DAZ White Dwarf



Initial transport: Tidal disruption of asteroids creates particles subject to Poynting-Robertson drag,

followed by sublimation that produces gas. This gas then creates a drag on the particles that assists the inward migration of solids onto the star.

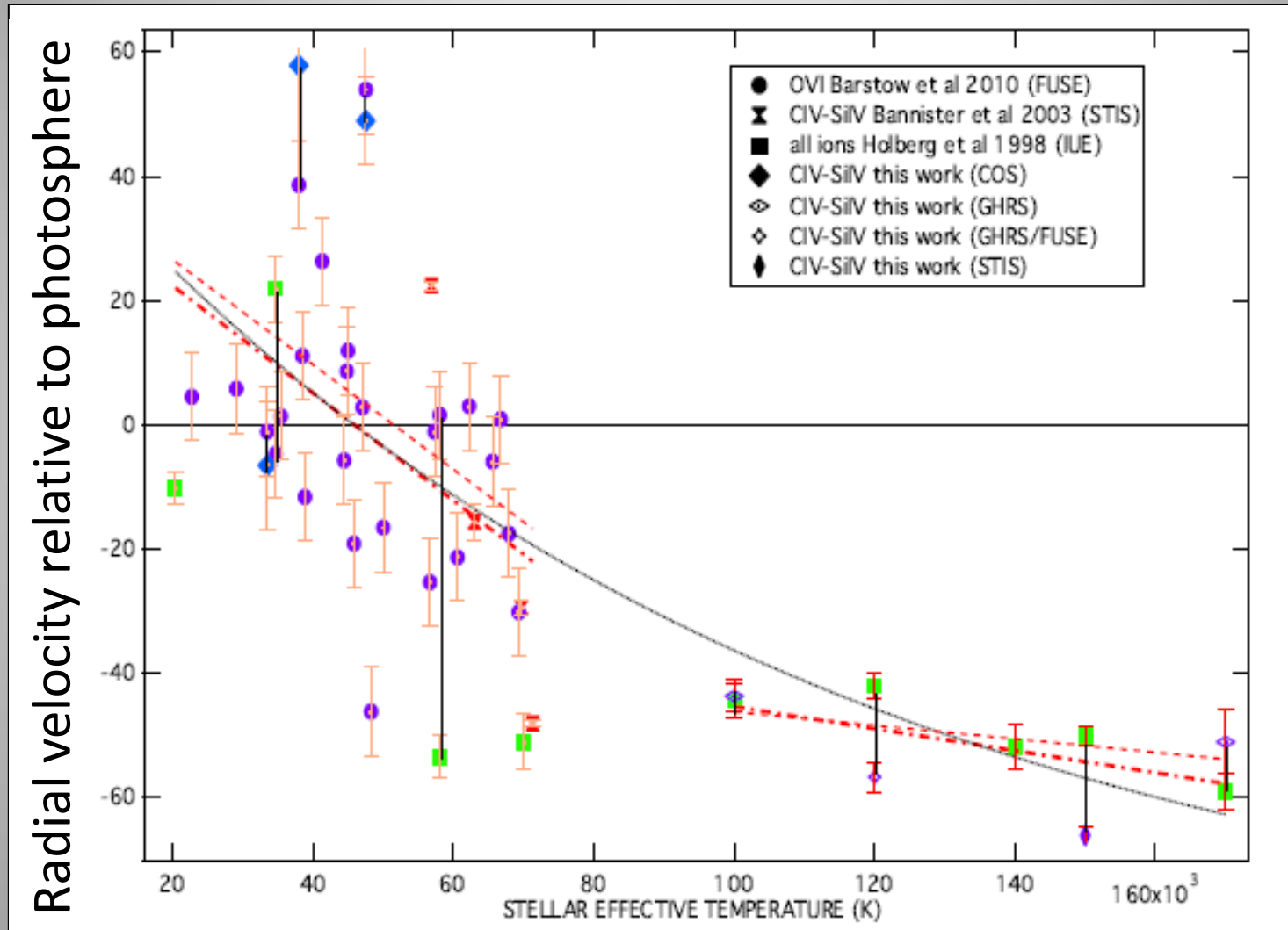
Metzger et al. (2012)



Some of these stars show 10 μm silicate emission from their debris disks

Jura, Farihi & Zuckerman (2009)

Hot Winds from White Dwarfs

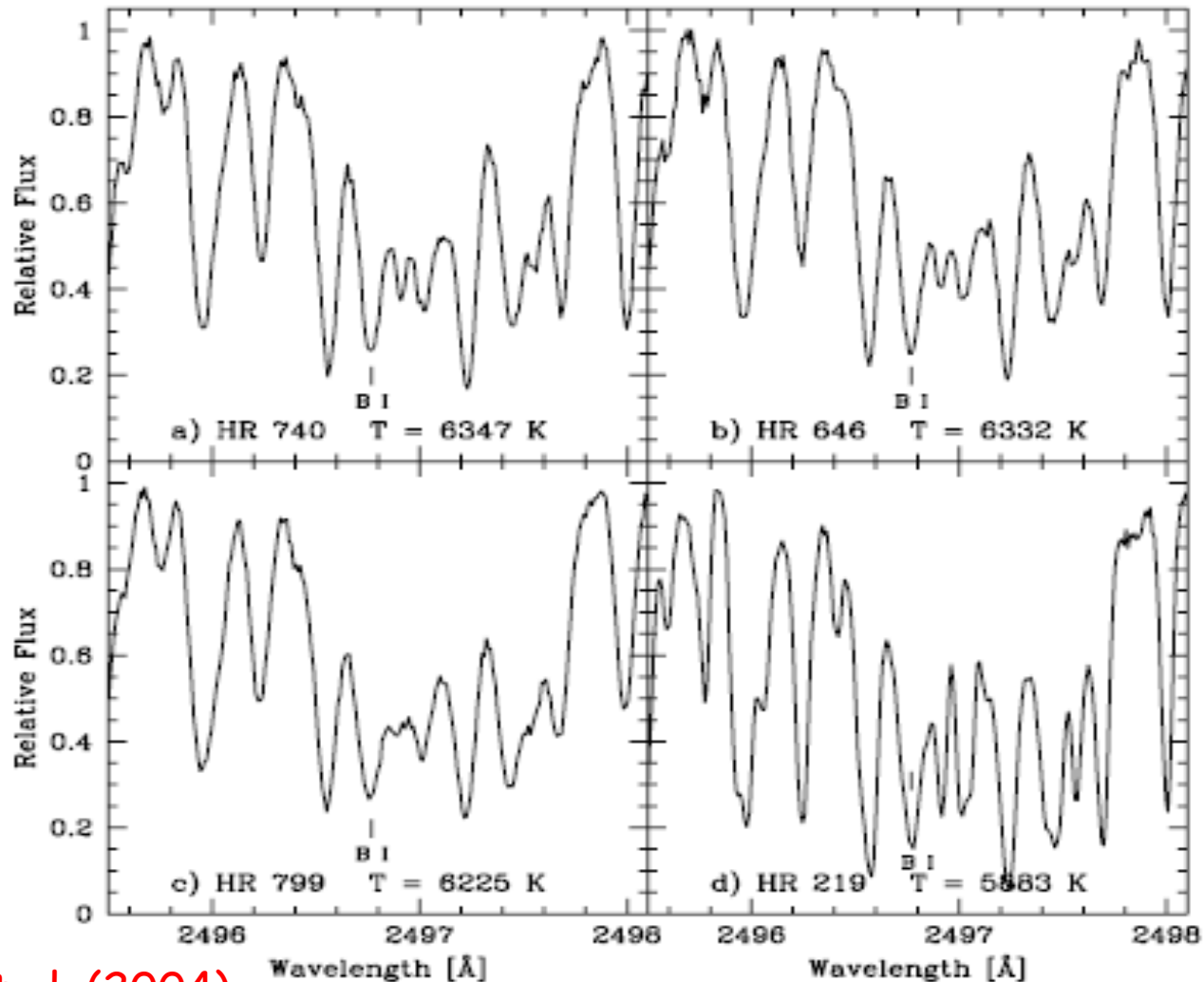


Lallement et al. (2011)

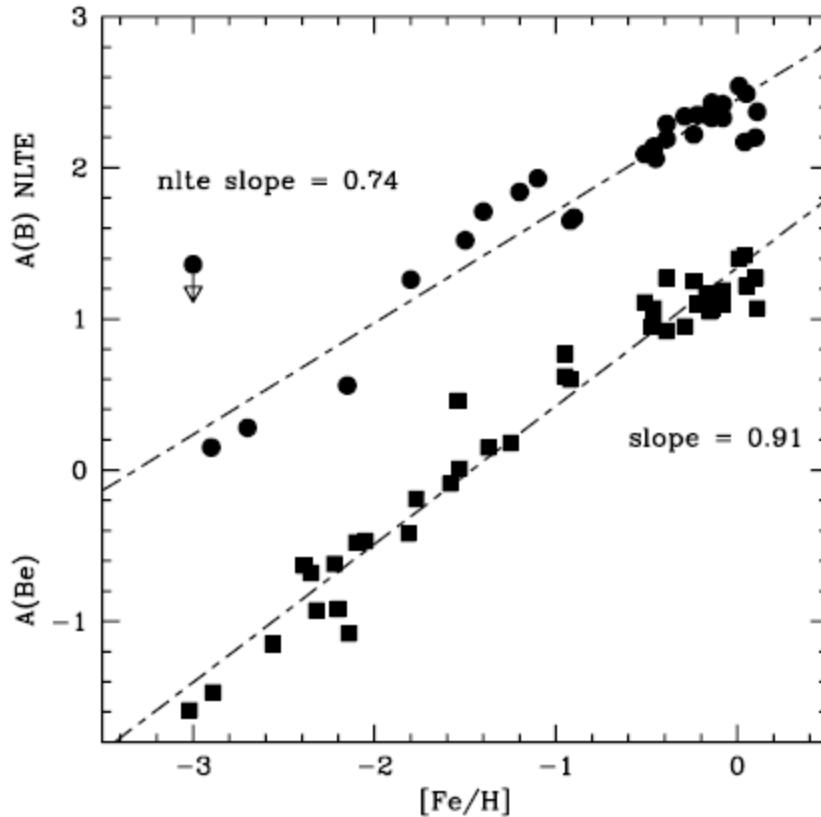
Some Element Abundances in Stars that Require UV Observations

- Some peculiar elements in chemically peculiar stars
- Absorption lines of some neutron-capture elements can be seen in the visible, but many others (e.g., 3rd r-process peak) require UV spectra. Can study correlations, or lack thereof, of various abundances with each other and with [Fe/H]
- Boron abundances and how they scale with [Fe/H] — insights on light-element production by spallation

Boron Abundances vs. [Fe/H]



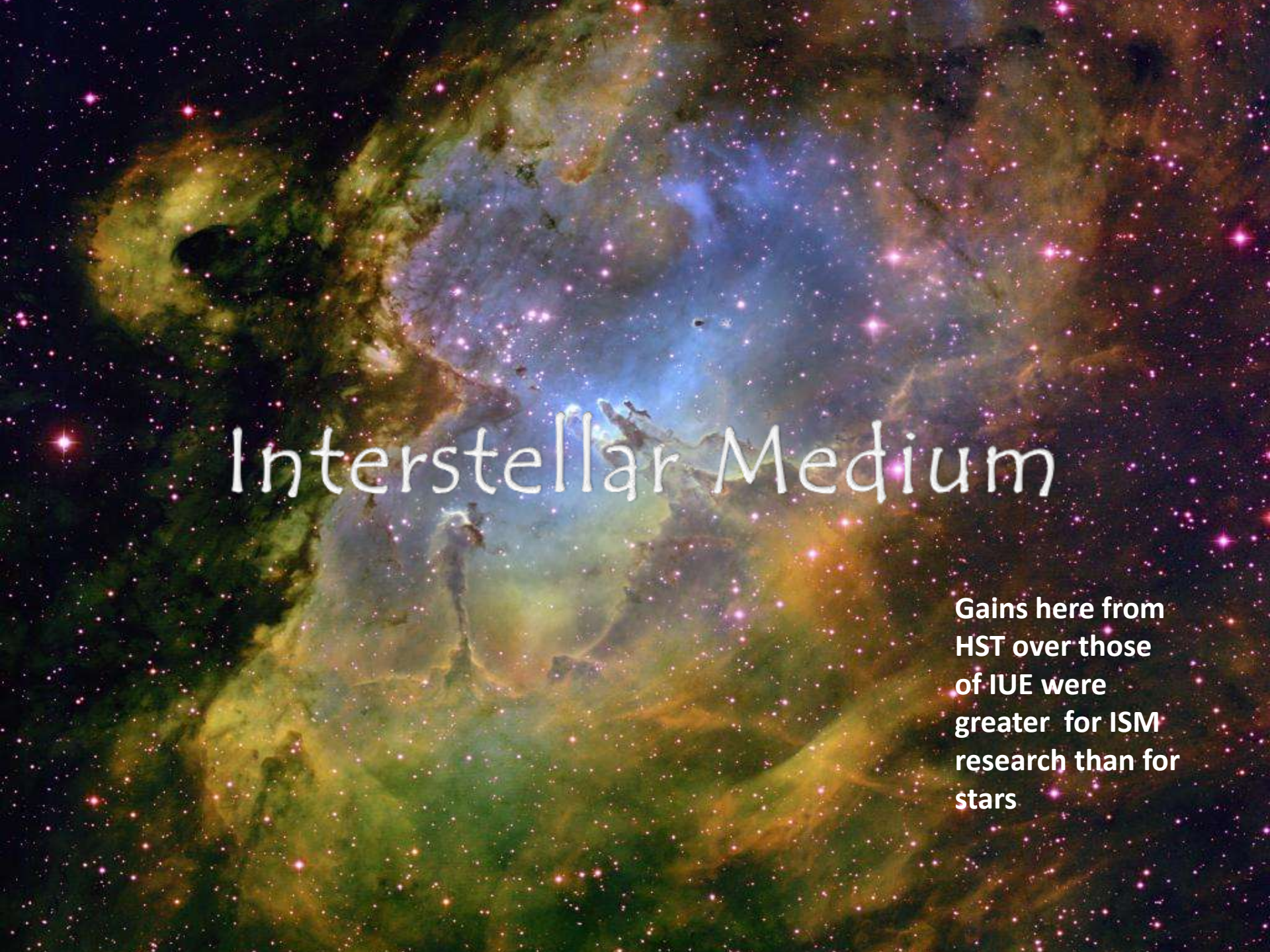
Boron Abundances vs. [Fe/H]



Boesgaard et al. (2004)

**CR protons \rightarrow C,N,O (ISM)
should produce slope = 2,
whereas
C,N,O (CR) \rightarrow protons (ISM)
would produce slope = 1
(Duncan et al. 1997)**

We can guard against being misled by stellar burning of B by monitoring the abundances of Be and Li, which will be destroyed at lower temperatures.



Interstellar Medium

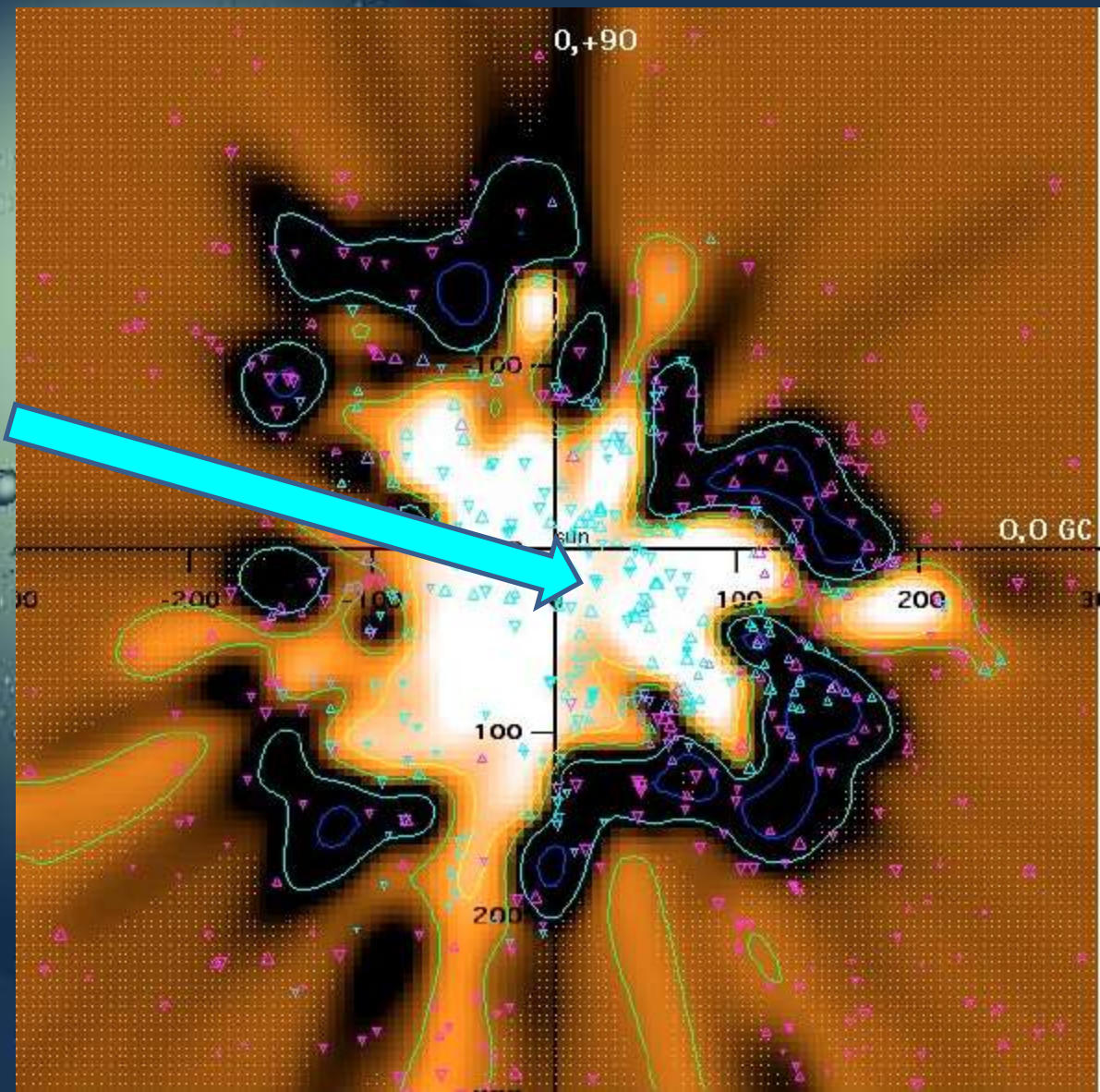
Gains here from HST over those of IUE were greater for ISM research than for stars



THE LOCAL BUBBLE

HST spectra of cool stars inside the Local Bubble indicate that there are warm, low density clouds embedded within the void shown in white.

Redfield & Linsky, (2008)



Temperatures and Turbulent Velocity Dispersions

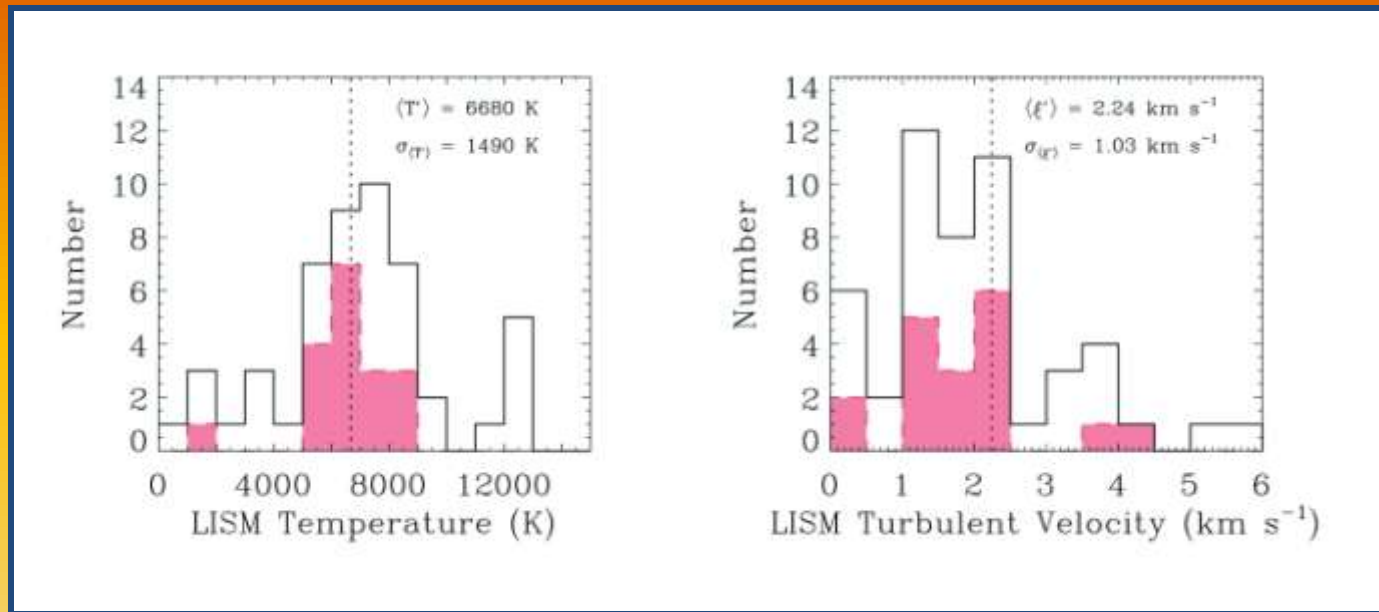
- Basic Formula – Doppler velocity dispersion adds in quadrature with turbulent velocities:

$$b^2 = \frac{2kT}{m} + \xi^2 = 0.016629 \frac{T}{A} + \xi^2$$

This term
varies with
mass

This one
doesn't

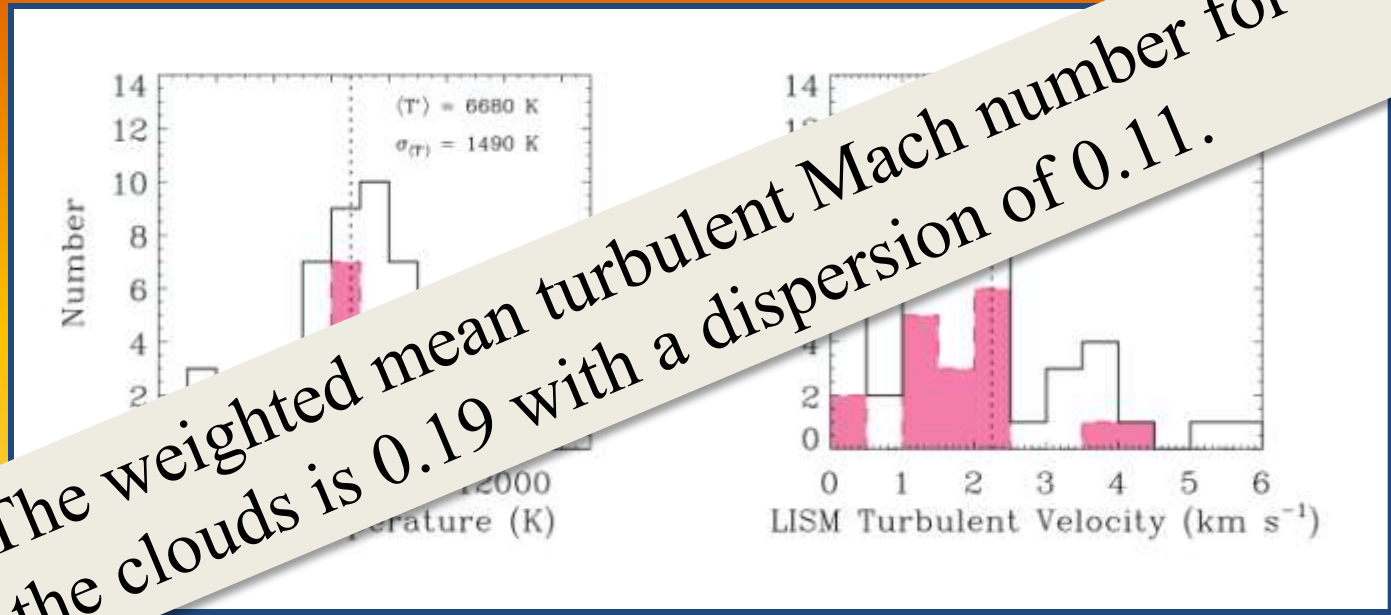
Temperatures and Turbulent Velocity Dispersions



Redfield & Linsky (2004)

Red portions indicate more precise measurements, i.e., those with errors less than the overall dispersion

Temperatures and Turbulent Velocity Dispersions



The weighted mean turbulent Mach number for the clouds is 0.19 with a dispersion of 0.11.

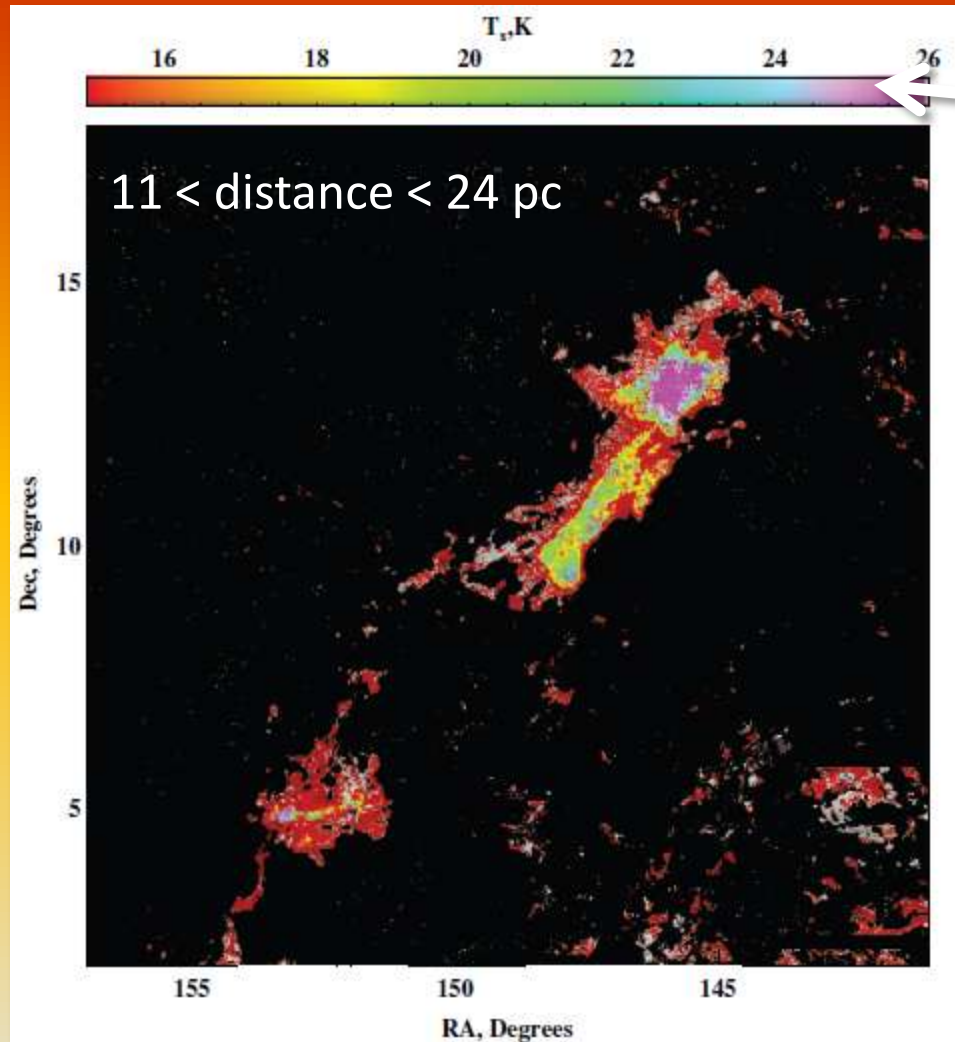
Redfield & Linsky (2004)

Red portions indicate more precise measurements, i.e., those with errors less than the overall dispersion

Temperatures and Turbulent Velocity Dispersions

However, there's an
interesting exception to
this picture

The Local Leo Cold Cloud



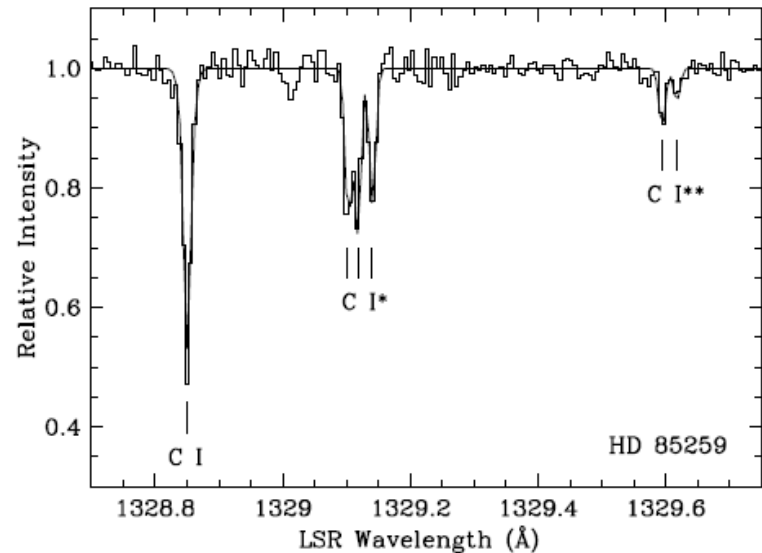
Very cold!

Peek et al. (2011)

The Local Leo Cold Cloud

Findings from high resolution
STIS spectroscopy of stars behind
the cloud

- C I fine-structure excitation and temperatures indicate that this cloud has a thermal pressure $p/k \approx 60,000 \text{ cm}^{-3}\text{K}$, which is far above normal.
- This condition could arise from the compression that occurs when two warm clouds collide.

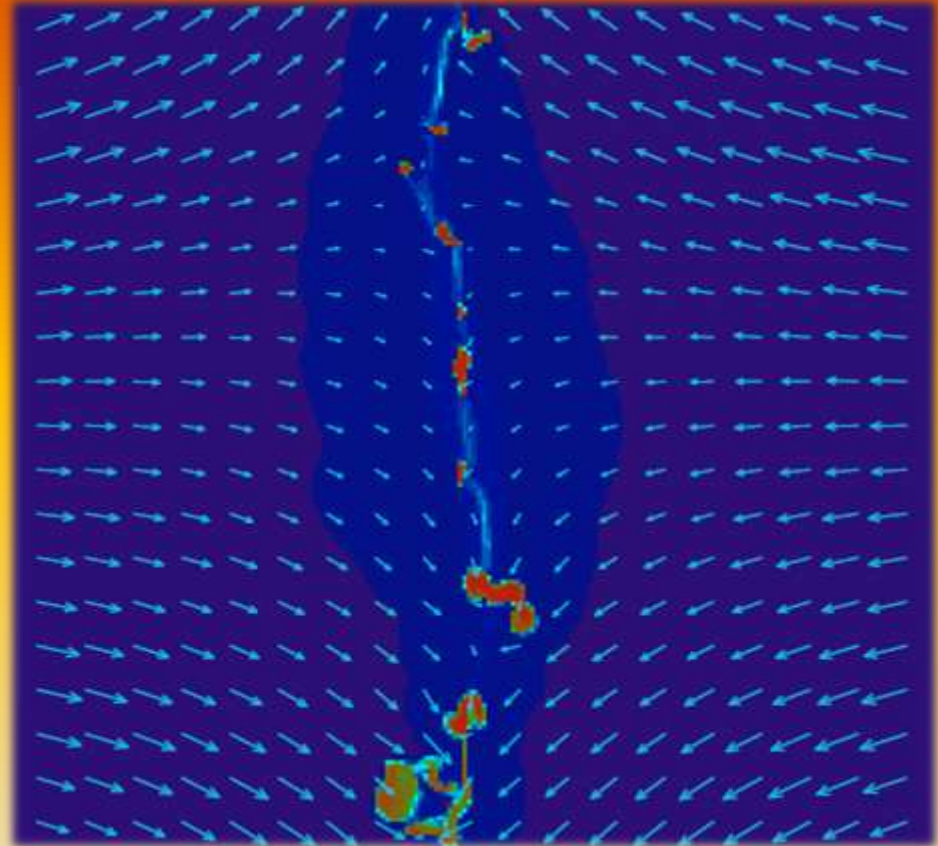


Meyer et al. (2012)

The Local Leo Cold Cloud

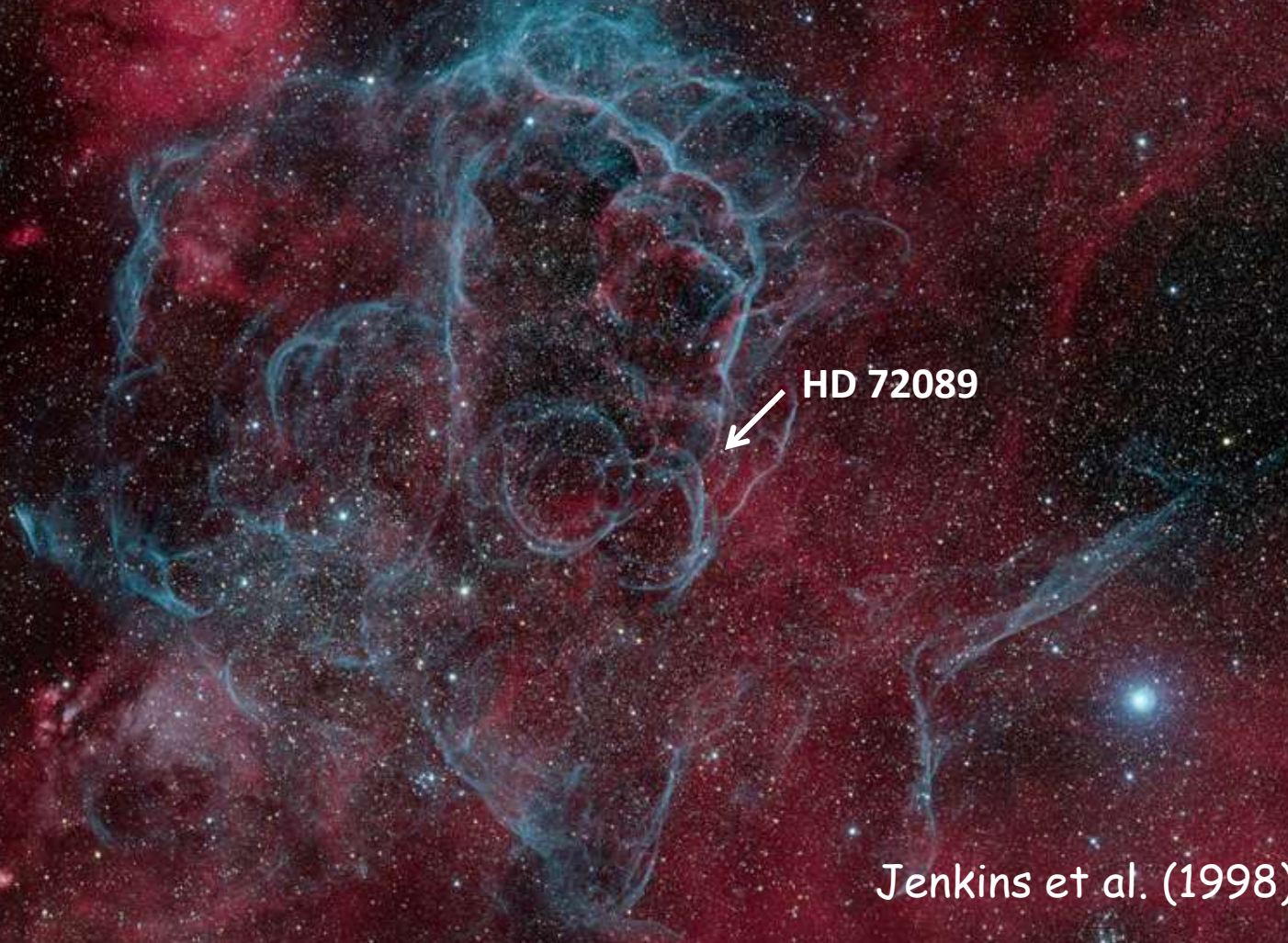
Findings from high resolution
STIS spectroscopy of stars behind
the cloud

- C I fine-structure excitation and temperatures indicate that this cloud has a thermal pressure $p/k \approx 60,000 \text{ cm}^{-3}\text{K}$, which is far above normal.
- This condition could arise from the compression that occurs when two warm clouds collide.



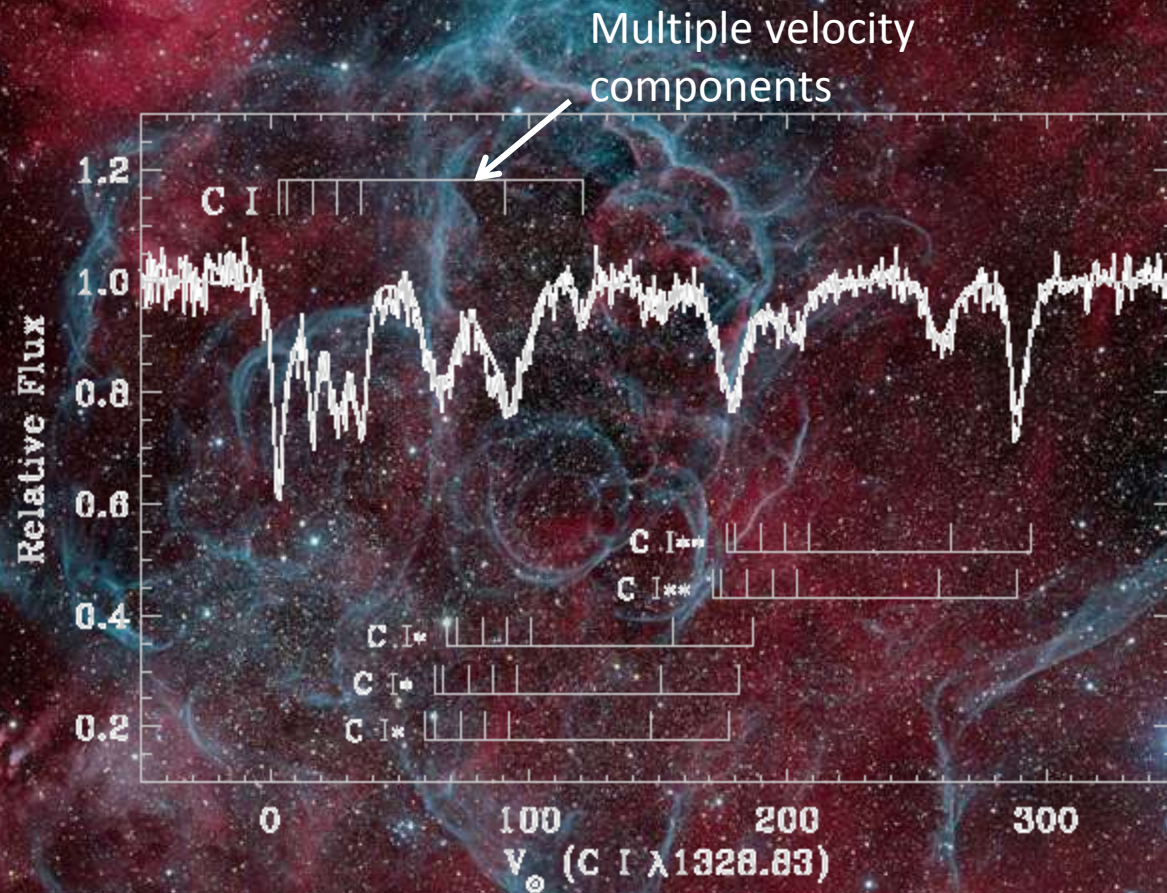
Audit & Hennebelle (2005)

Another Instance of High Thermal Pressure:
Absorption by the C I Multiplet at 1329 Å for the
Star HD 72089 Behind the Vela SNR



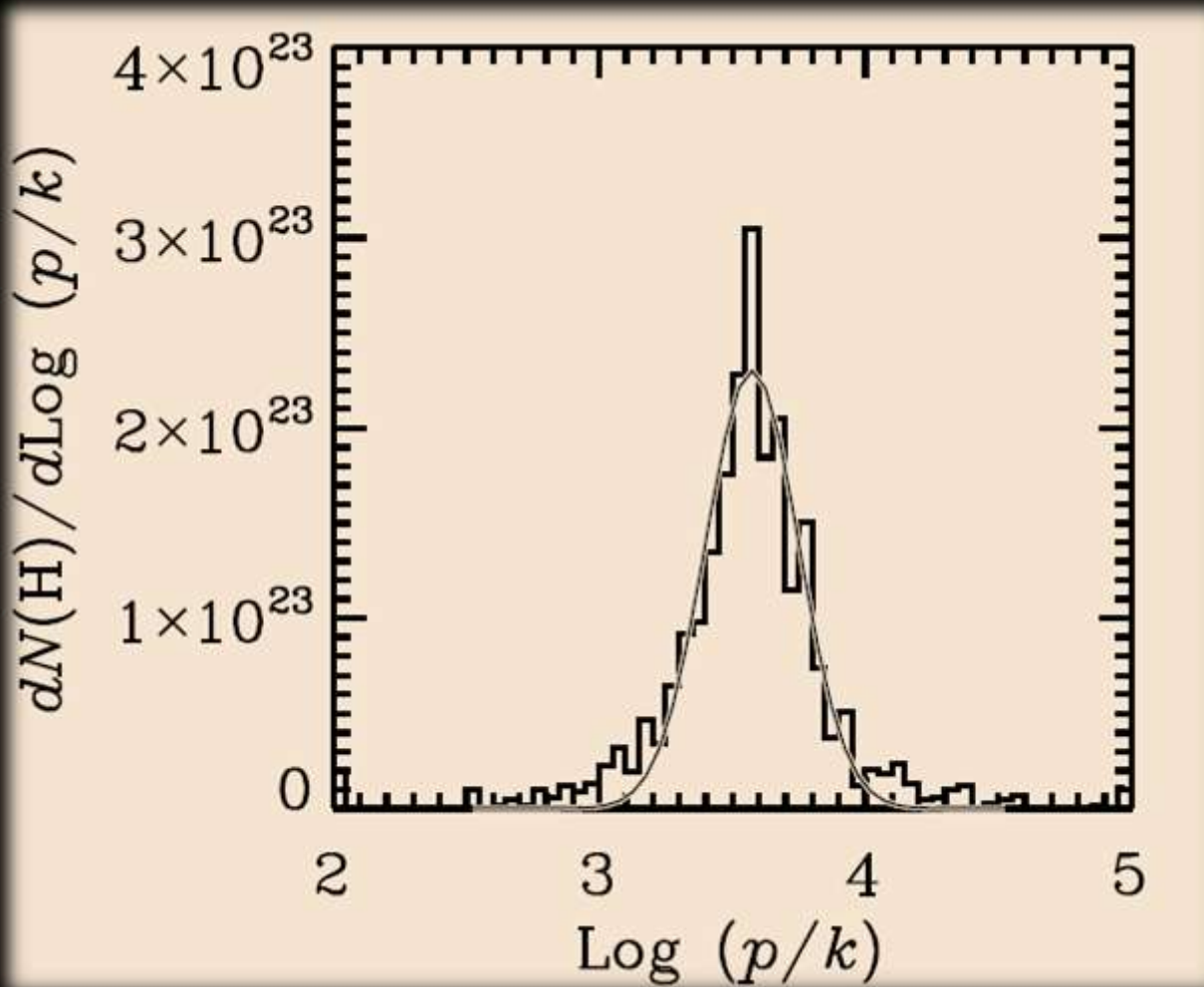
Jenkins et al. (1998)

Another Instance of High Thermal Pressure: Absorption by the C I Multiplet at 1329 Å for the Star HD 72089 Behind the Vela SNR



Jenkins et al. (1998)

Thermal Pressure Distribution for Typical Translucent Interstellar Clouds



Jenkins & Tripp (2011)

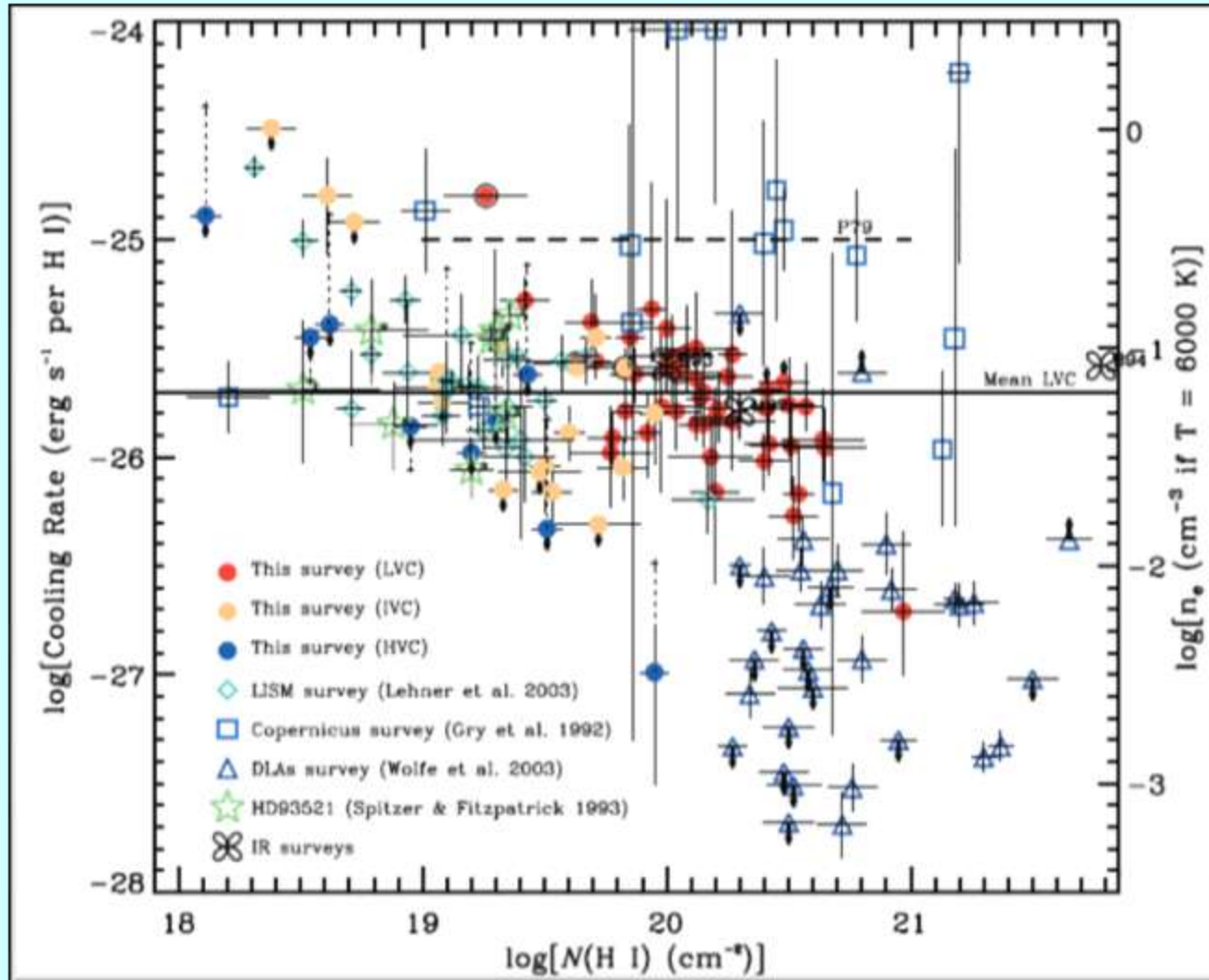
Cooling of the ISM

Principal coolant is C⁺ in an excited fine-structure level which radiates at 158μm

$$\begin{aligned}\Lambda(\text{C}^+) &= h\nu_{21}A_{21}n(\text{C}^{++}) \\ &= 2.89 \times 10^{-20}n(\text{C}^{++}) \text{ ergs s}^{-1} \text{ cm}^{-3}\end{aligned}$$

$$l_c \equiv \frac{\int \Lambda(\text{C}^+) ds}{\int n(\text{H}^0) ds} = 2.89 \times 10^{-20} \frac{N(\text{C}^{++})}{N(\text{H}^0)} \text{ ergs s}^{-1} (\text{H atom})^{-1}$$

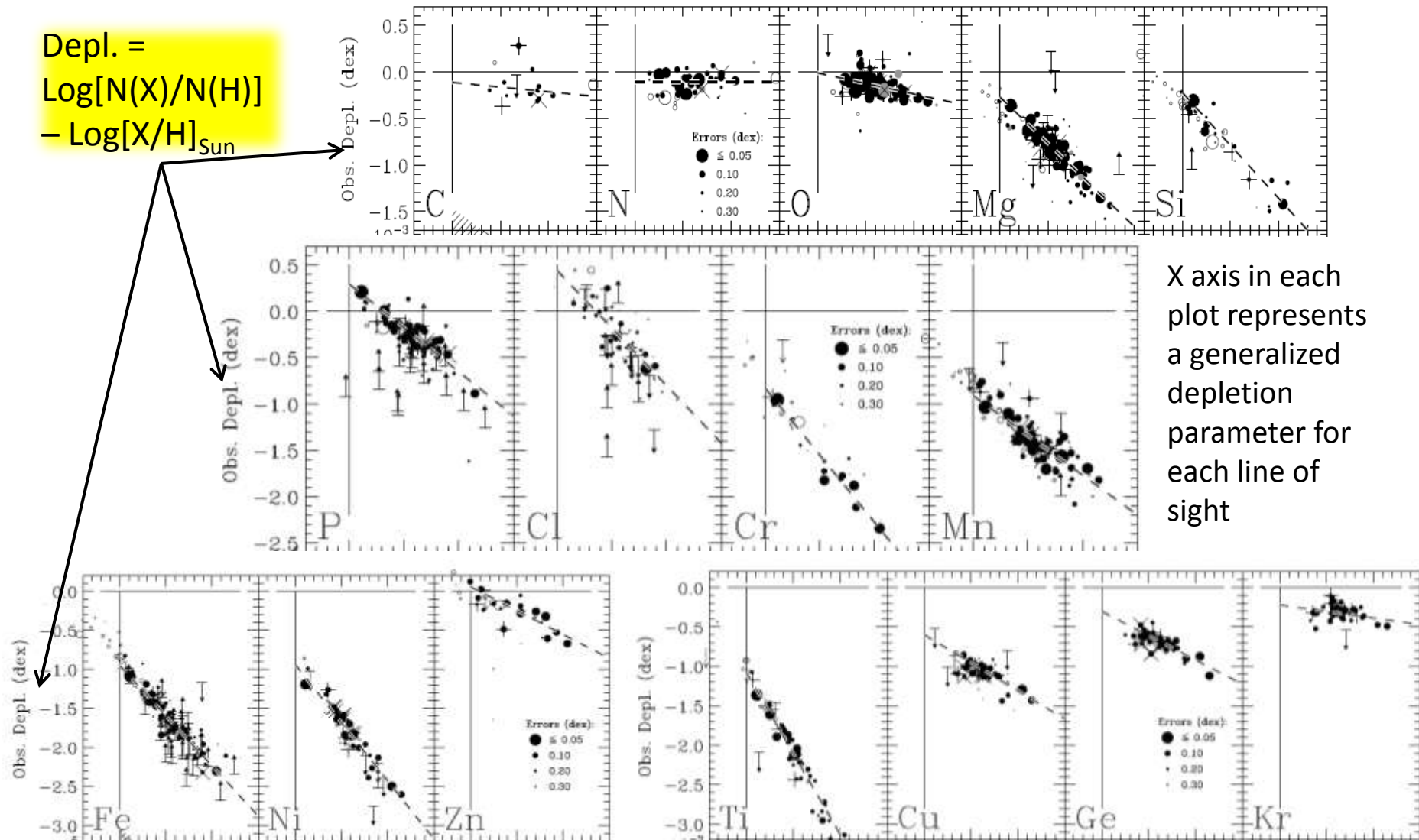
Cooling of the ISM



Lehner, Wakker & Savage (2004)

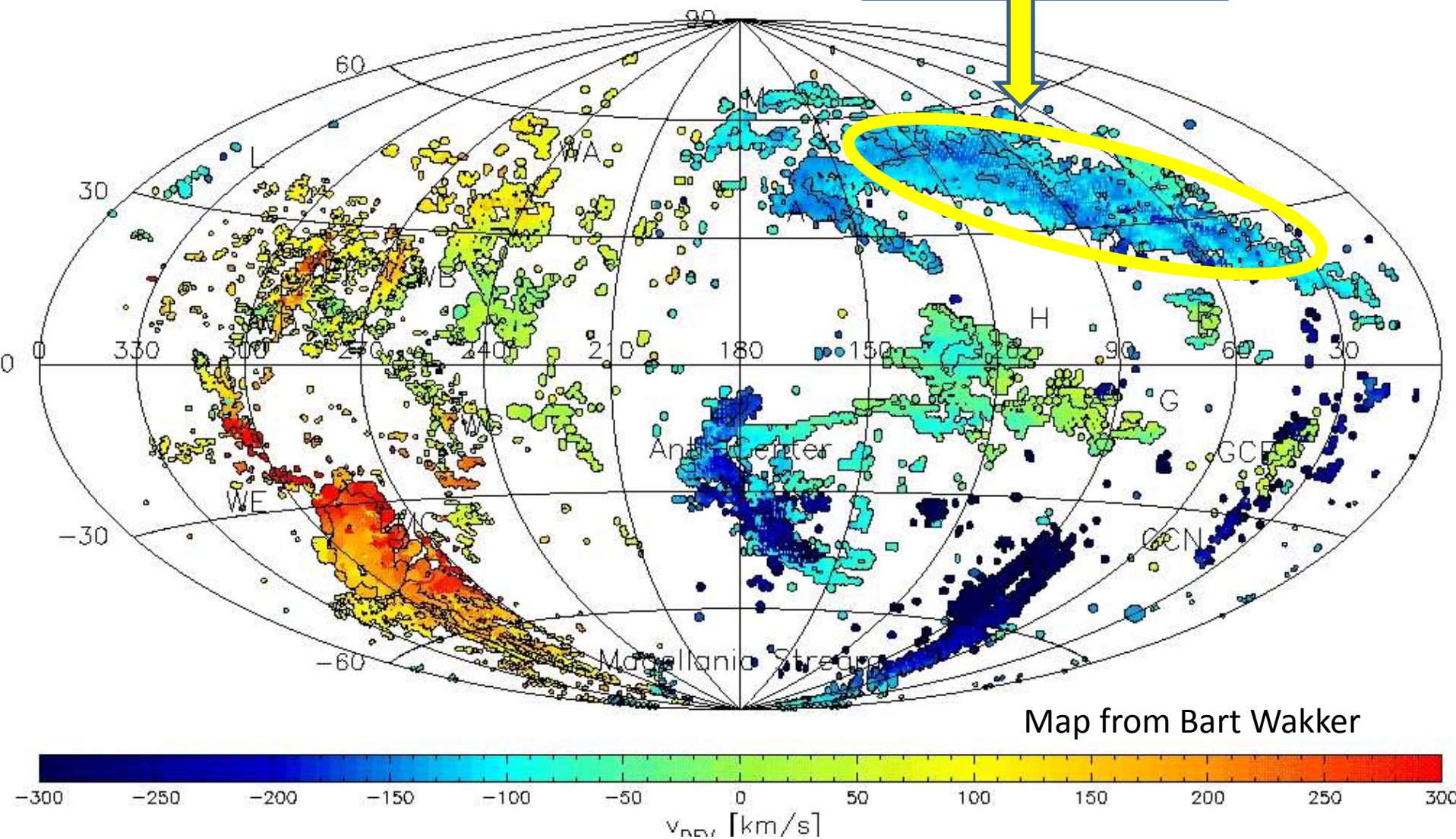
Depletions of Atoms in the Gas Phase

Depl. = $\text{Log}[N(X)/N(H)] - \text{Log}[X/H]_{\text{Sun}}$

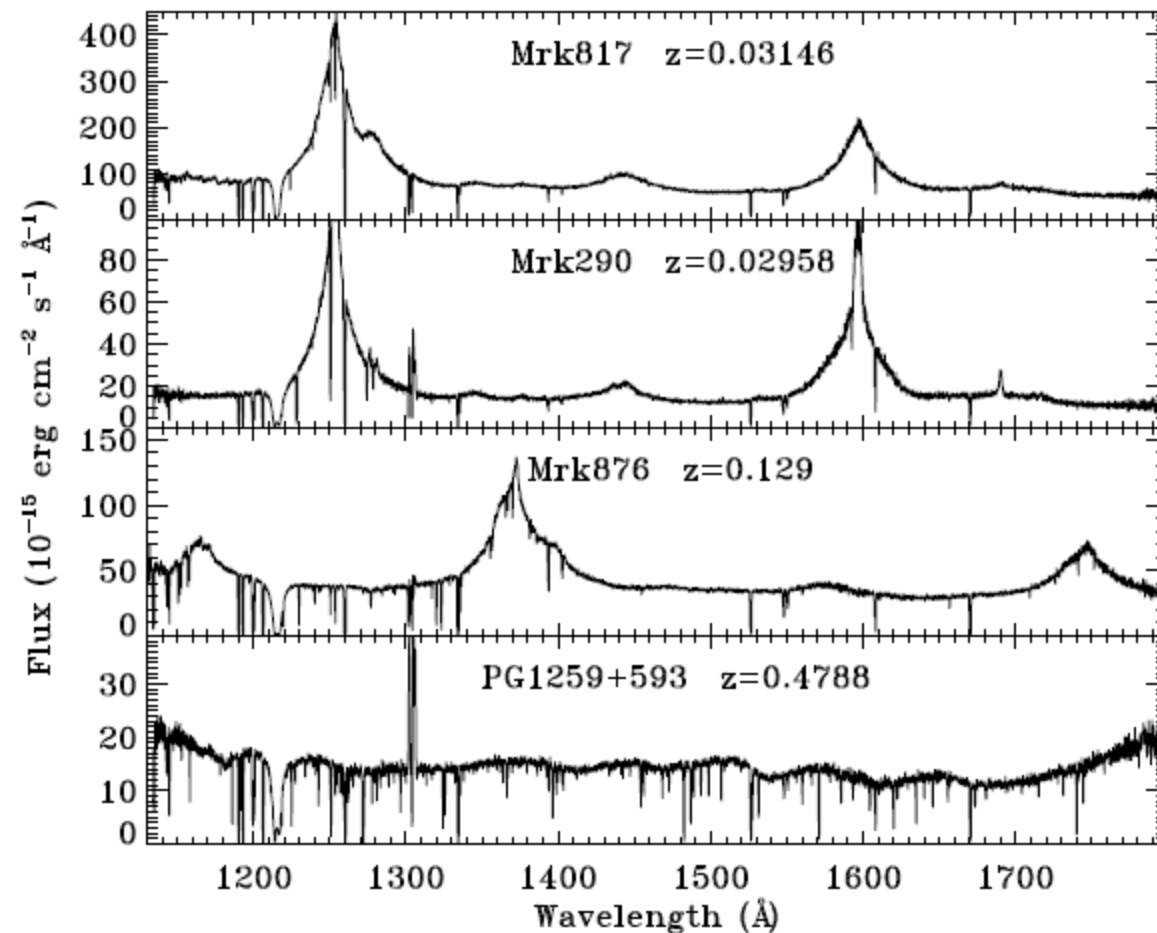


X axis in each plot represents a generalized depletion parameter for each line of sight

High Velocity Gas Clouds at High Galactic Latitudes: **Complex C**



High Velocity Gas Clouds at High Galactic Latitudes: Complex C

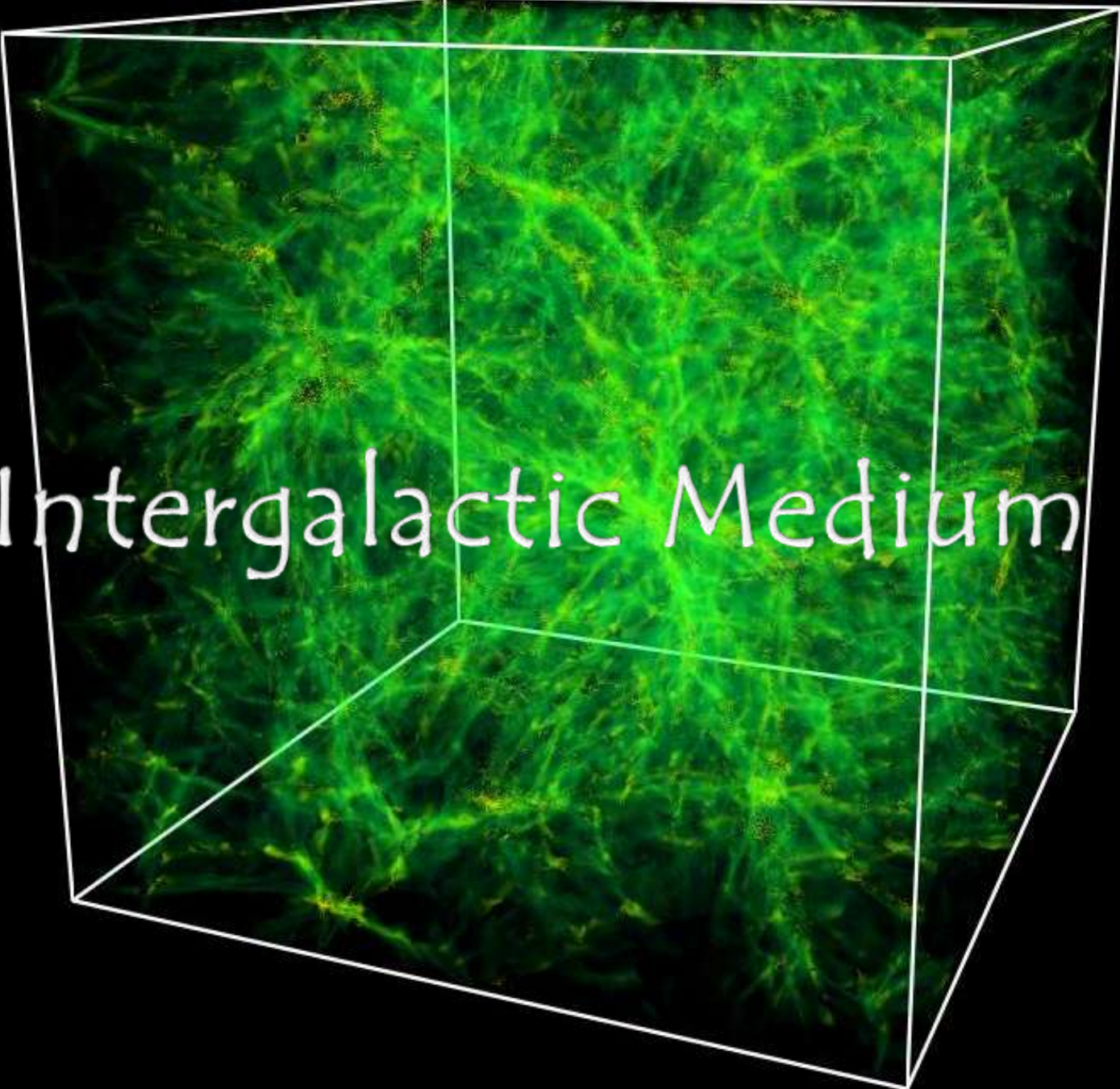


Conclusions from this and earlier investigations:

Metallicity of the gas is about 10-30% of the solar value.

Ratios of N V, C IV and O VI (measured by FUSE) are consistent with non-equilibrium ion ratios in cooling gas and with conductive heating.

Shull et al. (2011)

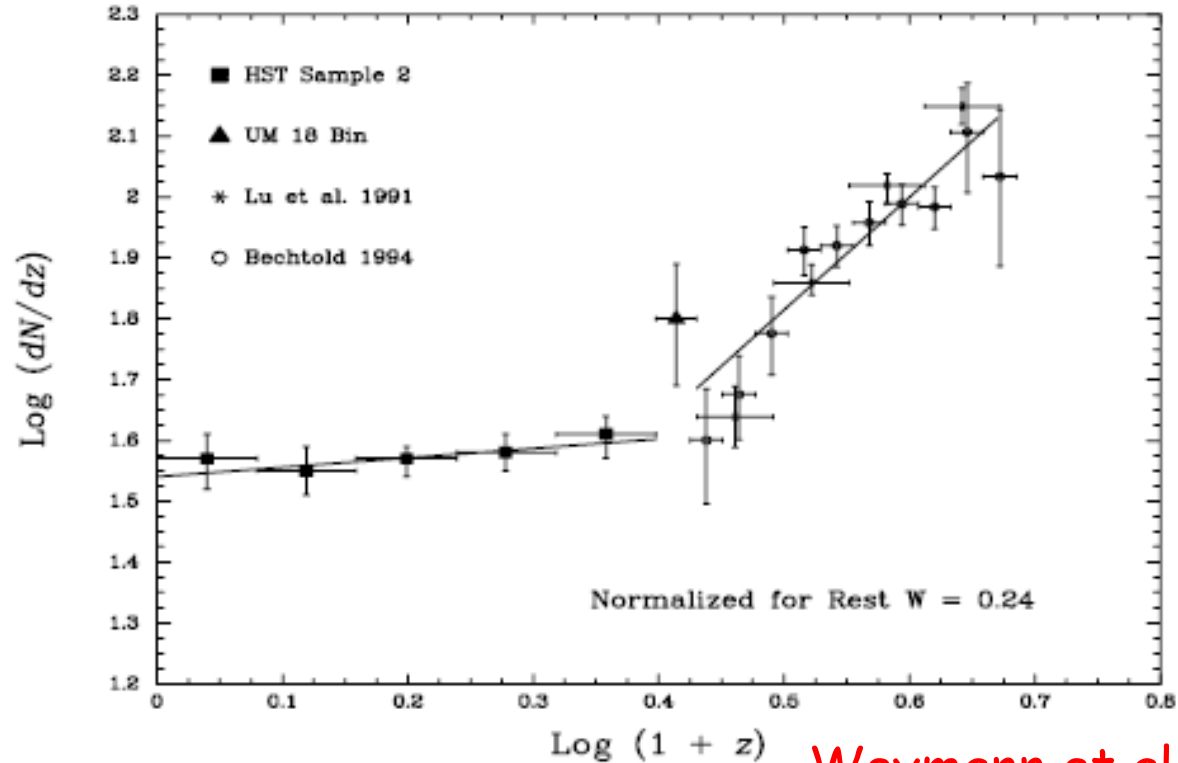
A 3D wireframe cube is shown, containing a complex, green, filamentary structure representing the intergalactic medium. The structure consists of numerous interconnected filaments and clusters, creating a dense, web-like appearance. The text "Intergalactic Medium" is overlaid in white on the central part of the cube.

Intergalactic Medium

Evolution of the Lyman- α Forest with Redshift

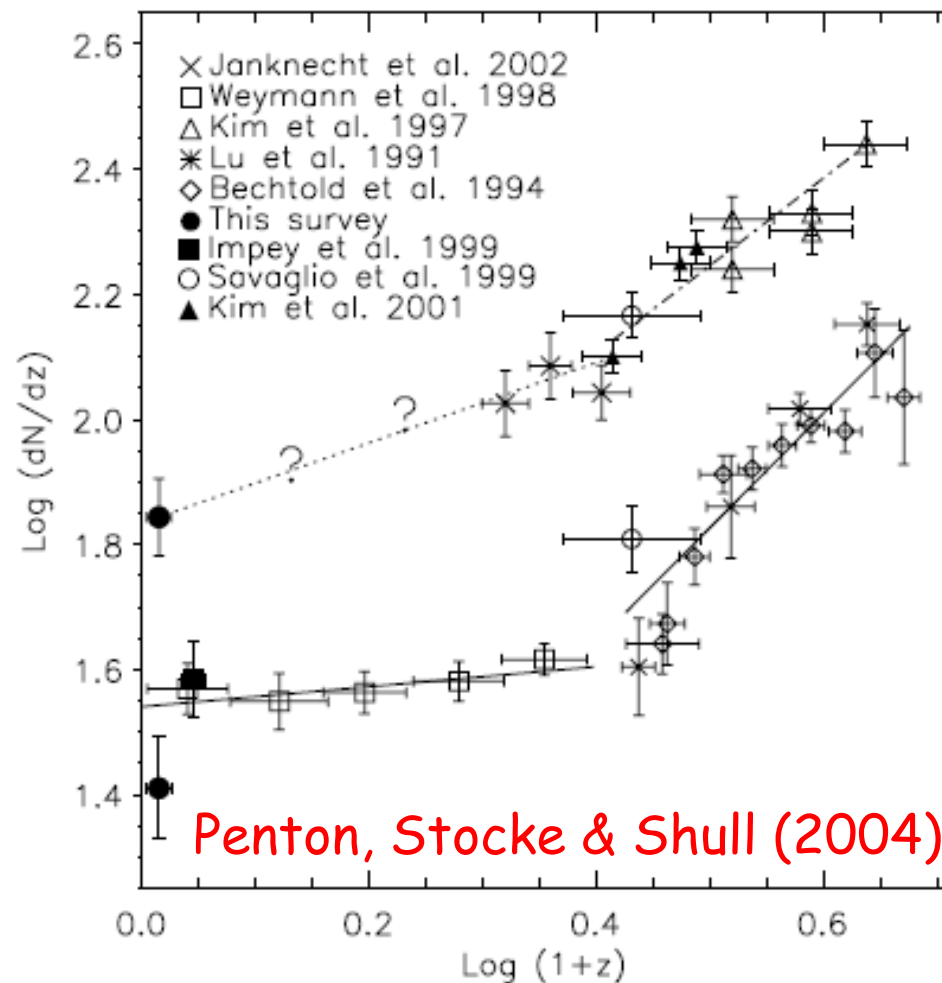
If we assume that the distribution of Ly α lines as a function of redshift and EW has the form and parameters derived at high redshift (as in Murdoch et al. 1986), then over the redshift range of 0.016–0.151 one predicts 0.8–2.1 lines with rest EW greater than 50 mÅ, whereas we observed 10. One predicts 0.9–2.3 lines with rest EW greater than 25 mÅ, whereas we have possibly observed 14. *Morris et al. (1991)*

Evolution of the Lyman- α Forest with Redshift

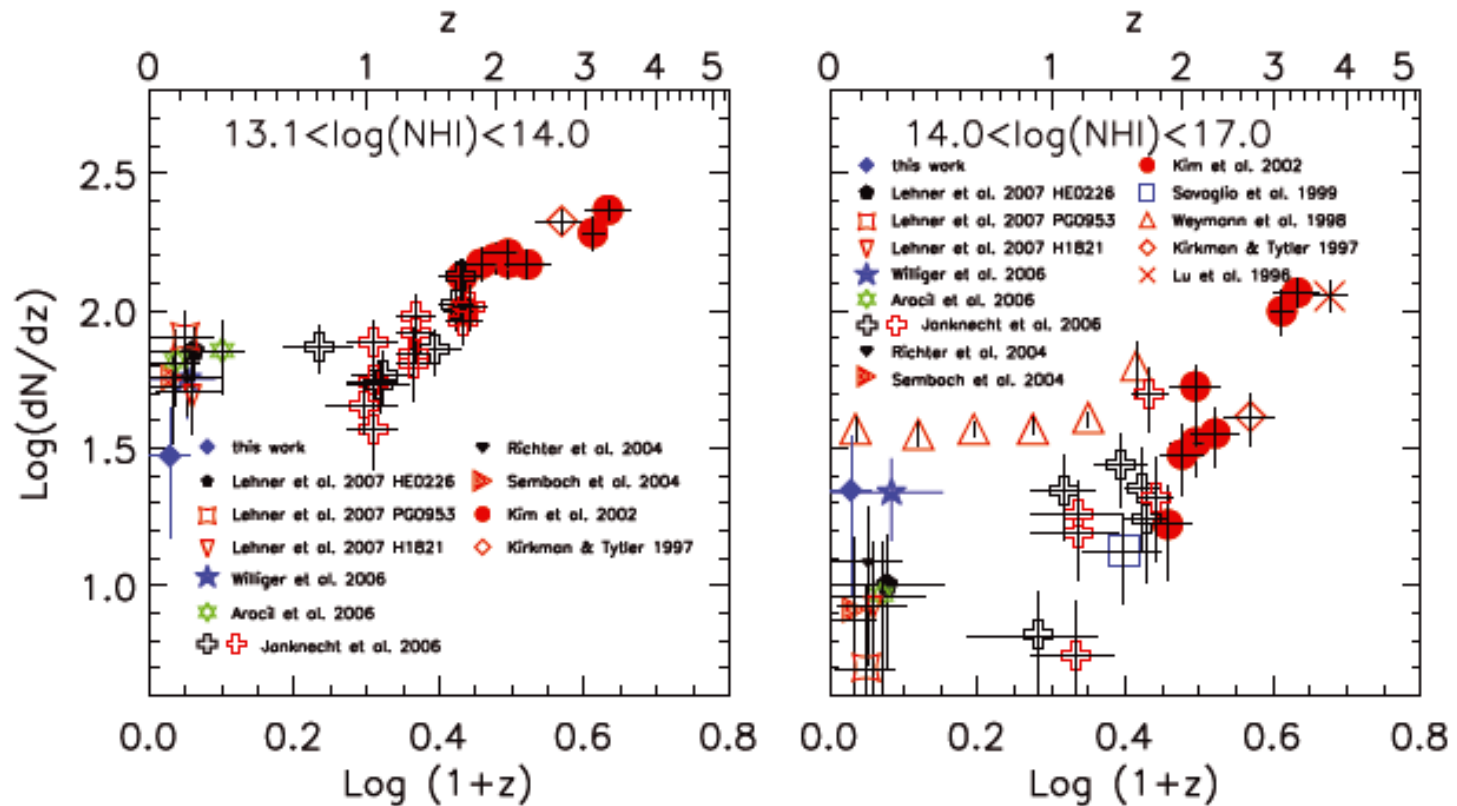


Weymann et al. (1998)

Evolution of the Lyman- α Forest with Redshift

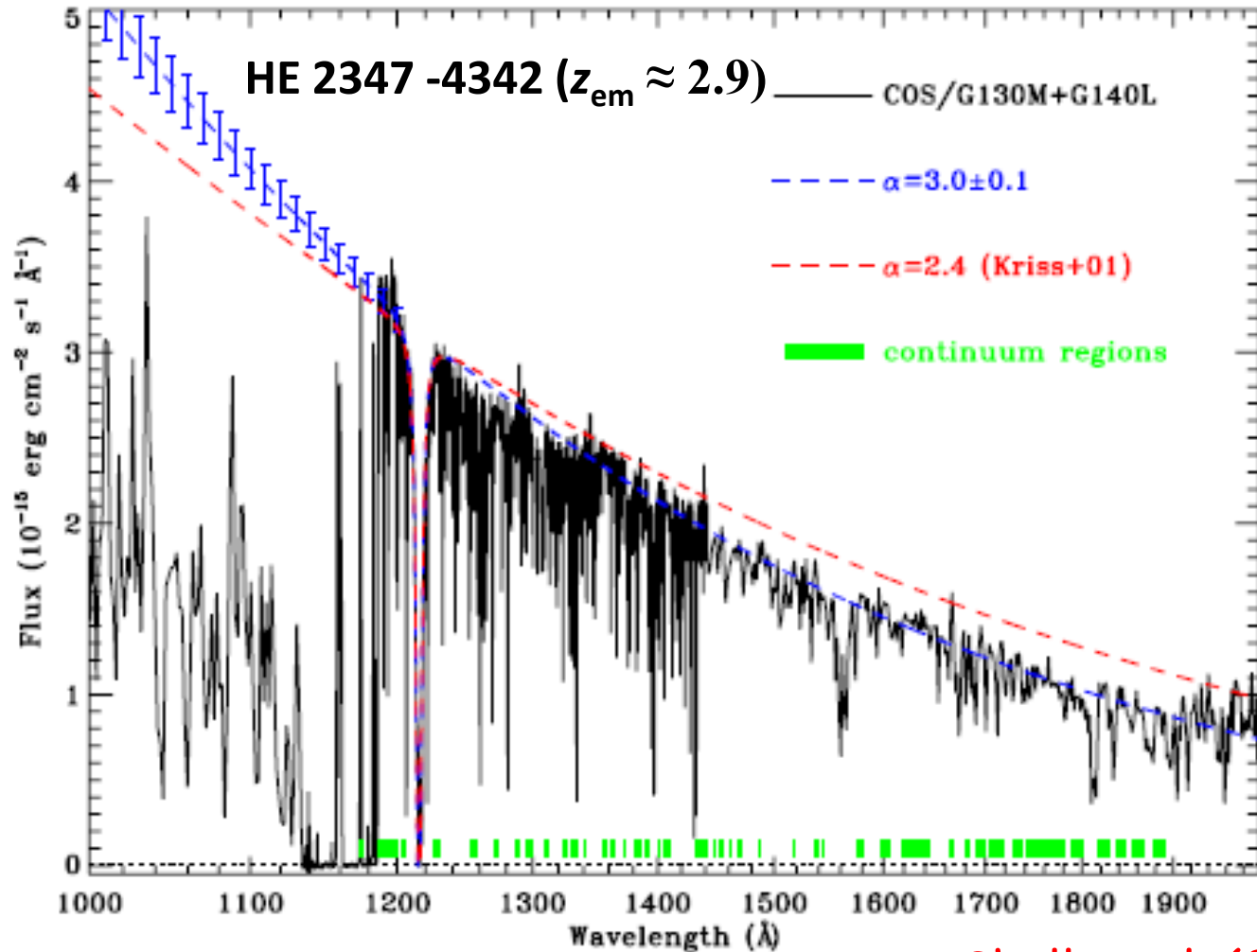


Evolution of the Lyman- α Forest with Redshift



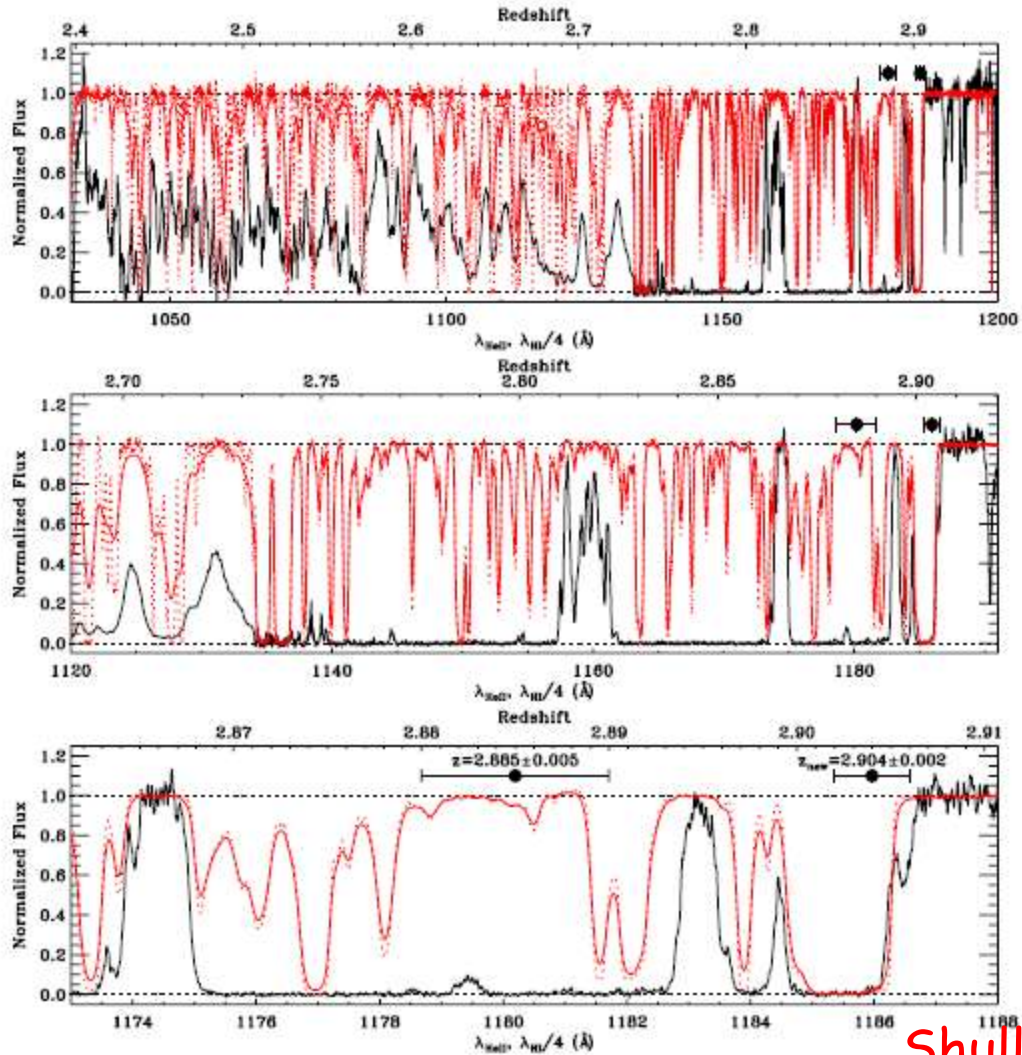
Williger et al. (2010)

He II Gunn-Peterson Absorption



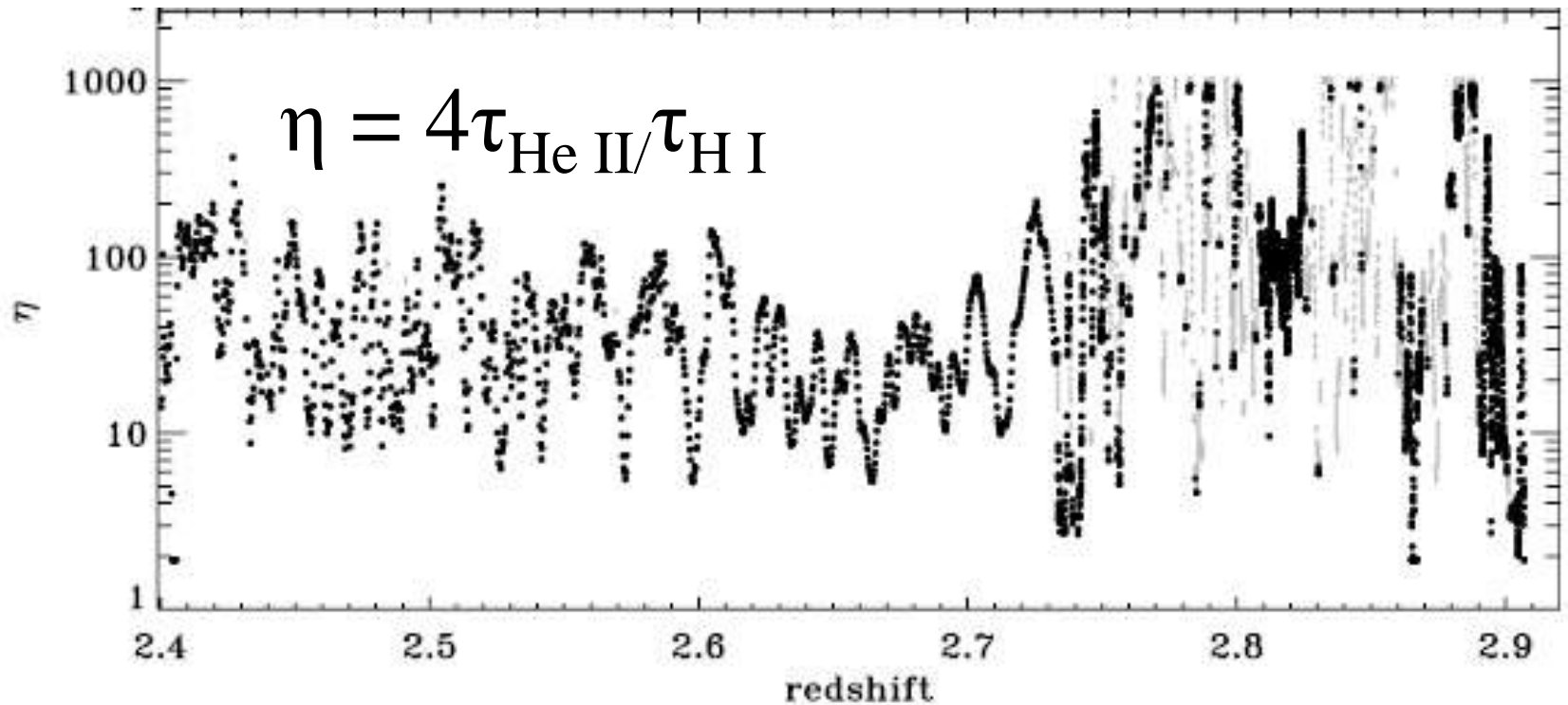
Shull et al. (2010)

He II Gunn-Peterson Absorption



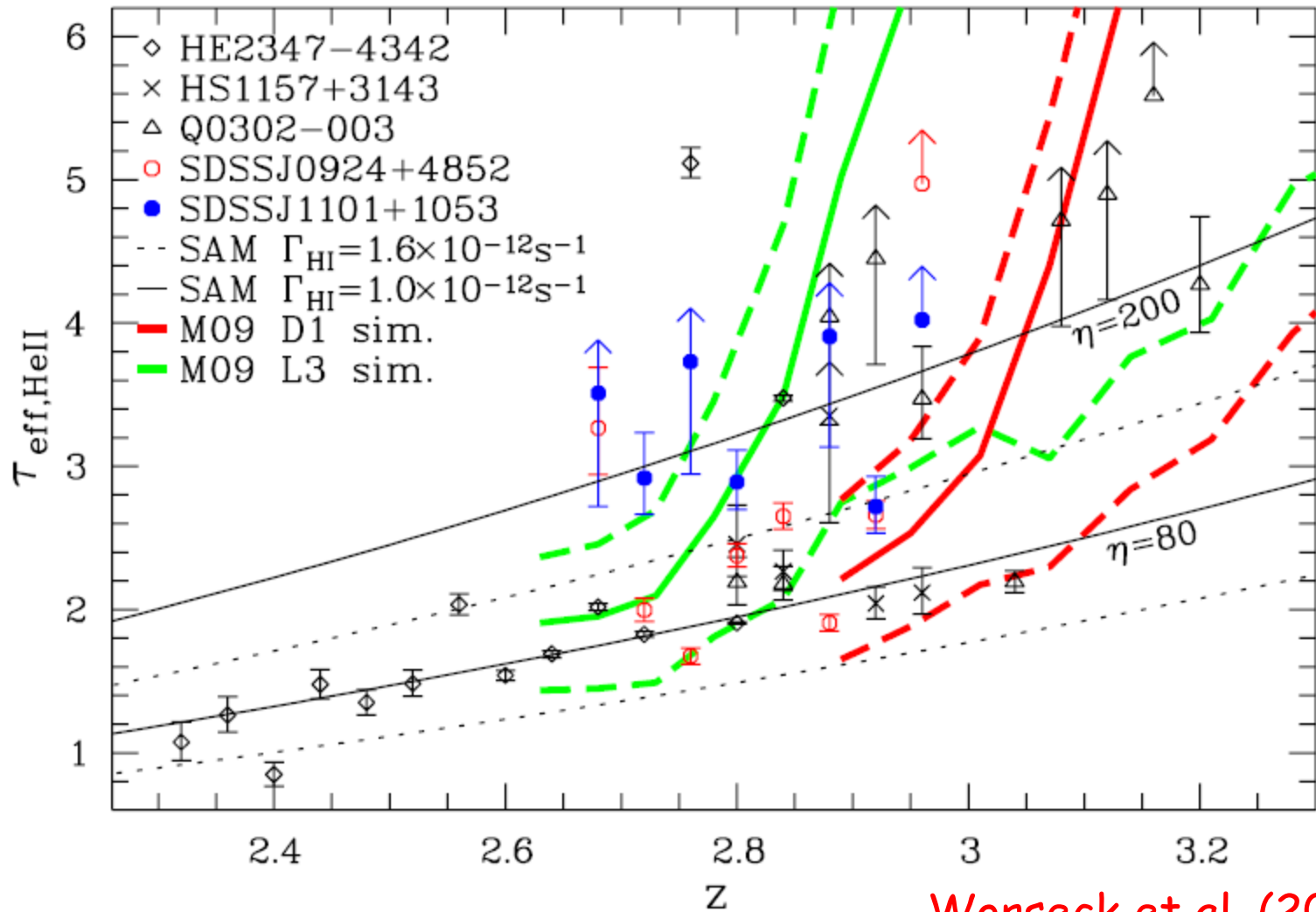
Shull et al. (2010)

He II Gunn-Peterson Absorption



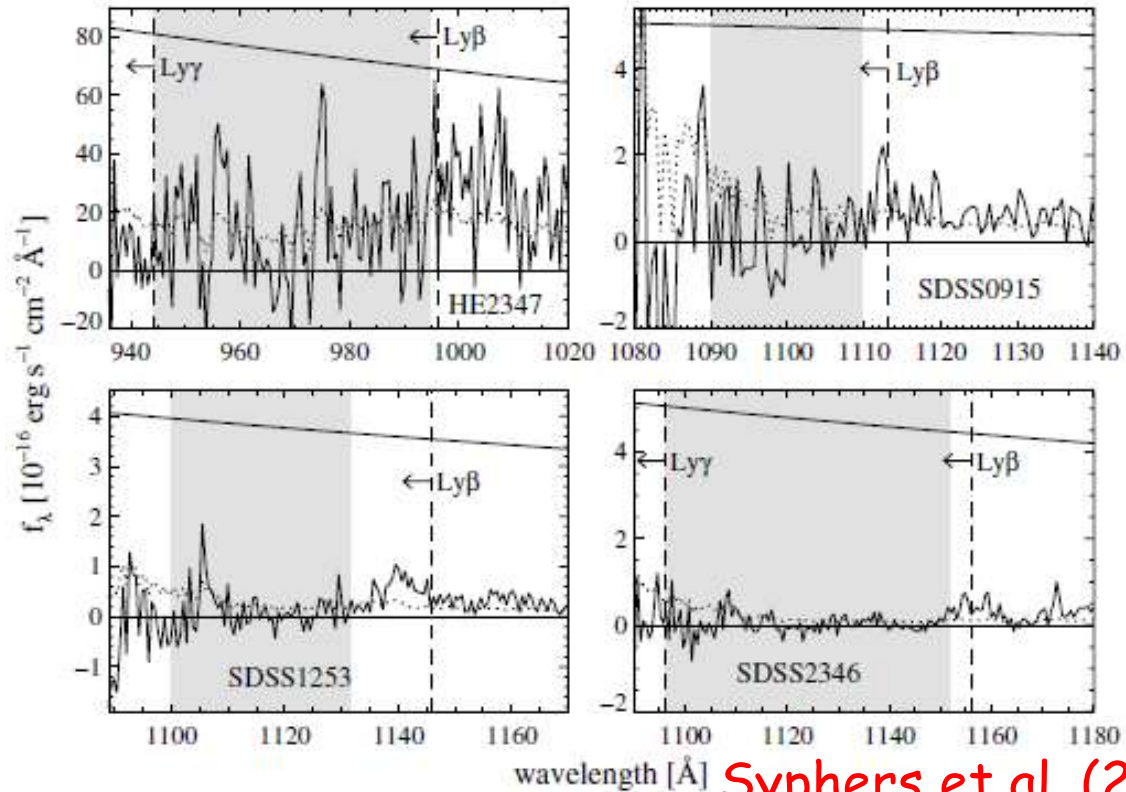
Shull et al. (2010)

He II Gunn-Peterson Absorption



Worseck et al. (2011)

He II Gunn-Peterson Absorption

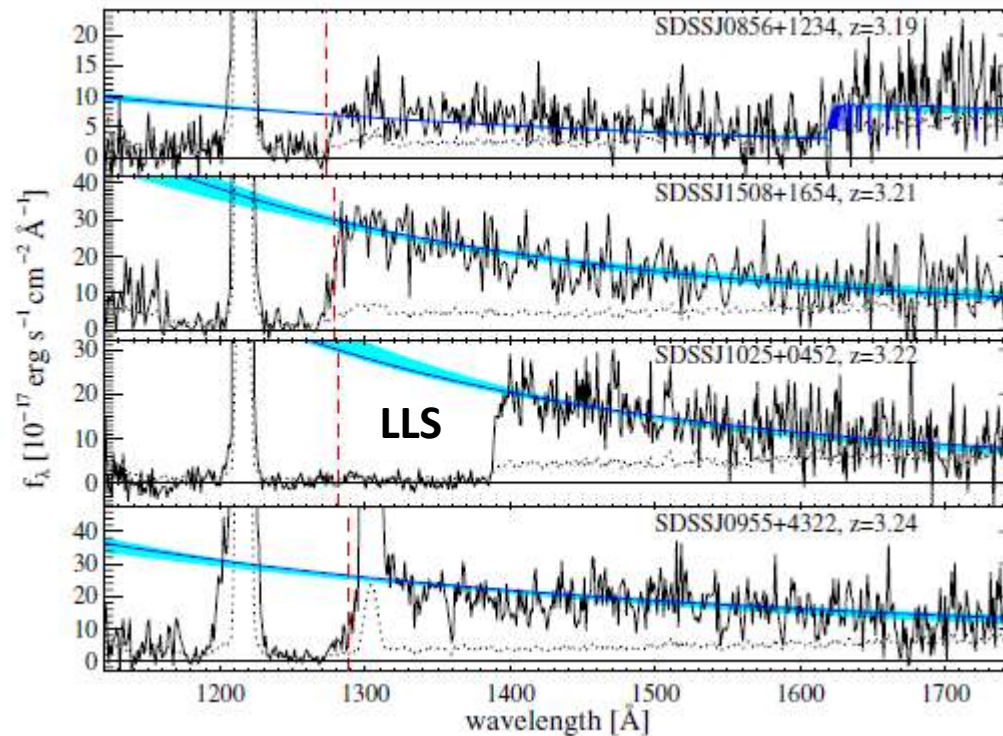


Syphers et al. (2011)

He II Gunn-Peterson Absorption

Use of GALEX and SDSS to find new target QSOs

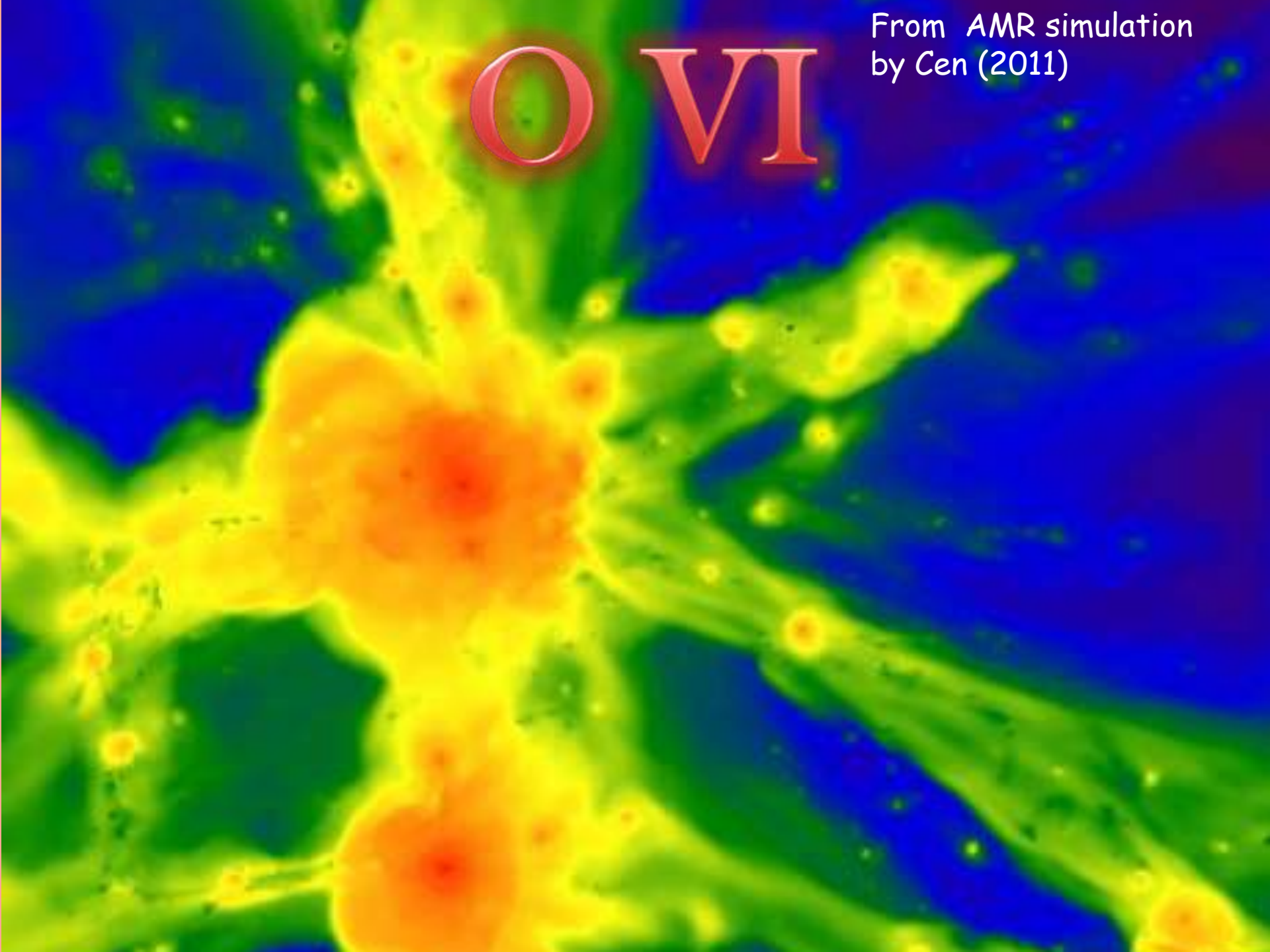
G140L
mode
of COS



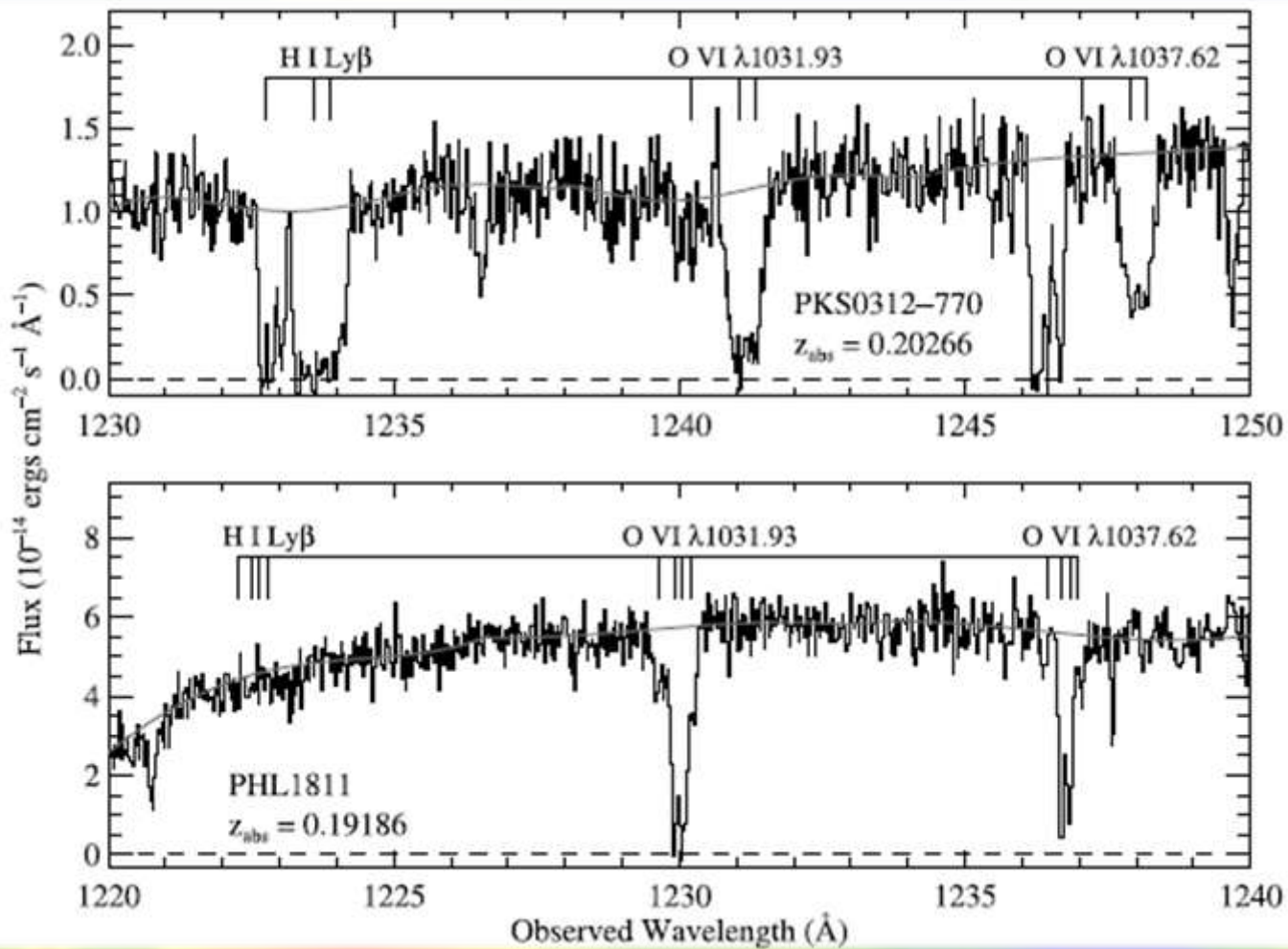
Syphers et al. (2012)

From AMR simulation
by Cen (2011)

O VI

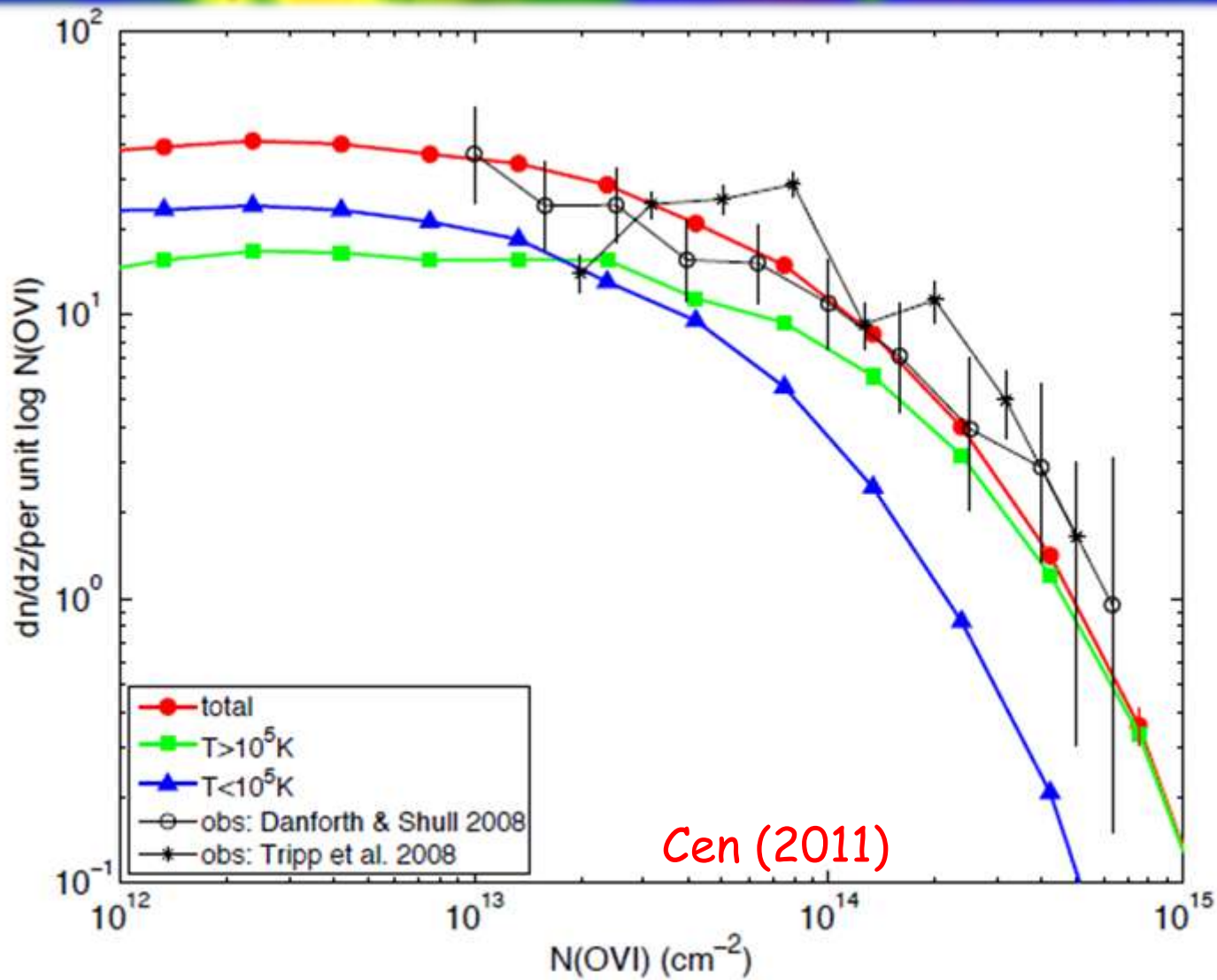
The image displays a simulated O VI absorption line profile. The background is a color map where blue represents low absorption, green represents moderate absorption, and yellow to red represents high absorption. The absorption is most intense in a central, irregularly shaped region. Several elongated, filamentary structures extend from this central region, showing varying degrees of absorption. Numerous small, bright spots are scattered throughout the field, indicating localized regions of high absorption. The overall appearance is that of a complex, multi-phase interstellar or circumgalactic medium.

O VI



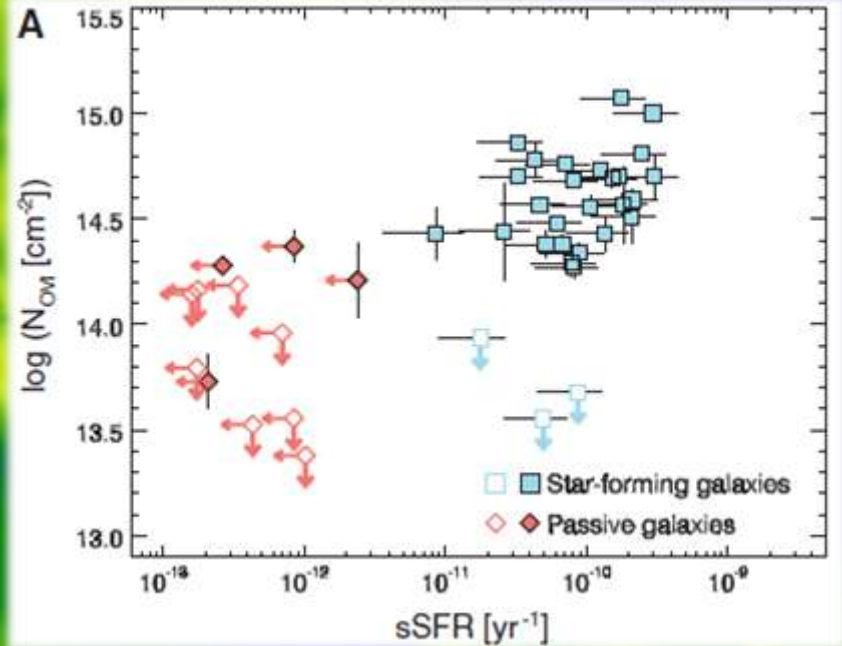
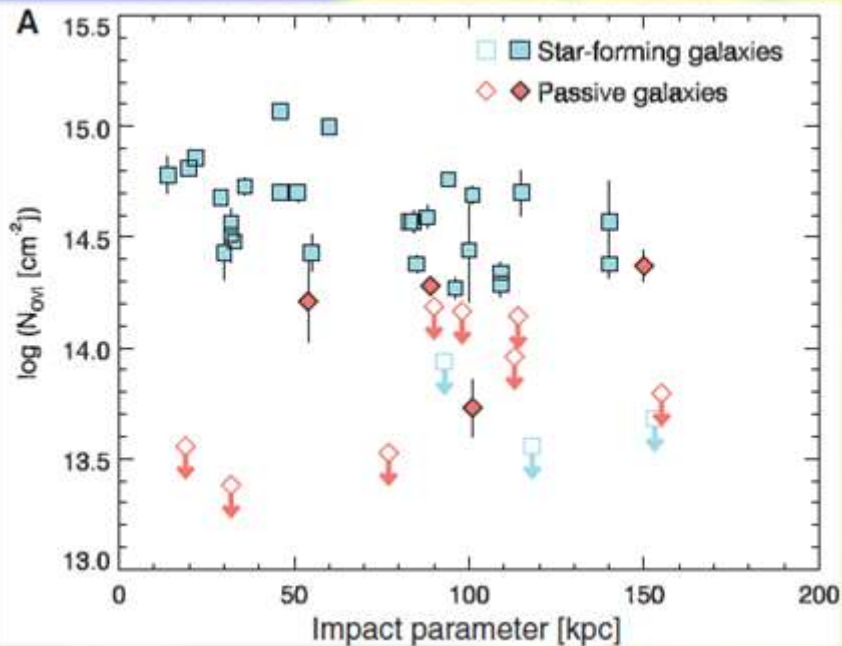
Tripp et al. (2008)

OVI



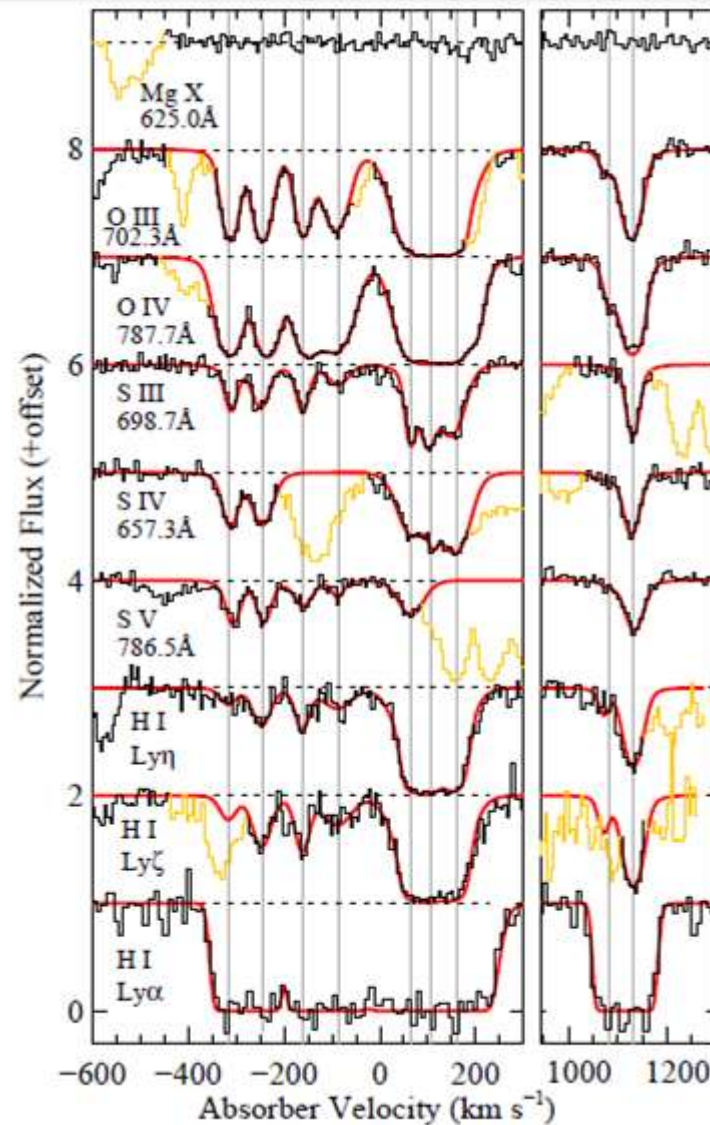
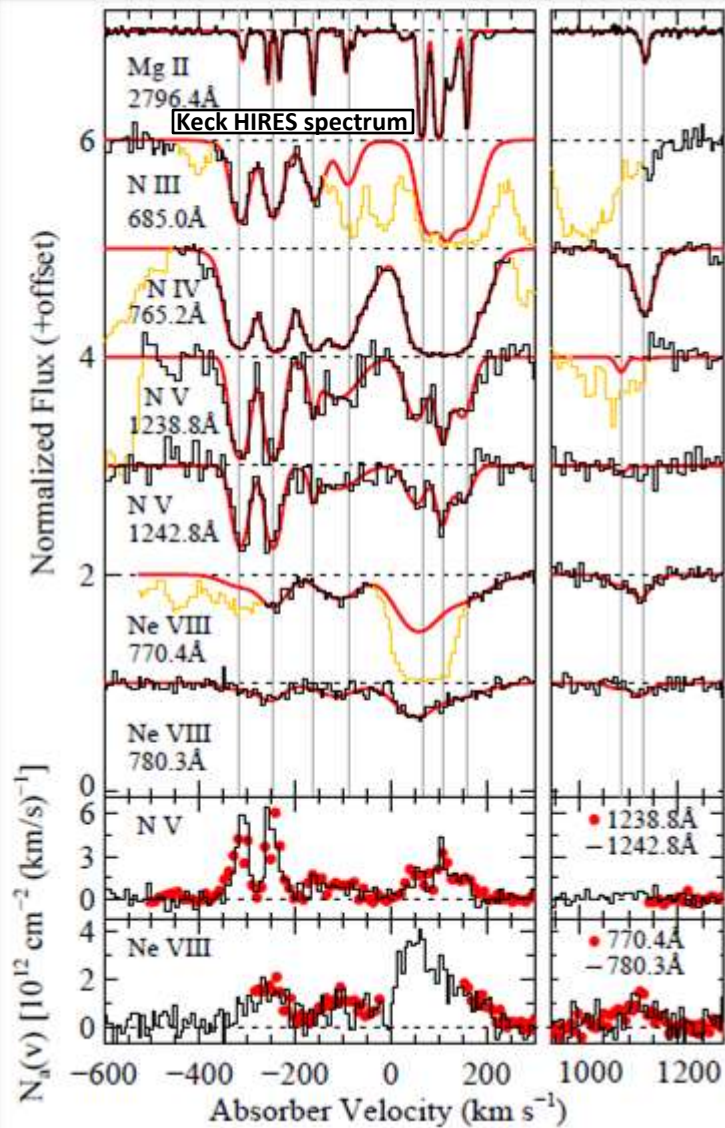
O VI

O VI in the vicinities of foreground galaxies



Tumlinson et al. (2011)

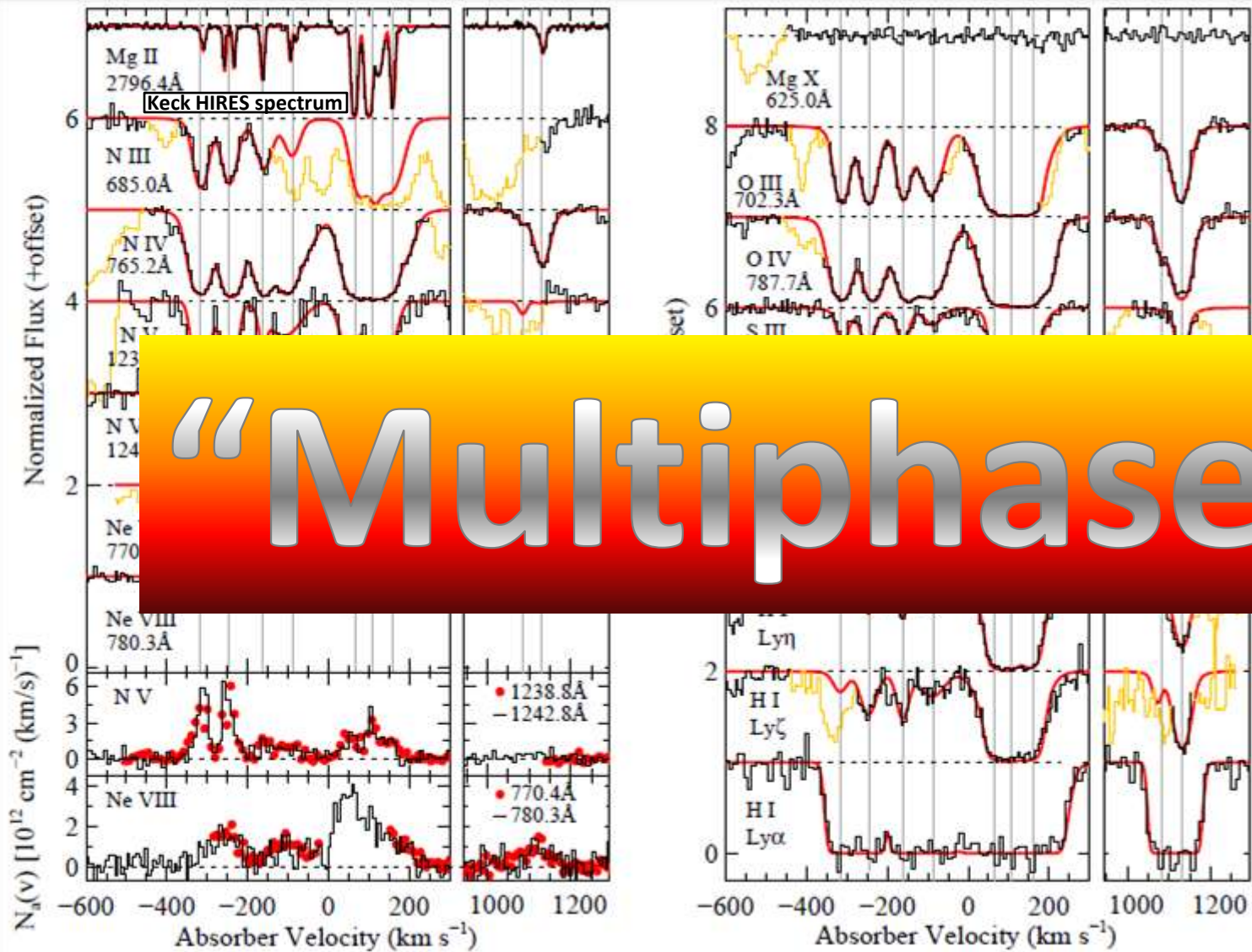
Absorption Systems at Moderately High z



$z_{\text{abs}} = 0.927$

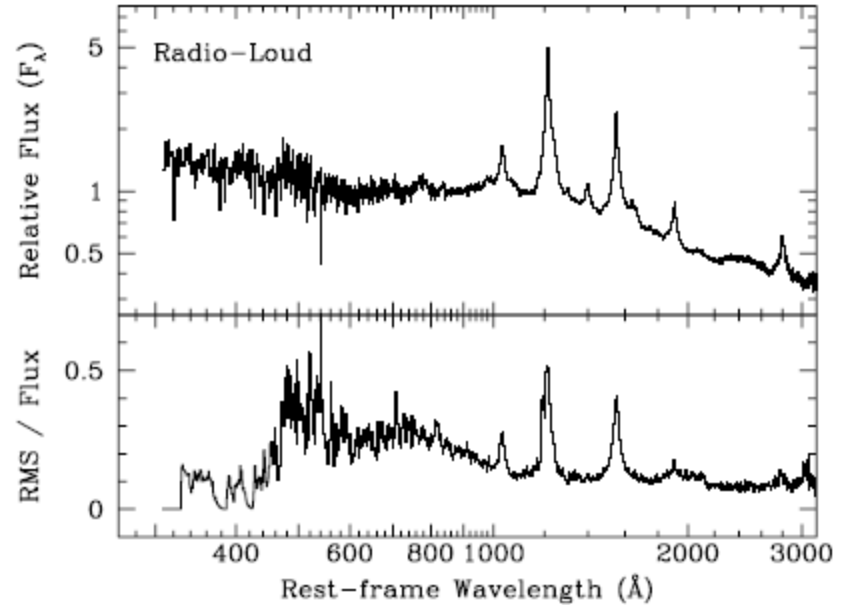
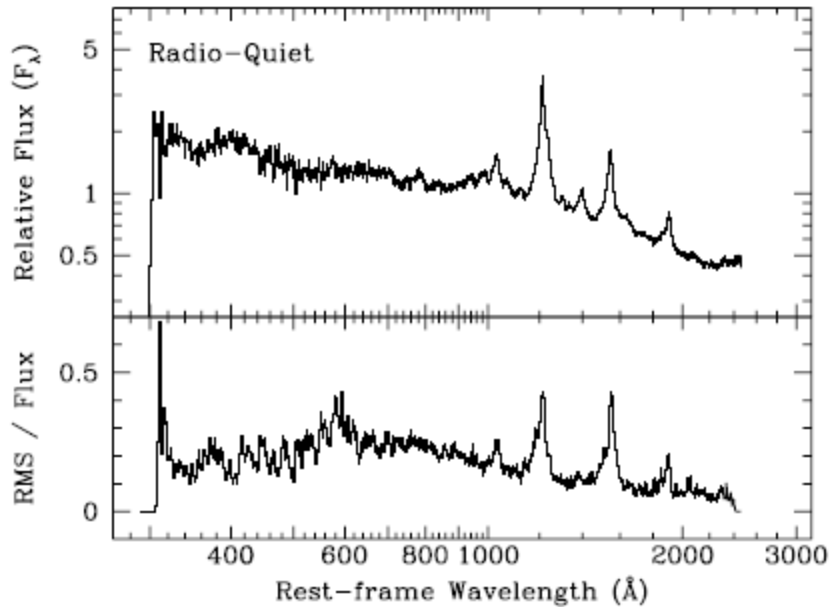
Tripp
et al
(2011)

Absorption Systems at Moderately High z



Tripp
et al
(2011)

Composite Spectra of Quasars

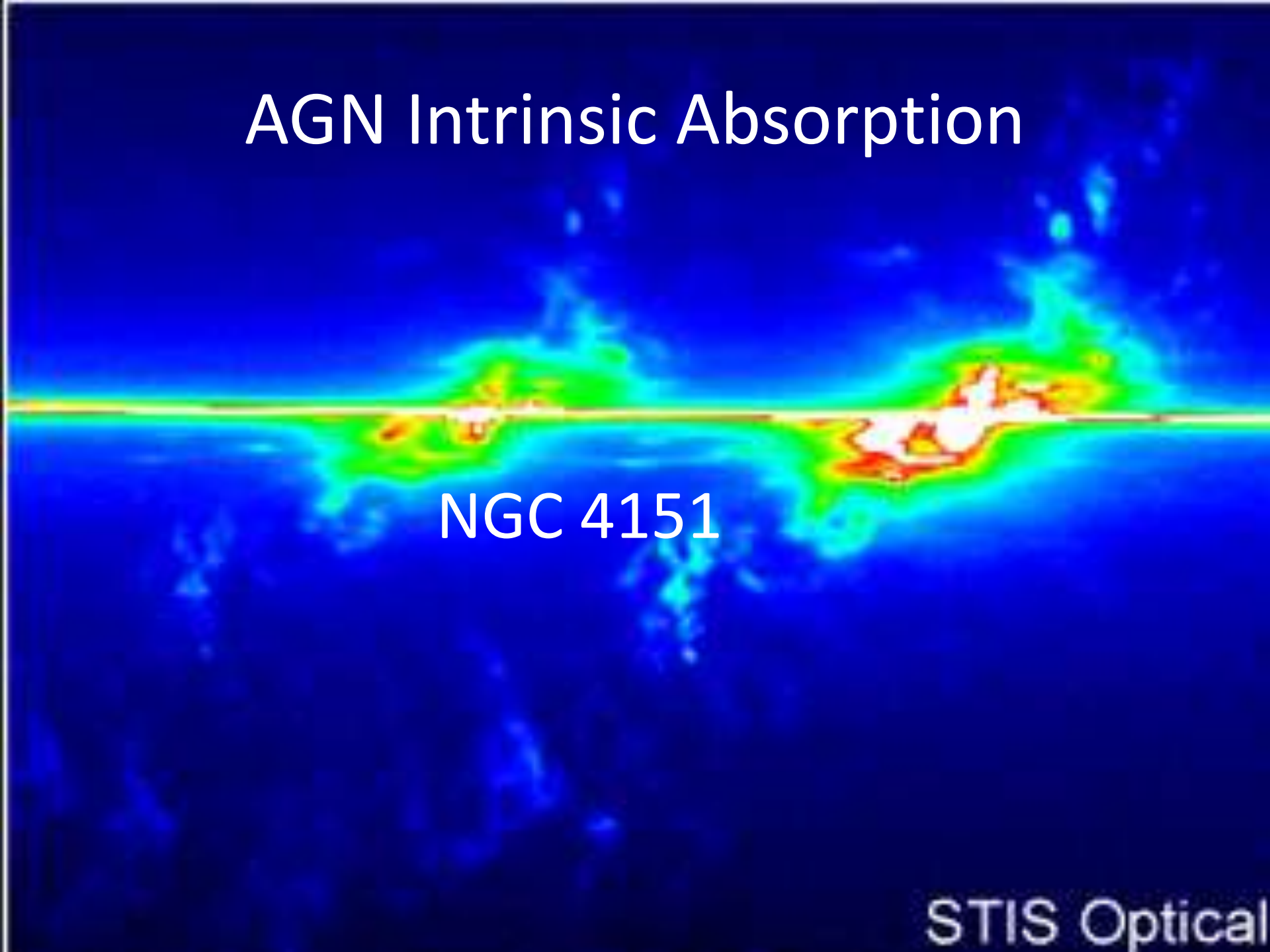


Telfer et al. (2002)

Spectral energy distributions are of relevance to our understanding of the ionization of the IGM

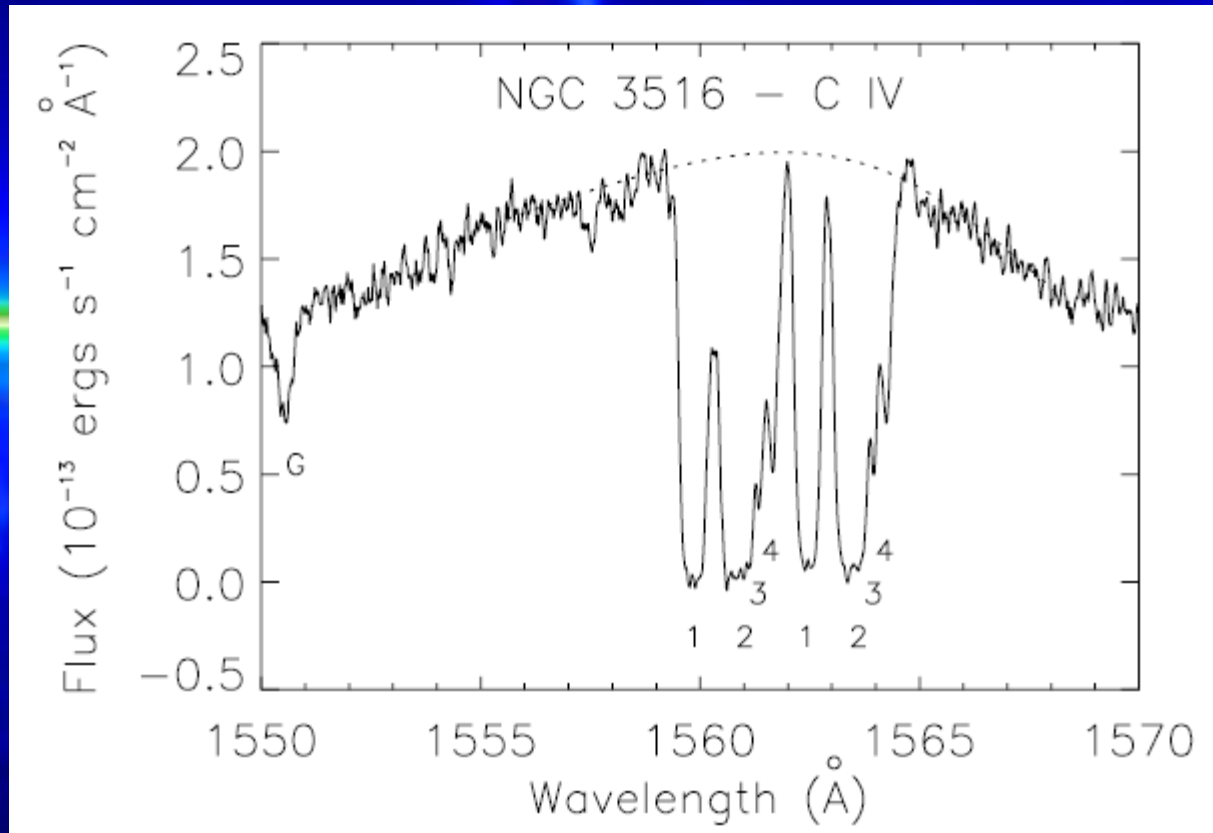
AGN Intrinsic Absorption

NGC 4151

The image is a false-color optical spectrum of the galaxy NGC 4151, captured by the Space Telescope Imaging Spectrograph (STIS). The horizontal axis represents the rest-frame wavelength, and the vertical axis represents flux. The spectrum shows a broad emission line profile with a significant absorption dip at approximately 4130 Å, which is characteristic of AGN intrinsic absorption. The absorption is deepest in the central region of the galaxy, as indicated by the darker blue color in the center of the image. The overall color scheme ranges from dark blue (low flux) to white (high flux).

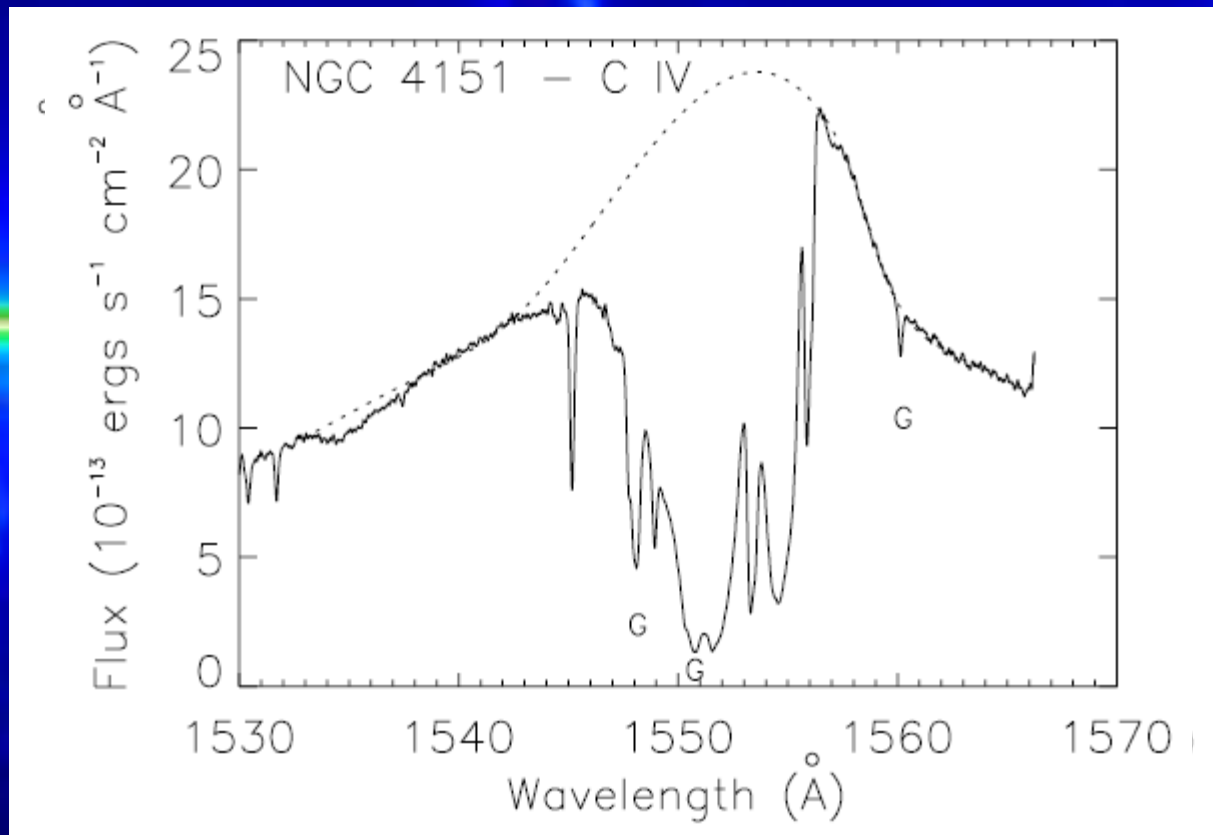
STIS Optical

AGN Intrinsic Absorption



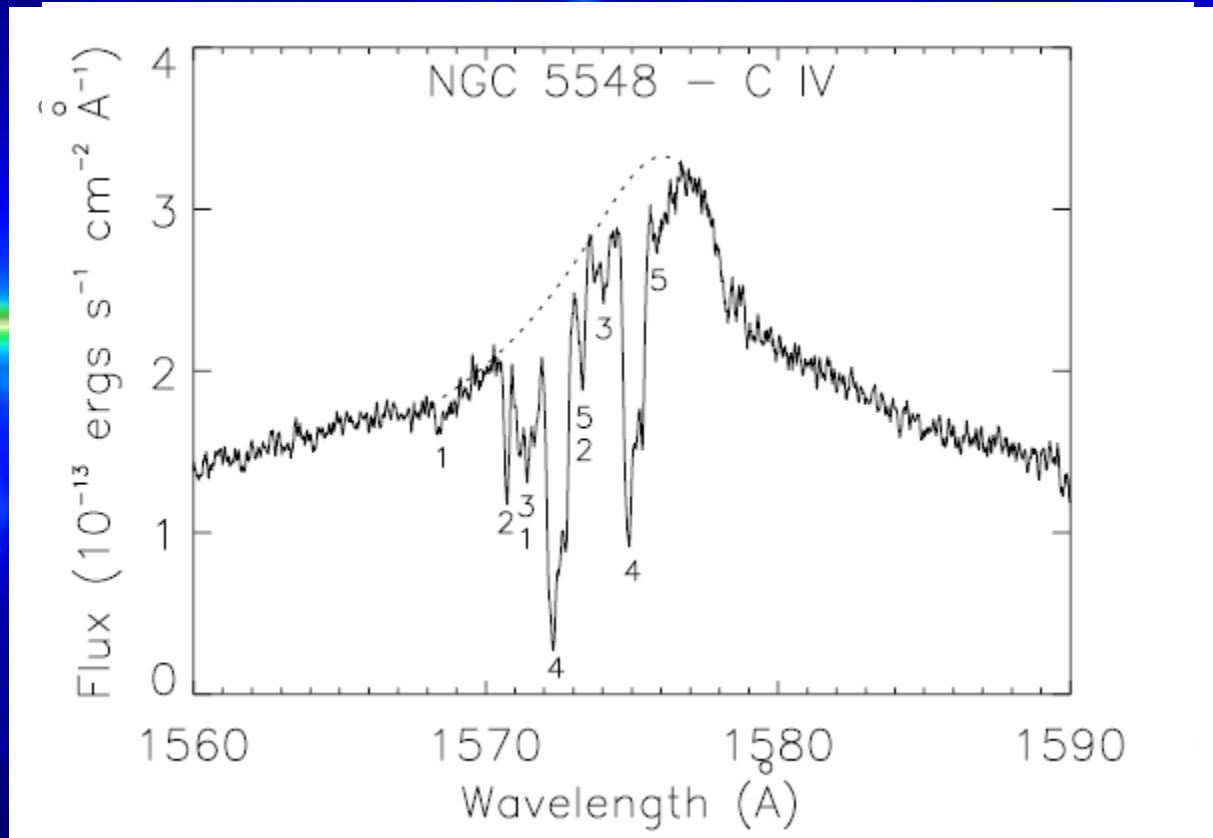
Crenshaw et al. (1999)

AGN Intrinsic Absorption



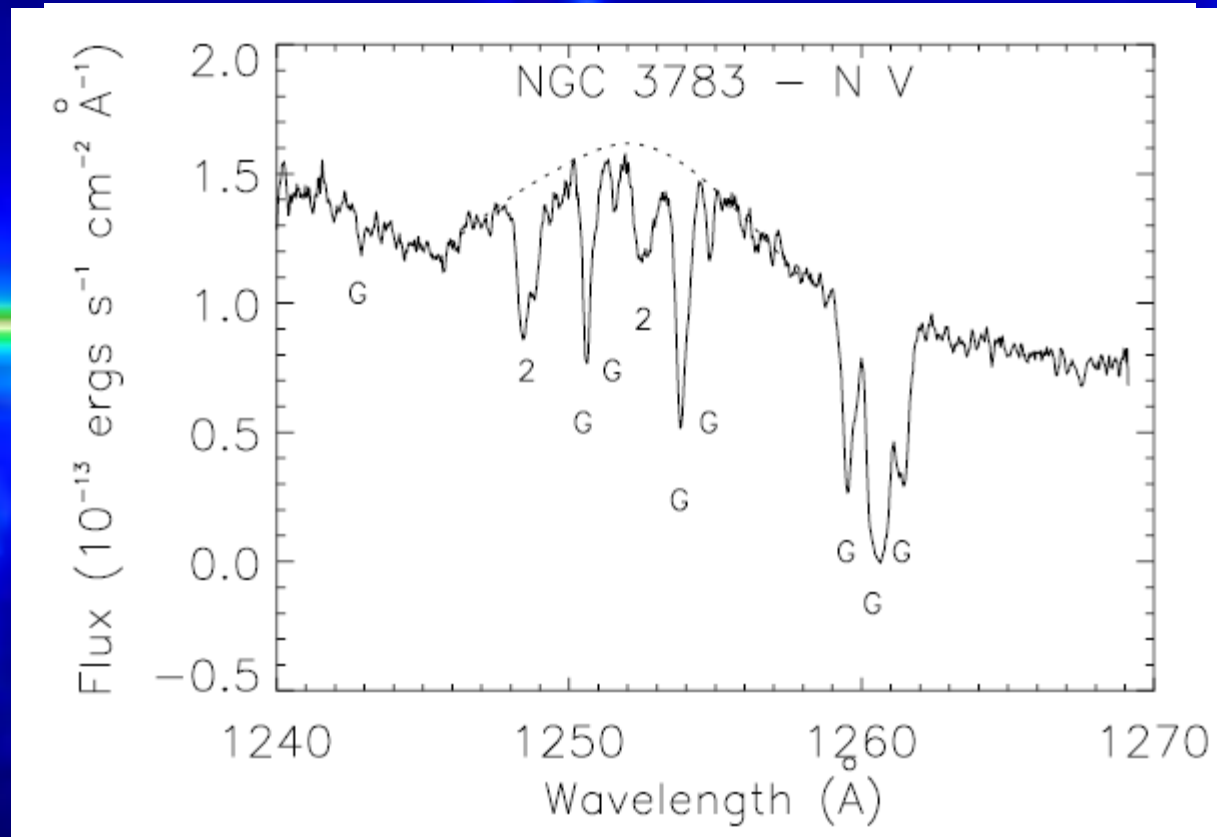
Crenshaw et al. (1999)

AGN Intrinsic Absorption



Crenshaw et al. (1999)

AGN Intrinsic Absorption



Crenshaw et al. (1999)

AGN Intrinsic Absorption

Conclusions:

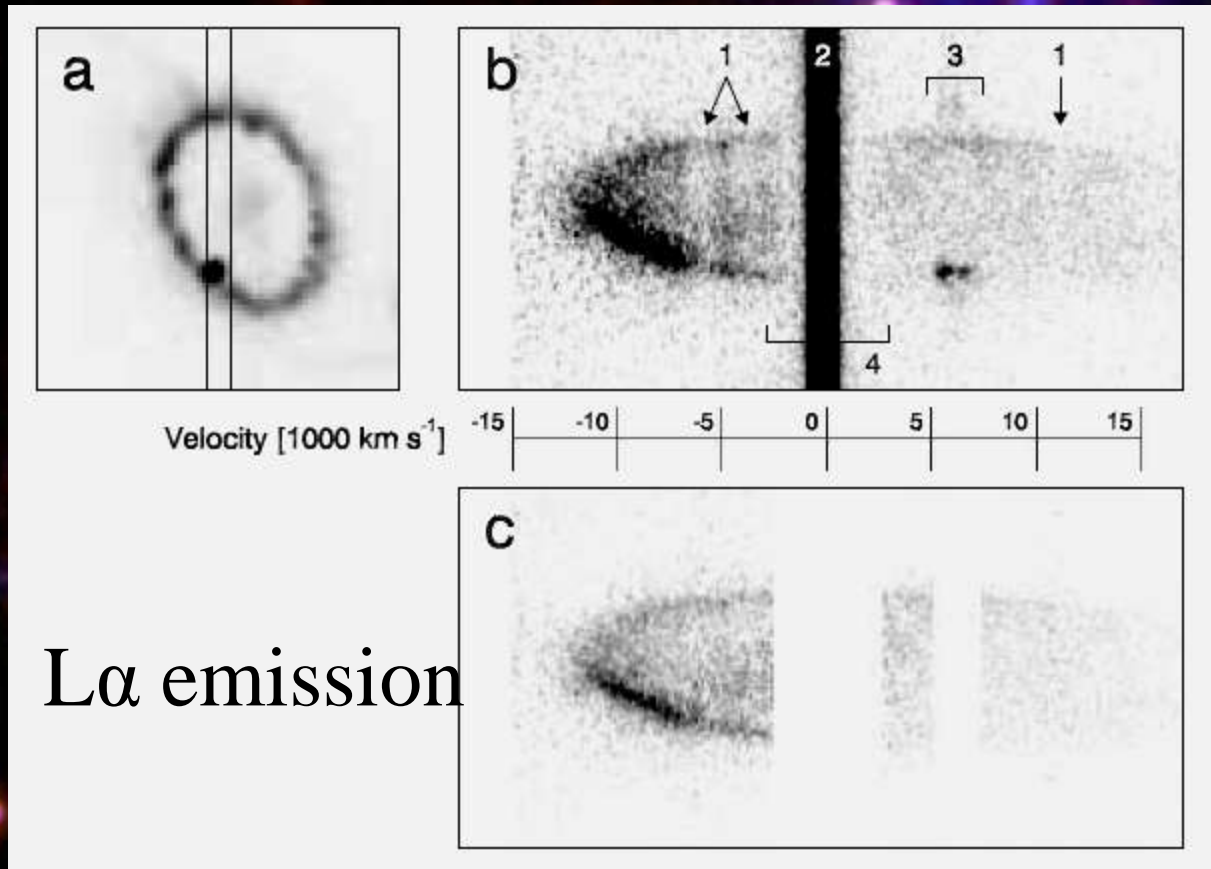
1. Prominent features in high ionization stages of atoms
2. Frequency of appearance indicates that the covering factor $\approx 50\%$ of the broad line region.
3. Features show time variability (indicates characteristic distances $100 - 10^4$ lt-days) and have multiple narrow velocity components.

Supernovae: SN 1987A in the LMC

The image shows a field of stars in the Large Magellanic Cloud. A prominent feature is a bright, circular ring of light in the center, which is the H-alpha emission from the supernova remnant of SN 1987A. Two bright, star-like sources are visible: one in the upper right and one in the lower left, both exhibiting prominent diffraction spikes. The background is dark with numerous other stars of varying colors and brightness.

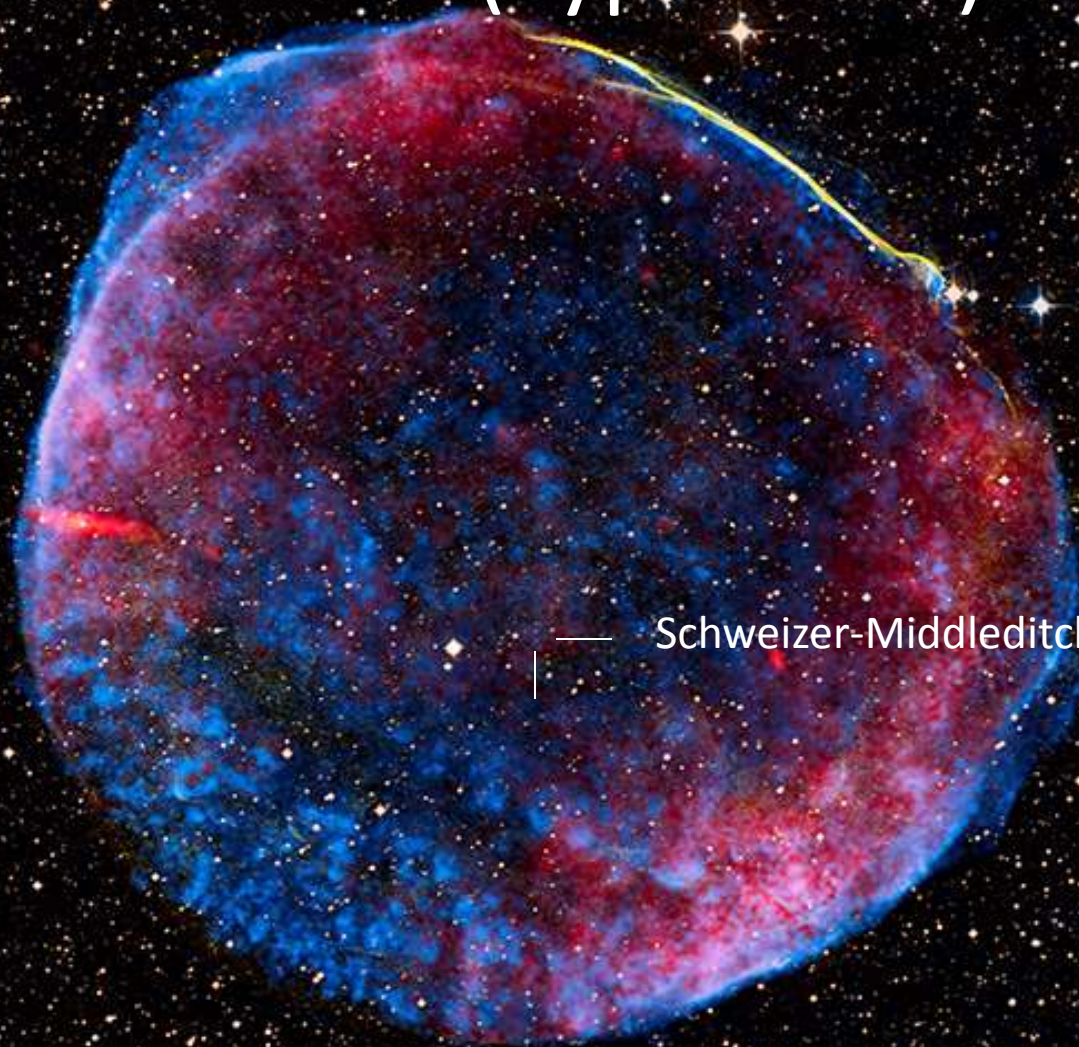
H α emission

Supernovae: SN 1987A in the LMC



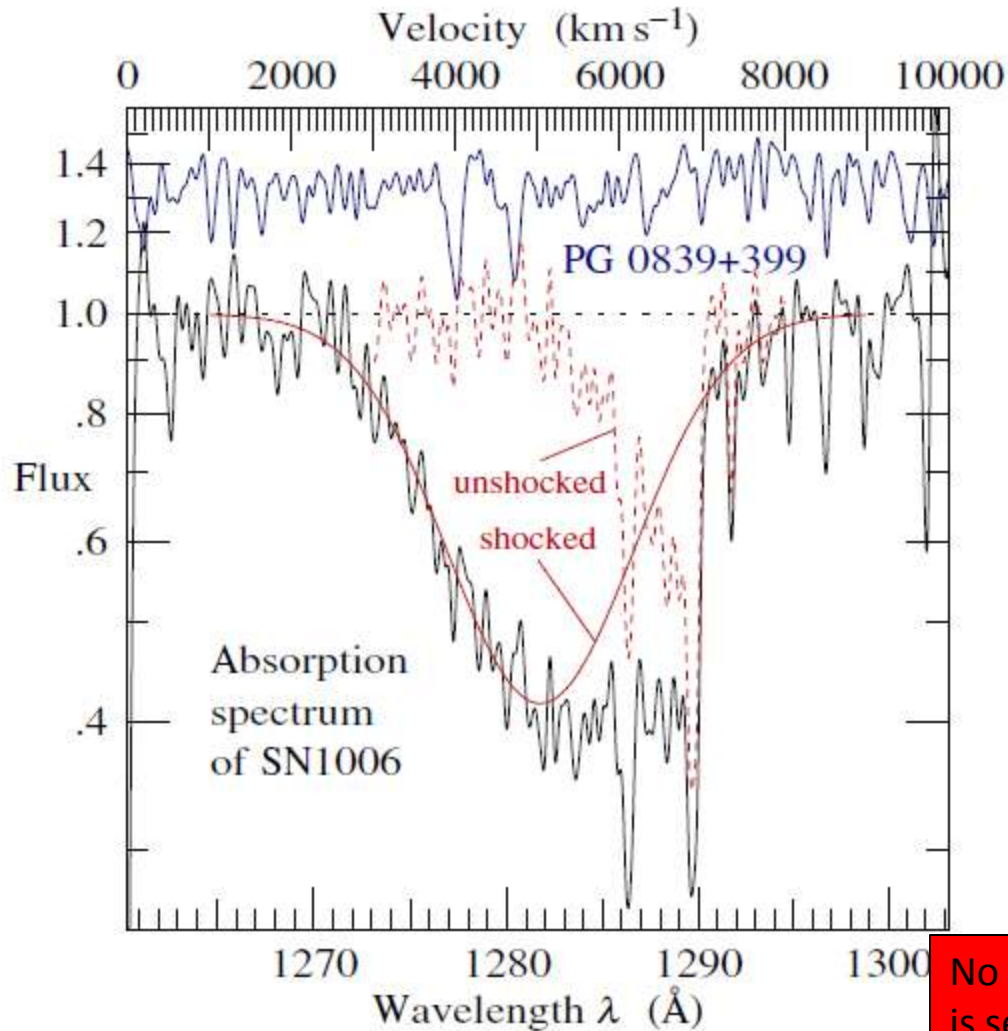
Michael et al. (2003)

Supernovae: SN 1006 (Type Ia SN)



Schweizer-Middleditch star ($V = 16.7$)

Supernovae: SN 1006 (Type Ia SN)



The sharp edge on the right-hand side has moved to lower velocities by $44 \pm 11 \text{ km s}^{-1}$ between a STIS exposure taken in 1999 and a COS exposure taken in 2010, indicating that the reverse shock is intercepting more slowly moving gas further inside the outflow.

*Winkler
et al.
(2011)*

No blueshifted counterpart to this absorption is seen. Possible reasons for this are discussed by Hamilton et al. (1997)

THE LEGACY OF HST SPECTROSCOPY





Barbara A.

MIKULSKI ARCHIVE OF SPACE TELESCOPES

High Level Science Products

High-Level Science Products (HLSP) are community contributed, fully processed (reduced, co-added, cosmic-ray cleaned etc.) images and spectra that are ready for scientific analysis. HLSP also include files such as object catalogs, spectral atlases, and README files describing a given set of data.

Spectral Atlases

Search [10 Lac \(O9V\) Spectral Atlas \(HST/GHRS\)](#) PI: Brandt, J.C.

Search [A FUV Atlas of Low-Resolution HST spectra of T Tauri Stars](#) PI: Gregory Herczeg

Search [AGN and Quasar Spectral Atlas \(HST/FOS\)](#) PI: Ian Evans

- [alpha Ori Spectral Atlas \(HST/GHRS\)](#) PI: GHRS Team

- [chi Lupi \(B9.5 pHgMn\) Spectral Atlas \(HST/GHRS\)](#) PI: GHRS GTO team

Search [CoolCAT - A cool-star UV spectral catalog](#) PI: Thomas Ayres

- [Copernicus Atlases of 6 Selected Stars](#) PI: Copernicus Project

Search [Detailed Far-UV Spectral Atlas of B Main Sequence Stars](#) PI: Myron Smith

Search [EUV Spectral Atlas of Stars \(EUVE\)](#) PI: N. Craig

Search [FUSE Atlas of Starburst Galaxies](#) PI: Anne Pellerin

Search [FUSE Magellanic Clouds Legacy Project](#) PI: William Blair

Search [FUSE Spectral Atlas of Wolf-Rayet Stars](#) PI: Allan J. Willis

Search [OB Stars \(Galactic\): FUSE Spectral Atlas](#) PI: Anne Pellerin

Search [OB Stars \(Magellanic\): FUSE Spectral Atlas](#) PI: Nolan Walborn

Search [Pre-Main Sequence Stars: IUE Spectral Atlas](#) PI: Jeff Valenti

- [Procyon \(FV-IV\) Spectral Atlas - Chromospheric Lines \(HST/GHRS\)](#) PI: Brian Wood

- [Standard Stars: IUE](#) PI: Chi-Chao Wu

Search [StarCat: HST STIS Echelle Spectral Catalog of Stars](#) PI: Thomas Ayres

Search [STIS Next Generation Spectral Library \(AR10659\)](#) PI: Sally Heap

- [White Dwarf Spectral Atlas: High dispersion IUE](#) PI: Jay Holberg